# Development of Fragility Curves for Cold-Formed Steel Light-Framed Structural Systems: a Two-Pronged Approach

By

Alexander Grummel

A thesis submitted in partial fulfillment of
the requirements for the degree of

MASTER OF SCIENCE IN CIVIL ENGINEERING

WASHINGTON STATE UNIVERSITY
Department of Civil and Environmental Engineering

AUGUST 2010

To the Faculty of Washington State University:

The members of the Committee appointed to examine the thesis of Alexander Conrad Grummel find it satisfactory and recommend that it be accepted.

J. Daniel Dolan, Ph.D., Chair

William Cofer, Ph.D.

Bonnie Manley

# ACKNOWLEDGEMENT

Sincere gratitude goes to Dr. Daniel Dolan for his continued support and technical advice throughout the development of this thesis. I would also like to thank Dr. Daniel Dolan and Dr. William Cofer for their superb teaching over the years. Their thorough knowledge of engineering principles and practices and passion for teaching has consistently reaffirmed the quality of education at Washington State University.

Additionally, I would like to thank Professor Shiling Pei, the developer of SAPWood. His willingness to provide technical support with a cheerful attitude is greatly appreciated.

Many thanks to Bonnie Manley and Kelly Cobeen for providing data and reports for use in this thesis. Without their connections in the industry, data gathering would have been a daunting task.

Lastly, I would like to thank my mother and father Esther and Michael Grummel. They have instilled in me the belief that with a combination of skill and perseverance anything is possible.

# Development of Fragility Curves for Cold-Formed Steel Light-Framed Structural Systems: a Two-Pronged Approach

## Abstract

by Alexander Conrad Grummel, MSCE
Washington State University
August 2010

Chair: J. Daniel Dolan

The use of Cold-Formed Steel (CFS) shear walls has become increasingly prevalent in the construction of low-rise residential structures. Due to the increase of CFS construction in low-rise residential structures, there is an increased demand for performance based seismic analysis of CFS shear walls. Fragility functions were developed to aid in the performance based seismic analysis of CFS structures. Fragility functions are a very useful tool for such an analysis as they are used to estimate the probability of damage that a structure may incur when subject to seismic loading.

Fragility curves in this document were constructed using two separate approaches. The first approach was to develop fragility curves based on test data. Fragility curves based on test data were developed using Inter-Story Drift (ISD) as the Engineering Demand Parameter (EDP). Cyclic and monotonic test data from experiments conducted by Chen (2004), Serette (1997), Nguyen, Hall and Serette (1996), Boudreault (2005), Branston, Boudreault and Chen (2004), Blais (2006), Hikita (2006), Rokas (2006) and Branston (2004) was used to construct fragility curves for the following wall systems:

- CFS System #1: CFS walls with wood structural panel sheathing (plywood or OSB), seismic hold-downs and various fastener spacing.

- CFS System #2: CFS walls with 8 mil or 23 mil exterior steel sheathing, seismic hold-downs and various fastener spacing.
- CFS System #3: CFS walls with exterior flat strap X-bracing and seismic hold-downs.

The second approach to construct fragility curves for above mentioned CFS wall systems used Peak Ground Acceleration (PGA) as the EDP. The development of fragility curves of this nature involved the use of the program SAPWood to perform an Incremental Dynamic Analysis (IDA) based on idealization of wall specimens as Single-Degree of Freedom (SDOF) spring elements.

# Table of Contents

# List of Figures

# List of Tables

# Dedication

This thesis is dedicated to my beloved girlfriend Jennifer Kaye.  Her continued love, and support of all my endeavors made it possible for me to keep a smile on my face during stressful times.

# Chapter 1

# Introduction

## 1.1 General Overview

The use of cold-formed steel (CFS) stud framing with structural panels has been prevalent in commercial construction for quite some time. However, in recent years, CFS framing with structural panels has become increasingly popular in the construction of low-rise residential structures. Low-rise structures are defined by ASCE-07 to be structures with a mean roof height less than 60 feet and not greater than the least horizontal dimension of the structure. This method of shear wall construction typically consists of CFS framing with Wood Structural Panels (WSP) screwed to the CFS framing at predetermined fastener schedules. However, in some cases diagonal X-bracing or steel structural panels may be used to provide horizontal reinforcement in place of WSP's. A typical light-gauge CFS framed house sheathed with WSP's is shown in Figure 1.

**Figure 1-Typical Residential Construction Using CFS Framing with WSP sheathing (left: interior view of CFS wall; right: exterior view) (Branston, 2004)**

As part of a larger project to develop a basis for performance based seismic design, the Applied Technology Council (ATC) has begun to seek help from the engineering community to develop the required information for CFS light-frame shear walls. One common means of gauging a structure's seismic performance involves the use of fragility functions. Fragility functions provide the information required to do performance based seismic design since they are used to estimate the reliability of structural components when subject to seismic loading. The various levels of damage a structural component might incur can then be related to the amount of repair and cost of repair to return the component to a serviceable state. Therefore, fragility functions pertaining to various structural components of a building can be used to estimate the cost of returning the building to an operable state. For this reason, fragility functions are an extremely efficient way to estimate the amount of monetary and physical resources needed to repair the structures in a given area after an earthquake has impacted that area. Additionally, fragility functions are useful when analyzing the costs and benefits of structural components in the preliminary design stage of a structure. For example, building developers can work with engineers to choose a structural component based not only on initial cost but also on the cost of repairing the structure after a seismic event.

While many low-rise residential structures consist of wood-frame shear walls, for which fragility curves have already been developed (Ekiert and Filiatrault 2008), the increased use of CFS framing in residential structures warranted development of fragility curves for CFS light-frame shear walls. Therefore, Chapter 3 of this thesis is based on a report entitled "Fragility Curves for Cold-Formed Steel Light-Frame Structural Systems." This report was developed by the author and co-authored by Dr. J. Daniel Dolan. Empirical data from various researchers was used to develop the fragility curves in the aforementioned report. Following development of the ATC report, further analysis was performed to develop fragility curves based on wall performance when subjected to various historical earthquake trace accelerations. A list of earthquakes used for the analysis is presented in Table 17. A program entitled SAPWood (Seismic Analysis Package for Woodframe Structures) was used to idealize structural walls as Single Degree of

Freedom (SDOF) spring elements and impose loading on these idealized walls via ground acceleration records from various earthquakes. The final product of this two-pronged approach to the development of fragility curves for CFS light-frame shear walls is quite versatile as this document can be used to assess the probability of damage to a CFS shear wall based on the amount of horizontal drift of the shear wall or based on the peak acceleration the shear wall is subjected to.

## 1.2 Fragility Curves Explained

As was previously mentioned, fragility functions are used to determine the probability that a given structural component will incur a given amount of damage when subjected to seismic loading. It should be noted that the development of fragility curves need not be constrained to structural components only. Fragility functions may, and have been, developed for non-structural elements and systems such as office furniture and appliances. However, this document focuses solely on the development of fragility curves for CFS light-frame shear walls.

The method of developing fragility functions is governed by the ATC-58 project (Porter, 2007). The ATC-58 document lays out specific guidelines for developing fragility curves for a given component or system, all of these protocols must be followed to insure the development of accurate and reliable fragility curves.

Fragility curves are constructed using lognormal cumulative distribution functions. These functions are based on two fragility parameters; a median value θ, and dispersion value β, which is the lognormal dispersion value of the function. Fragility curves/functions are developed using the following mathematical formula:

$$F_i(D) = \Phi\left(\frac{(\ln(\frac{D}{\theta_i})}{\beta_i}\right)$$

Where: $F_i(D)$ is the probability that the component of interest will reach or exceed the damage state "i". $\Phi$ denotes the standard normal Gaussian cumulative distribution function. $\theta_i$ and $\beta_i$ denote the median value and dispersion value of the Damage State "i" respectively. Therefore, θ and β must be established for each damage state identified. Additionally, the conditional probability that the component of interest will be damaged to Damage State "i" and not to a lesser or greater damage state is given by the equation:

$$P[i|D|] = F_{i+1}(D) - F_i(D)$$

Where: $F_{i+1}(D)$denotes the conditional probability that the component of interest will be damaged to a more severe Damage State ("i+1"). An example of a fragility function with probability of exceedence graphed against demand parameter D (definition of demand parameter to be explained further) is shown in Figure 2.

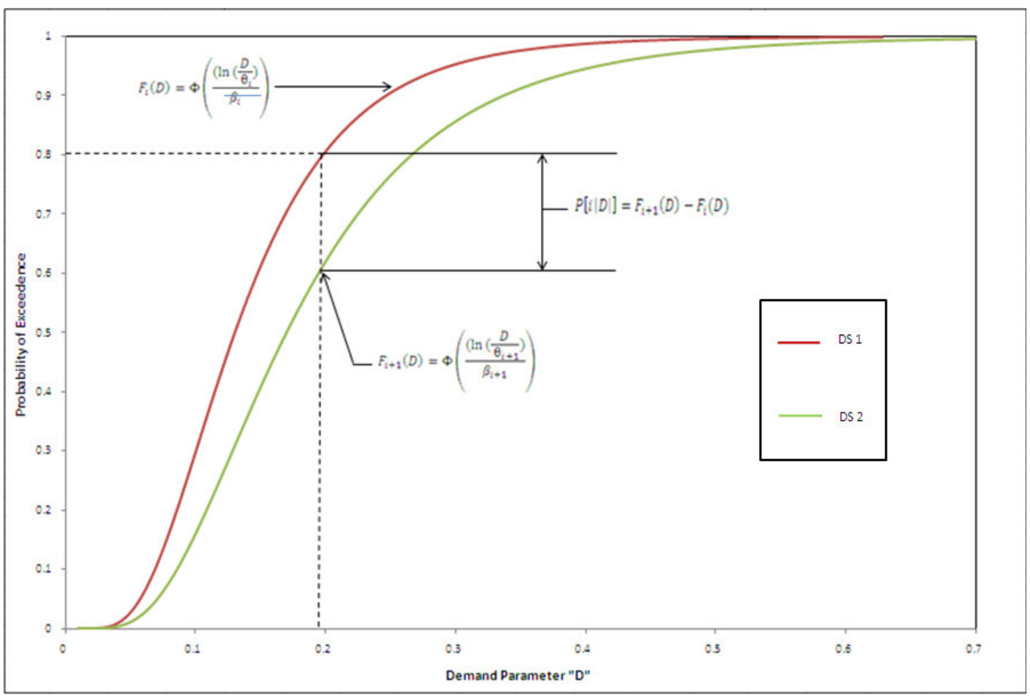


**Figure 2-Example Fragility Curve Showing Probability Functions For Two Damage States**

The Demand Parameter, commonly referred to as the Engineering Demand Parameter (EDP) when developing fragility curves for structural components, can be either expressed in terms of Inter Story Drift

(ISD%) where ISD(%)=(horizontal deflection/wall height) x100) or in terms of ground acceleration (i.e. PGA). Whether using ISD or PGA values as the governing demand parameter, damage states for the component of interest must be defined. A Damage State (DS) is typically defined in terms of the deteriorated condition of the component of interest and the amount of repair needed to return the component to its original undamaged state (i.e. condition it was in prior to seismic loading). For example, an interior wall with gypsum wallboard may experience three damage states when subjected to seismic loading. $DS_1$ may be defined as cracking of gypsum wallboard over fastener heads (a condition which involves repainting and some spackle work). $DS_2$ may be defined as rotation of gypsum panels (a condition which involves complete replacement of all panels and refinishing of the wall). Lastly, $DS_3$ may be defined as complete failure of the wall, requiring the wall be rebuilt. Damage States are defined by the level of damage and associated repairs to insure that fragility curves which are developed based on these damage states can be used for a probabilistic analysis for the cost to repair a structural system or component after a seismic event.

When developing fragility curves, ATC-58 "Guidelines for Seismic Performance Assessment of Buildings" stipulates that specific procedures and associated functions be used to develop mean ($\theta$) and dispersion ($\beta$) values. These methods are described in ATC-58 and are as follows:

Method A: Actual Demand Data: When test data is available from M number of specimens and each tested component actually experienced the damage state of interest at a known value of demand, D.

Method B: Bounding Demand Data: When test data or earthquake experience data are available from M number of specimens, however, the damage state of interest only occurred in some specimens. For other specimens, testing was terminated before the damage state occurred or the earthquake did not damage the specimens. The value of the maximum demand, $D_i$ , to which each specimen was subjected to is known for each specimen. This maximum demand need not necessarily be the demand at which the damage state initiated.

Method C: Capable Demand Data: When test data or earthquake experience data are available from M number of specimens, however, the damage state of interest did not occur in any of the specimens. The maximum value of demand, $D_i$ , to which each specimen was subject is known.

Method D: Derivation (analysis): When no test data are available, however, it is possible to model the behavior and estimate the level of demand at which the damage state of interest will occur.

Method E: Expert Opinion: When no data are available and analysis of the behavior is not feasible, however, one or more knowledgeable individuals can offer an opinion as to the level of demand at which damage is likely to occur, based either on experience or judgment.

Due to the fact that Method A in conjunction with Method E were used to develop the fragility curves presented in this document, only the formulas pertaining to derivation of fragility parameters (θ and β) for Method A are presented here. They are as follows:

$$\theta = e^{\left(\frac{1}{M}\sum_{i=1}^{M} \ln d_i\right)}$$

where:

M= total number of specimens tested to the initiation of the respective damage state "i"

$d_i$=demand in test "i" at which the damage state was first observed to occur.

Additionally, the value of dispersion β is calculated as:

$$\beta = \sqrt{\left(\frac{1}{M-1}\sum_{i=1}^{M}\left(\ln\left(\frac{d_i}{\theta}\right)\right)^2\right)}$$

with M, $d_i$ and θ defined as before.

Finally, the fragility functions must be tested for goodness of fit. Testing for goodness of fit is performed at the 5% significance level using the Lilliefors Goodness of Fit testing method (Lilliefors, 1967). The testing method is as follows:

$$D = max_x |F_i(d) - S_M(d)|$$

Where: $S_m(d)$ denotes the sample cumulative distribution function

$$S_M(d) = \frac{1}{M} \sum_{i=1}^{M} H(d_i - d)$$

where H is taken to be:

- 1.0 if $d_i$-d is positive
- ½ if $d_i$-d is zero
- 0 if $d_i$-d is negative

If D > $D_{crit}$ than the function fails the Goodness of Fit test. At the 5% significance level, $D_{crit}$ is taken as:

$$D_{crit} = \frac{0.895}{(M^{0.5} - 0.01 + 0.85M^{-0.5})}$$

# Chapter 2

# Literature Review

## 2.1 Summary of CFS wall Testing

Although the emergence of CFS framing in low-rise residential construction is fairly new, testing of CFS light-frame shear walls has been going on for quite some time. Testing on CFS walls began in the 1970's with tests performed by Tarpy at Vanderbilt University (McCreless & Tarpy, 1978; Tarpy & Hauenstein, 1978). Following these tests, many other researchers have tested CFS walls with structural panels to further knowledge of CFS building performance in the engineering community.

Since the fragility curves presented in this document were constructed using Method A (based on raw data), the development of these curves would not have been possible without data and field observations from numerous researchers.

The first sets of data analyzed for purposes of fragility curve construction came from Serrette et al. (1996, 1997). Both the '96 and '97 reports were sponsored by the American Iron and Steel Institute (AISI). The purpose of the '96 report entitled "Shear Wall Values for Light Weight Steel Framing" was to investigate the behavior of CFS light-frame shear walls sheathed with various structural panels. Shear wall specimens sheathed with gypsum wallboard (GWB), oriented strand board (OSB) and plywood were tested using both monotonic and cyclic loading protocols. A total of 48 wall specimens were tested. Data from 16 of the 48 walls tested was used in the construction of fragility curves for this document. The 16 wall specimens were sheathed with either OSB or plywood, with numerous fastener schedules. All data used from Serrette's report was based on cyclic loading conditions. From these cyclic tests, it was found that while tighter screw schedules produced substantial increases in the shear capacity of a wall, the constraining failure mode moved from fastener pull through to buckling of the wall chord studs.

Serrette's report therefore recommended that designers size chord studs to develop the nominal capacity of the wall, thus insuring that the chord studs do not buckle.

Testing protocols used in the '97 report were identical to those used in Serrette's '96 report. However, the 1997 report entitled "Additional Values for Light Weight Steel Framing" focused on testing of walls with high aspect ratios, walls sheathed with flat strap X-bracing and walls with steel sheathing. From the '97 tests it was reported that the use of thicker steel sheathing increased the capacity of the wall, yet the failure mode of the wall moved from sheathing rupture to screw pullout from the framing. Additionally, the report recommends that when designing walls with flat strap X-bracing, the designers should design the chord studs of the wall for 150% of the flat strap X-brace design strength to insure that buckling of the chord studs does not occur. From the '97 report, data and observations from 28 wall specimens was analyzed to develop fragility curves.

While test data was only available from 1996 and 1997 testing, it should be noted that recent tests have been conducted to improve the performance of CFS shear walls. The documents entitled "Inelastic Performance of Welded CFS Strap Braced Walls" and "Inelastic Performance of Screw Connected Cold-Formed Steel Strap Walls" written by Kostadin Velchev and Gilles Comeau respectively, each focused on the improved connections for CFS light-frame shear walls with X-bracing. These documents provide connection specifications to insure against failure of X-braced walls prior to the X-brace design capacity.

Vagh and Dolan (2000) and Salenikovich, Dolan and Easterling (1999) also published reports for the AISI entitled "Effect of Anchorage and Sheathing Configuration on the Cyclic Response of Long Steel-Frame Shear Walls." Although no test data was used from this report, findings from the report relating to damage characteristics and failure modes of CFS walls were used to develop this thesis. One important conclusion from these reports was that the behavior of CFS shear walls is similar to wood-frame shear walls both in design capacity and observed failure mechanisms.

Additionally, data and observations from numerous theses under the direction of Dr. Collin Rogers at McGill University were used to develop fragility curves for this document. An extensive test program to analyze the behavior of CFS light-frame shear walls has been in the works since 2001. The objective of the test program at McGill University was to develop design standards for CFS walls since, at the time no specific design method for CFS light-frame shear walls existed in the National Building Code of Canada (NBCC). Zhao (2002), Branston (2004), Chen (2004), Boudreault (2005), and Blais (2006) have all published theses on the performance of CFS walls. Additionally, technical reports from Rokas (2006) and Hikita (2006) examined the behavior of CFS shear walls. Since only data and observations from the aforementioned theses and technical reports was used for this document, specifics regarding the scope of each authors individual research are omitted here for brevity. Data from 183 wall specimens was analyzed for the purposes of this document. Wall specimens were tested using both monotonic and cyclic loading protocols.

## 2.2 Summary of Software Used

While many of the fragility curves presented in this document were developed from raw test data from the aforementioned researchers, numerous computer programs were used to develop fragility curves for which PGA was the controlling Engineering Demand Parameter (EDP). One program used was NONLIN, developed by Dr. Finley Charney. NONLIN is a program used for the dynamic analysis of Single Degree of Freedom (SDOF) structural systems. This program allows users to model structures as either perfectly elastic or as elastic plastic. Additionally, NONLIN allows users to input trace ground accelerations from various earthquakes. From these ground accelerations, NONLIN can compute, Spectral Acceleration (Sa), Velocity, etc. as a function of the natural period (T) of a structure. NONLIN was used for the purposes of this thesis to develop Sa vs. T graphs from earthquake acceleration files.

Another program used to aid in the development of fragility curves for which PGA was the EDP was SAPWood (Seismic Analysis Package for Woodframe Structures). SAPWood was developed by Shiling Pei and John Van de Lindt in conjunction with the NEESWood project. The objective of the NEESWood project is to develop a seismic design philosophy which can be used to safely and efficiently increase the height of wood-frame construction. SAPWood was used to model each analyzed wall specimen as a SDOF spring element and then to perform Incremental Dynamic Analysis (IDA) on the idealized wall models.  Output from the IDA was used to construct plots of PGA vs. horizontal displacement for given records of ground acceleration.

# Chapter 3

# Development of Fragility Curves From Test Data

## 3.1 Introduction to the Development of Fragility Curves From Test Data

The objective of this section was to develop fragility curves for CFS light-frame shear walls. While many light-frame structures consist of wood-frame shear walls, for which fragility curves have already been developed (Ekiert and Filiatrault 2008), the use of CFS light-frame shear walls has become increasingly popular in low-rise residential construction and has been used for quite some time in commercial construction. Therefore, when analyzing damage to a structure with CFS shear walls, it is necessary to utilize CFS shear wall fragility functions. All walls analyzed in this report are considered part of a platform frame structural system. Balloon framed structural systems are not considered. The cold-formed steel (CFS) shear wall systems considered in this document are as follows:

- CFS System #1: CFS walls with wood structural panel sheathing (plywood or OSB), seismic hold-downs and various fastener spacing.
- CFS System #2: CFS walls with 8 mil or 23 mil exterior steel sheathing, seismic hold-downs and various fastener spacing.
- CFS System #3: CFS walls with exterior flat strap X-bracing and seismic hold-downs.

Fragility curves for walls with Wood Structural Panel (WSP) sheathing were developed based on fastener spacing (i.e. 6/12 in, 4/12in, etc.). In addition to this, one set of fragility curves was also developed to include all walls with wood structural panel sheathing regardless of fastener spacing. The user of these fragility curves can therefore perform damage assessment on CFS structures with walls of known fastener spacing or can perform a more general analysis to save time or in any instance where individual wall fastener spacing is unknown.

None of the test data analyzed for the purpose of this document included walls with gypsum wallboard (GWB) due to the unavailability of experimental data. However the results of monotonic and cyclic tests of full-size CFS shear walls sheathed with OSB (Salenikovich and Dolan 1999) revealed that CFS shear walls had a similar capacity to wood-frame shear walls. Additionally, it was shown that failure modes of CFS shear walls were similar to those present in tests conducted on wood-frame shear walls (Salenikovich, et al., 1999), with the primary failure mode being head pull through of sheathing screws. Although CFS shear walls experience slightly more flexure in the framing than wood-frame shear walls due to local elastic buckling (dimpling) of the wall stud or track around the fastener, deformation patterns observed for CFS shear walls and wood-frame shear walls are very similar. It is therefore the judgment of the authors that when analyzing CFS shear walls with GWB, the fragility parameters derived for Damage States 1 and 2 ($DS_1$ and $DS_2$) in “Fragility Curves for Wood Light-Frame Structural Systems” (Ekiert and Filiatrault, 2008) should be used.

CFS shear wall specimens tested by the aforementioned authors were subjected to one of the following four loading protocols:

1) Monotonic Loading-wall specimens were loaded to a displacement of 0.5in of lateral deflection after which the load was released. The specimens were then loaded to 1.5in of lateral deflection after which the load was released. The specimens were then loaded to failure.
2) Monotonic Loading-wall specimens were loaded until failure with no release of load.
3) Cyclic Loading-wall specimens were subjected to the Sequential Phase Displacement (SPD) protocol with a cyclic rate of displacement of 1.0Hz.
4) Cyclic Loading-CUREE-Caltech loading protocol.

It is recognized by the author that wall response will differ between testing protocols. However, the predominant mechanism of failure in CFS shear walls results from local elastic buckling of framing members around fastener penetrations and not fatigue failure of individual fasteners which is the predominant failure mode of wood-frame shear walls when tested using a SPD loading protocol. Furthermore, test data used to develop fragility curves for this document showed no drastic differences between peak load capacities of similar walls tested with various loading protocols. Therefore fragility curves were developed based on the type of wall system not the loading protocol used to induce failure of the wall.

A set of fragility curves was developed for each CFS wall system included in this report. These fragility curves consist of an Engineering Demand Parameter (EDP) and a Damage State ($DS_i$) associated with the demand parameter. For each wall system, two or three damage states were included based on the type of structural configuration and whether the authors could confidently assert that a certain damage state occurred in a specimen based on test data. If the authors could not confidently assert that a test specimen exhibited a certain damage state, test data for that specimen was omitted from the respective fragility curve. However, test data for the specimen could still be used for lower bound damage states and their respective fragility curves. For example, data for a wall specimen that was not loaded until failure could still be used to generate a fragility curve associated with the damage state of wall panel replacement. Due to the fact that no wall specimens included finish cladding or multiple types of cladding (e.g. gypsum, stucco, etc.) each damage state was identified based on the amount of repair necessary to restore the structural integrity of the wall (e.g. re-fasten structural panel, replace buckled studs, etc.).

Each collection of fragility curves was generated using Inter-Story Drift (ISD) as the Engineering Demand parameter (EDP). ISD is taken to be the amount of horizontal drift the wall experienced expressed in % of story height (i.e. ISD= (horizontal drift/wall height) x100). All data analyzed for this report was checked for outliers using Pierce's criterion as outlined in Section 3.2 of "Developing Fragility Functions for Building Components for ATC-58," (Porter 2007). The probability that a given damage state is exceeded for a specific ISD was calculated using the Hazen plotting position. Once developed, each fragility curve was subjected to a goodness of fit test at the 5% significance level using the Lilliefors Test (Lilliefors 1967).

Included in the appendices of this document is the pertinent experimental data used to develop the fragility curves present within this document. Tables and figures in the appendices include raw test data as well as data obtained from best fit envelope curves developed from cyclic test data. Additionally, summaries of field reports for individual wall specimen damage states are included in Appendix B.

### 3.2 Fragilities of CFS Walls with WSP Sheathing and Various Fastener Spacing

To increase the versatility of this document, fragility curves were individually developed based on fastener spacing and were also developed for all walls with wood structural panel (plywood or OSB) sheathing regardless of fastener spacing. This section of the report includes fragility functions for all CFS System #1 wall types. These fragility curves will be especially useful when large scale damage assessments are performed in which there is not significant time to individually assess damage to numerous buildings based on the numerous fastener schedules of shear walls. These fragility functions will also be of great use when damage assessment is performed on a building comprised of CFS shear walls with unknown faster spacing.

Construction of the fragility curves for CFS shear walls with wood structural panel sheathing and various fastener spacing was based on cyclic and monotonic test data from experiments conducted by Chen (2004), Serette (1997), Nguyen, Hall and Serette (1996), Boudreault (2005), Branston, Boudreault and Chen (2004), Blais (2006), Hikita (2006), Rokas (2006) and Branston (2004). Specifications for the wall specimens tested are as follows:

- Walls 8ft in height by either 2ft, 4ft or 8ft in length
- 1-1/2"x3-1/2" A446 33ksi steel top and bottom tracks with 33 mil thickness
- 1-1/2"x3-1/2" A446 33ksi steel studs spaced at 24" o.c.
- No. 8-1" sharp point flat head screws for panel to framing connection for '96 and '97 wall specimens

- No. 8-1.5” self piercing bugle head screws for panel to framing connection for all other wall specimens
- Wood structural panel sheathing attached with long dimension parallel to studs
- Spacing of sheathing to framing fasteners at 2-6” on panel edges with 12” spacing in the field
- Seismic hold-downs at wall ends

### 3.2.1 Definition of Damage States

For all walls with wood structural panel sheathing, three damage states were defined based on the level of repair needed to restore the wall to a non-damaged state. The first type of repair ($DS_1$) consists of refastening the structural wall panel. The authors defined $DS_1$ to be the ISD (%) at which either monotonic curves or best-fit envelope curves from experimental data showed a 40-60% decrease in stiffness as evidenced by positive and negative envelope curves. This decrease in stiffness is caused by either pull through of the sheathing to framing connectors from the wood structural panel sheathing or local crushing of the wall panel at the connector to sheathing interface. Refer to Figure 3 for an example of a best fit envelope curve at which $DS_1$ is defined. The authors used both negative and positive displacements to establish average $DS_1$ values for each test specimen.

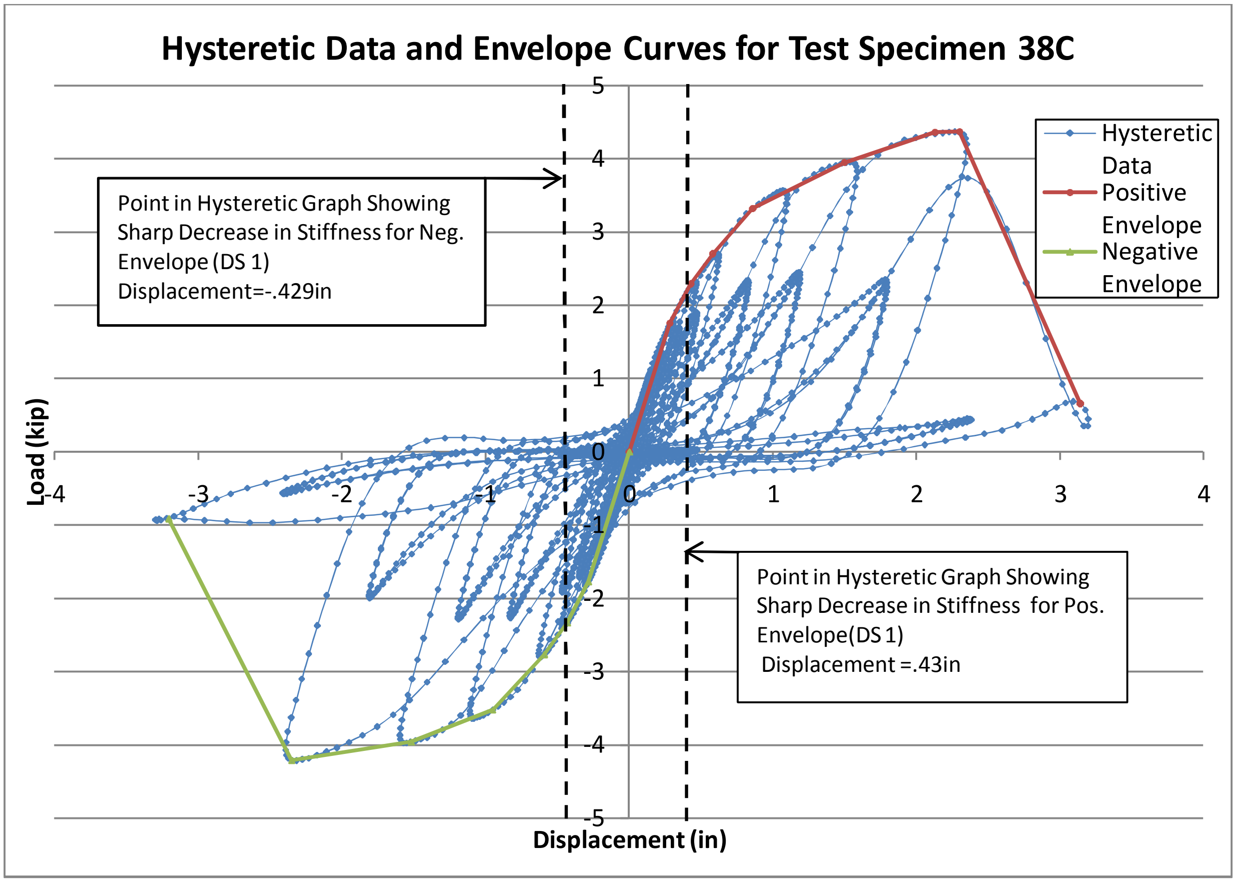


**Figure 3- Example of $DS_1$ Displacement Values from Hysteretic Data. Test Data from Rokas and Rogers (2006)**

A method similar to that defining $DS_1$ was used to define the second damage state ($DS_2$). The ISD at $DS_2$ was taken to be the ISD at which the wall specimens experienced peak load. Following peak load and corresponding ISD (%), the walls exhibited a sharp decrease in capacity prior to failure. At the point of peak load, wall specimens exhibited one or more of the following failure modes:

1) Permanent rotation of sheathing
2) Screw head pull-through of sheathing
3) Sheathing tear out at panel edges

Therefore, $DS_2$ repairs would entail complete replacement of all structural sheathing panels. In addition to this, the authors recommend inspecting all framing components (tracks and studs) for buckling. In the case of any track or flange yielding or buckling, the damaged framing components would need to be replaced in addition to the sheathing. Shown in Figure 4 is an example of $DS_2$ determination based on review of cyclic test data.

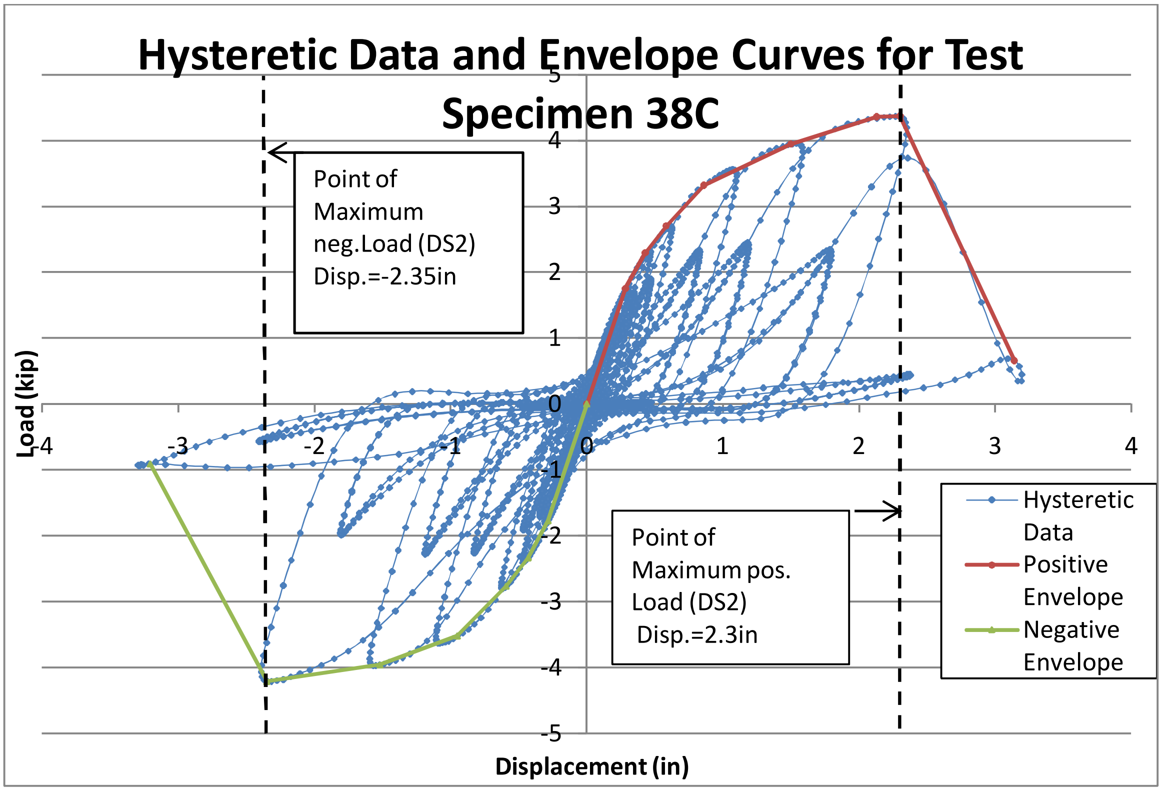


**Figure 4- Example of $DS_2$ Displacement Values from Hysteretic Data. Test Data from Rokas and Rogers (2006)**

In the case of $DS_3$, it is required that the wall be torn down and rebuilt. $DS_3$ was determined by the authors to correspond to the ISD at which the wall specimen experienced 80% of post peak loading. The definition of failure is defined at the point when the wall reaches a displacement with a load equal to 80% of the peak load for the wall. This definition has been used for several years in ASTM 2126 and other assembly test standards as well as research projects such as the CUREE-Caltech Woodframe project. When a wall specimen reached the ISD corresponding to the pre-determined failure load of 80% post peak load, the specimen exhibited physical deformations associated with $DS_2$ in addition to one or more of the following failure modes:

1) Wood bearing failure at panel to fastener interface

2) Local elastic buckling (dimpling) of studs at fastener penetrations

3) Global buckling of studs or tracks

4) Shear failure of fasteners

5) Withdrawal of fasteners from studs

The analysis procedure for $DS_3$ was similar to the procedures followed to obtain ISD (%)'s for $DS_1$ and $DS_2$. Both monotonic and cyclic test data was analyzed to determine 80% post peak load displacement values. Multiple specimens were encountered which, when subjected to cyclic loading, did not fail due to limitations of the test equipment. These specimens were omitted from the data set used to develop the $DS_3$ fragility curve. Additionally, some specimens failed at loads corresponding to displacements much lower than the mean 80% post-peak displacement value. The most common factor effecting premature failure is improper construction methods or pre-existing damage to construction components. Therefore, these specimens were omitted from the data set using Pierce's Criterion.

$DS_3$ ISD values for walls tested under cyclic loading protocol were obtained using the same method as shown for $DS_2$ and $DS_3$. Shown below in Figure 5 is an example of one $DS_3$ ISD value obtained from monotonic test data. The three damage states considered for all walls with structural panels are listed in Table 1 and illustrated in Figures 6, 7 and 8.

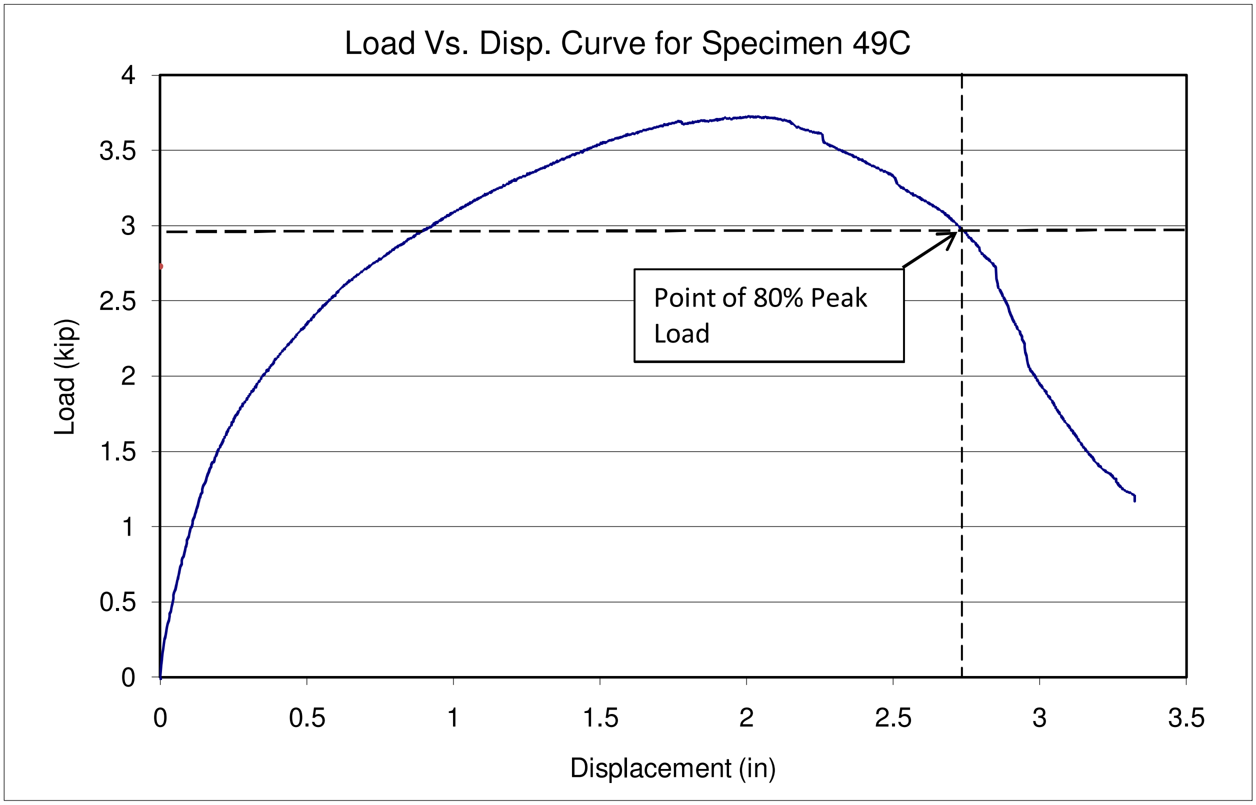


**Figure 5- Example of $DS_3$ obtained from Monotonic Test Data. Test data from Hikita (2006).**

**Table 1- Description of Damage States for all Walls with WSP Sheathing.**

| Damage States ($DS_i$) | Description of Damage State |
|---|---|
| $DS_1$ | Fastener Pull through-Refasten structural panels |
| $DS_2$ | Failure of structural panels-replace panels and inspect studs and tracks |
| $DS_3$ | Failure of wall-Replace wall |

(a) (b)

**Figure 6a and 6b – Screw Head Pull-Through of Sheathing ($DS_1$) (a) from Salenikovich and Dolan (1999), (b) from Rokas (2006)**

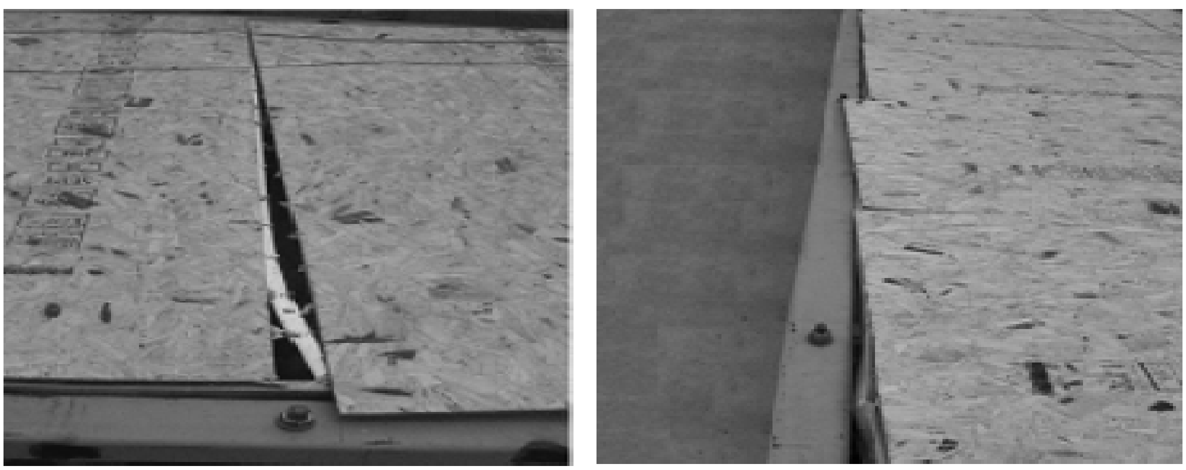

(a) (b)

**Figure 7a and 7b – Permanent Rotation of Sheathing with Fastener Pull-Through ($DS_2$) (Salenikovich and Dolan, 1999)**

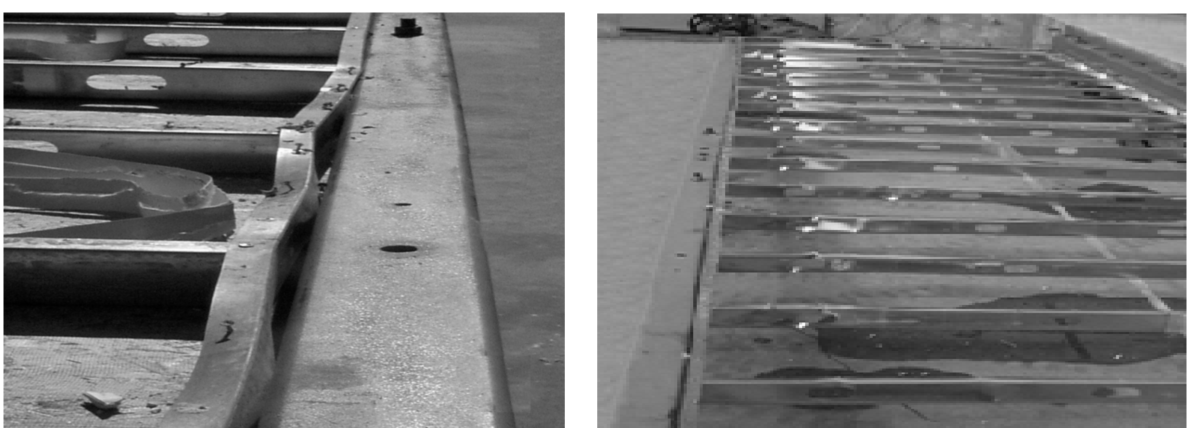

(a) (b)

**Figure 8a and 8b – $DS_3$: Buckling of Wall Track (a) and Buckling of Wall Studs (b) (Salenikovich and Dolan,1999)**

### 3.2.2 Development of Fragility Curves

The fragility curves constructed for all walls with structural panels are shown in Figure 9. The values for fragility parameters θ and β (mean and dispersion respectively) are given in Table 2.

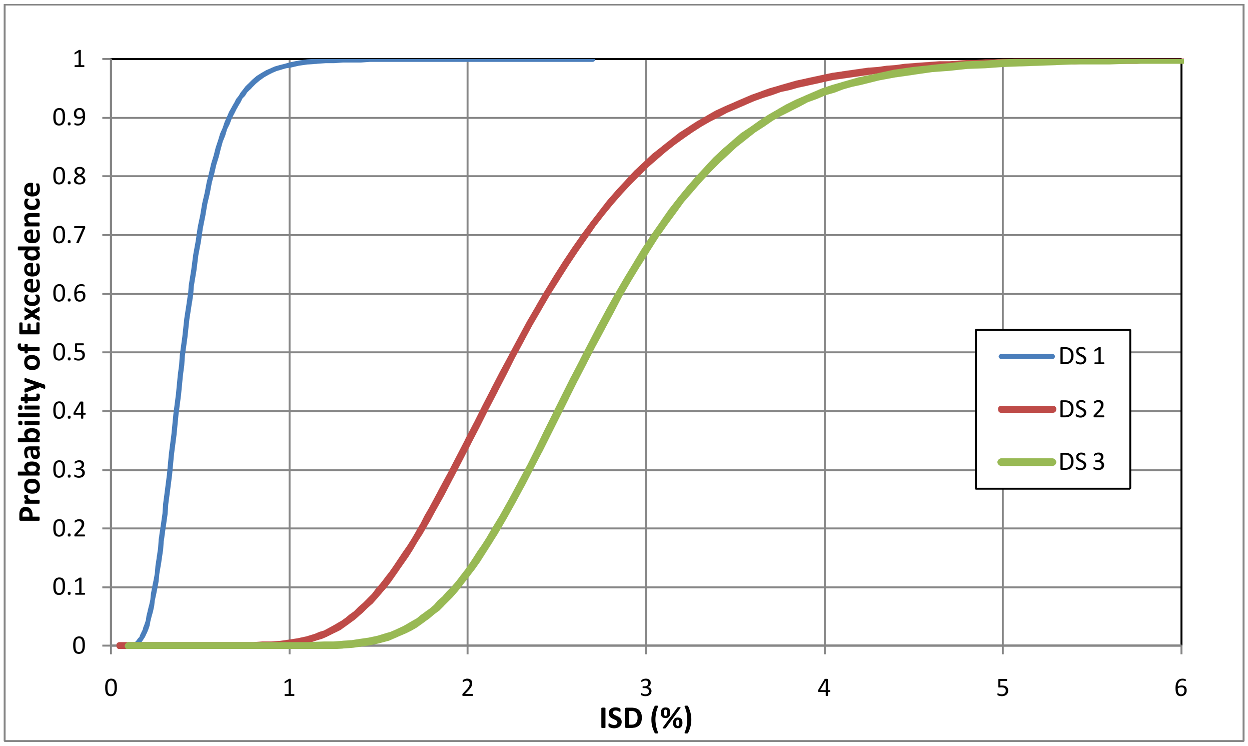


**Figure 9 – Fragility Curves for all Walls with WSP Sheathing**

**Table 2 – Median and Dispersion Values for all Walls with WSP Sheathing**

| Damage States | Demand Parameter (DP) | Median (θ) | Dispersion (β) |
|---|---|---|---|
| **$DS_1$** | **Inter-Story Drift ISD (%)** | 0.40 | 0.39 |
| **$DS_2$** | | 2.26 | 0.31 |
| **$DS_3$** | | 2.67 | 0.25 |

## 3.3 Fragilities of Shear Walls with WSP Sheathing and 6"/12" Fastener Spacing

All available test data for walls with 6"/12" fastener patterns (6" o.c. fastener spacing on the perimeter of each sheathing panel and 12" o.c. on the interior of the panel) was also used to generate fragility curves in Section 2. However, this section provides fragility curves pertaining to data solely from the testing of walls with 6"/12" fastener spacing. These fragility curves are to be used when the fastener spacing of a wall for which damage is to be assessed is known to be 6" on panel edges with 12" in the field. The methods used to determine ISD values corresponding with damage states are the same as those used in Section 3.2.1 of this report. The reader may examine Figures 3, 4 and 5 for examples of determining damage states from test data. The damage states defined in this section are also the same as those defined in Section 3.2.1, therefore pictures of damage states are omitted here for brevity. Specifications for the wall specimens tested are as follows:

- Walls 8ft in height by either 2ft, 4ft or 8ft in length
- 1-1/2"x3-1/2" A446 33ksi steel top and bottom tracks with 33 mil thickness
- 1-1/2"x3-1/2" A446 33ksi steel studs spaced at 24" o.c.
- No. 8-1" sharp point flat head screws for panel to framing connection for '96 and '97 wall specimens.
- No. 8-1.5" self piercing bugle head screws for panel to framing connection for all other wall specimens.
- Wood structural panel sheathing attached with long dimension parallel to studs
- Spacing of sheathing to framing fasteners at 6" on panel edges with 12" in field
- Seismic hold-downs at wall ends

### 3.3.1 Definition of Damage States

For detailed description of damage states refer to Section 3.2.1 with specific damage state definitions listed in Table 1. The descriptions of damage states for all walls with WSP Sheathing are listed in Table 3.

**Table 3 - Description of Damage States for all Walls with WSP Sheathing.**

| **Damage States ($DS_i$)** | **Description of Damage State** |
|---|---|
| $DS_1$ | Fastener Pull through-Refasten structural panels |
| $DS_2$ | Failure of structural panels-replace panels and inspect studs and tracks |
| $DS_3$ | Failure of wall-Replace wall |

### 3.3.2 Development of Fragility Curves

Displayed in Figure 10 are the fragility curves for walls with Wood structural panel sheathing and 6"/12" fastener spacing. The fragility parameters for walls with sheathing attached using 6"/12" fastener spacing are provided in Table 4.

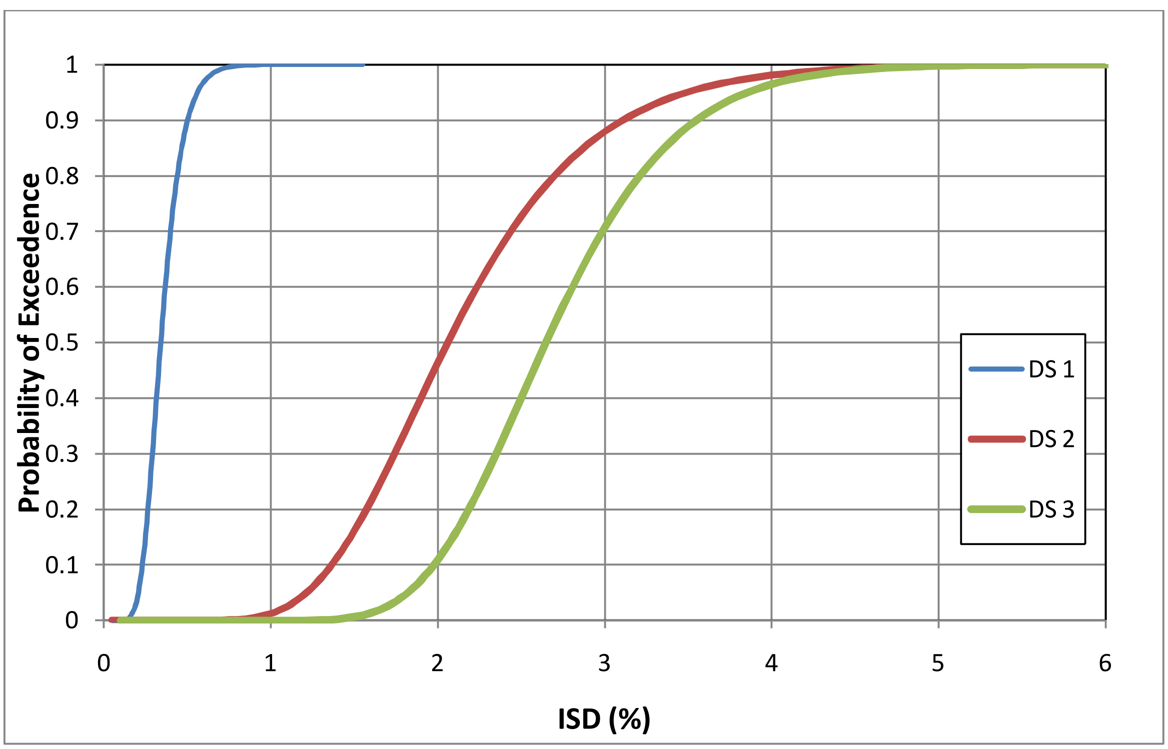


**Figure 10 - Fragility curves for Walls with WSP Sheathing and 6"/12" Fastener Spacing**

**Table 4 - Medians and Dispersions for Walls with WSP Sheathing and 6"/12" Fastener Spacing**

| Damage States | Demand Parameter (DP) | Median (θ) | Dispersion (β) |
|---|---|---|---|
| **$DS_1$** | **Inter-Story Drift ISD (%)** | **0.34** | **0.30** |
| **$DS_2$** | | **2.06** | **0.32** |
| **$DS_3$** | | **2.65** | **0.23** |

## 3.4 Fragilities of Shear Walls with WSP Sheathing and 4"/12" Fastener Spacing

This section includes the development of fragility curves from all monotonic and cyclic test specimens with wood structural panel sheathing and 4"/12" fastener spacing (4" o.c. fastener spacing on the perimeter of each sheathing panel and 12" o.c. on the interior of the panel). Methods used to determine ISD values corresponding with damage states are illustrated in Section 3.2.1. Specifications for the wall specimens tested are as follows:

- Walls 8ft in height by either 2ft, 4ft or 8ft in length
- 1-1/2"x3-1/2" A446 33ksi steel top and bottom tracks with 33 mil thickness
- 1-1/2"x3-1/2" A446 33ksi steel studs spaced at 24" o.c.
- No. 8-18x1in sharp point flat head screws for panel to framing connection for wall specimens from the '96 and '97 reports.
- No. 8-1.5" self piercing bugle head screws for panel to framing connection for all other wall specimens.
- Wood structural panel sheathing attached with long dimension parallel to studs
- Spacing of sheathing to framing fasteners at 4" spacing on panel edges with 12" in field
- Seismic hold-downs at wall ends

### 3.4.1 Definition of Damage States

Damage states defined for walls with wood panel structural sheathing and 4"/12" fastener spacing are identical to those defined in Section 3.2.1 and are listed in Table 5. Refer to Figures 6, 7 and 8 for photographs of damage states.

**Table 5 - Damage States for all Walls with WSP Sheathing and 4"/12" Fastener Spacing**

| Damage States ($DS_i$) | Description of Damage State |
|---|---|
| $DS_1$ | Fastener Pull through-Refasten structural panels |
| $DS_2$ | Failure of structural panels-replace panels and inspect studs and tracks |
| $DS_3$ | Failure of wall-Replace wall |

### 3.4.2 Development of Fragility Curves

Construction of the fragility curves for CFS walls with wood structural panel sheathing and 4"/12" fastener spacing was based cyclic and monotonic test data from experiments conducted by Chen (2004), Serette (1997), Nguyen, Hall and Serette (1996), Boudreault (2005), Branston, Boudreault and Chen (2004), Blais (2006), Hikita (2006), Rokas (2006) and Branston (2004). Fragility curves for walls with 4"/12" fastener spacing are shown in Figure 11. The median and dispersion values for these fragility curves are shown in Table 6.

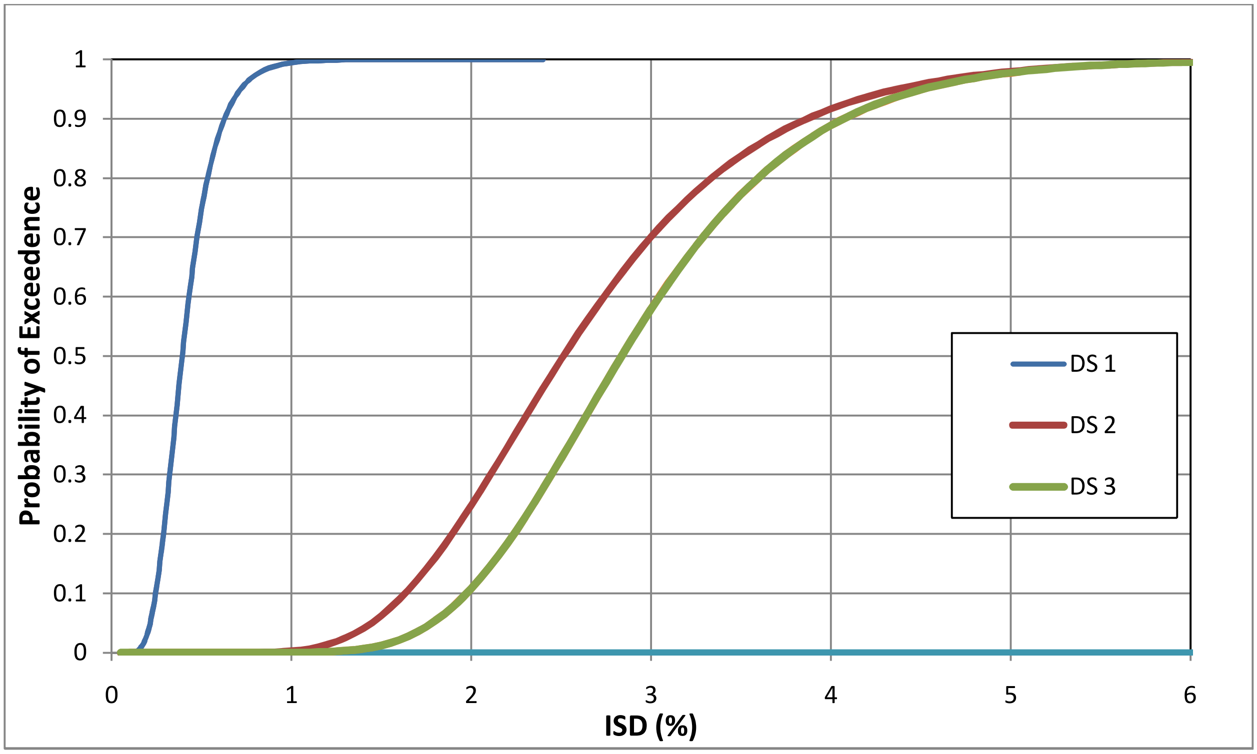


**Figure 11 - Fragility Curves for Walls with WSP Sheathing and 4”/12” Fastener Spacing.**

**Table 6 - Medians and Dispersions for Walls with WSP Sheathing and 4”/12” Fastener Spacing**

| **Damage States** | **Demand Parameter (DP)** | **Median (θ)** | **Dispersion (β)** |
|---|---|---|---|
| **$DS_1$** | **Inter-Story Drift ISD (%)** | 0.39 | 0.37 |
| **$DS_2$** | | 2.51 | .33 |
| **$DS_3$** | | 2.84 | 0.28 |

## 3.5 Fragilities of Shear Walls with WSP Sheathing and 3”/12” Fastener Spacing

This section includes the development of fragility curves from all monotonic and cyclic test specimens with structural sheathing and 3”/12” fastener spacing (3” o.c. fastener spacing on the perimeter of each sheathing panel and 12” o.c. on the interior of the panel). Methods used to determine ISD values corresponding with damage states are illustrated in Section 3.2.1. Specifications for the wall specimens tested are as follows:

- Walls 8ft in height by either 2ft, 4ft or 8ft in length
- 1-1/2"x3-1/2" A446 33ksi steel top and bottom tracks with 33 mil thickness
- 1-1/2"x3-1/2" A446 33ksi steel studs spaced at 24" o.c.
- No. 8-1" sharp point flat head screws for panel to framing connection for '96 and '97 wall specimens.
- No. 8-1.5" self piercing bugle head screws for panel to framing connection for all other wall specimens.
- Wood structural panel sheathing attached with long dimension of panel parallel to studs
- Spacing of sheathing to framing fasteners at 3" spacing on panel edges with 12" spacing in field
- Seismic hold-downs at wall ends

### 3.5.1 Definition of Damage States

Damage states defined for walls with structural sheathing and 3"/12" fastener spacing are identical to those defined in Section 2. Refer to Figures 6, 7 and 8 for photographs of damage states. The damage states for CFS walls with wood structural panel sheathing attached with 3"/12" fastener spacing are provided in Table 7.

**Table 7 - Damage States for all Walls with WSP Sheathing and 3"/12" Fastener Spacing**

| Damage States ($DS_i$) | Description of Damage State |
|---|---|
| $DS_1$ | Fastener Pull through-Refasten structural panels |
| $DS_2$ | Failure of structural panels-replace panels and inspect studs and tracks |
| $DS_3$ | Failure of wall-Replace wall |

### 3.5.2 Development of Fragility Curves

Construction of the fragility curves for CFS walls with wood structural panel sheathing and 3"/12" fastener spacing  was based cyclic and monotonic test data from experiments conducted by Chen (2004), Serette (1997), Nguyen, Hall and Serette (1996), Boudreault (2005), Branston, Boudreault and Chen (2004), Blais (2006), Hikita (2006), Rokas (2006) and Branston (2004).  Fragility curves for walls with 3"/12" fastener spacing are shown in Figure 12.  Median and dispersion values for these fragility curves are shown in Table 8.

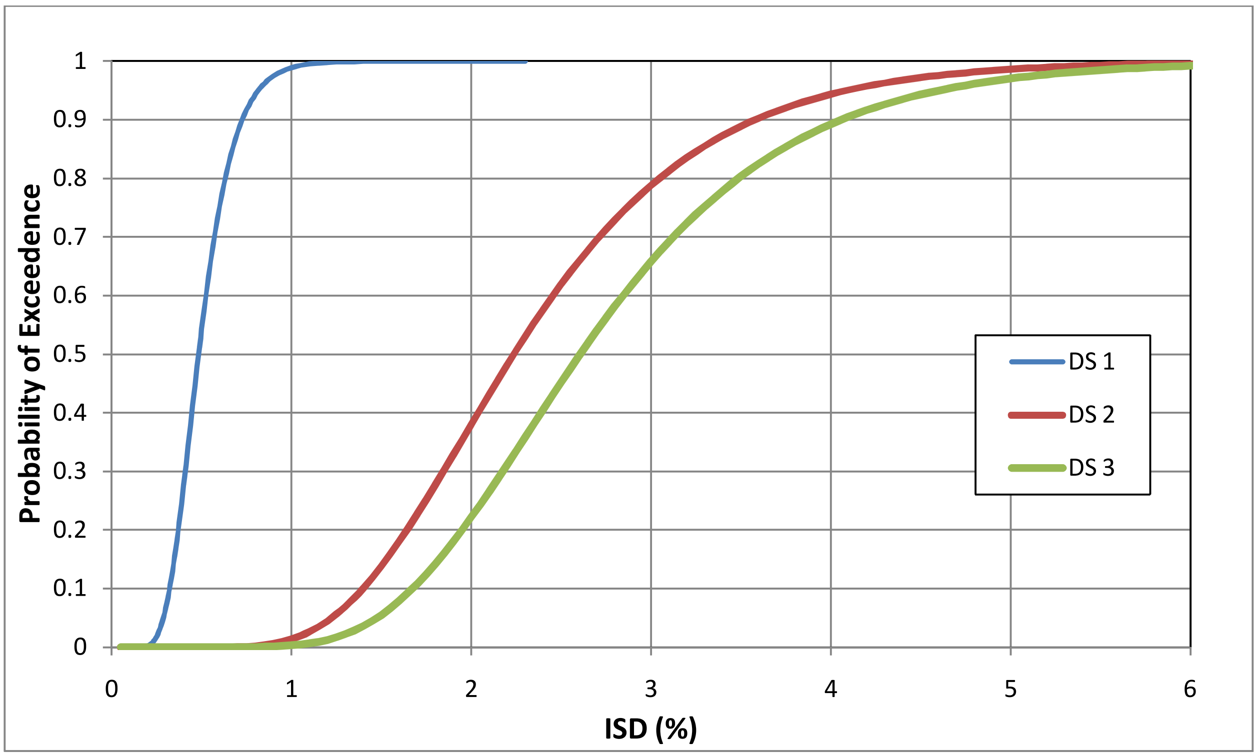


**Figure 12 - Fragility Curves for Walls with WSP Sheathing and 3"/12" Fastener Spacing**

**Table 8 - Medians and Dispersions for Walls with WSP Sheathing and 3"/12" Fastener Spacing**

| Damage States | Demand Parameter (DP) | Median (θ) | Dispersion (β) |
|---|---|---|---|
| **$DS_1$** | | 0.48 | 0.32 |
| **$DS_2$** | **Inter-Story Drift ISD (%)** | 2.23 | 0.36 |
| **$DS_3$** | | 2.6 | 0.34 |

## 3.6 Fragilities of Shear Walls with WSP Sheathing and 2"/12" Fastener Spacing

This section includes the development of fragility curves from all monotonic and cyclic test specimens with structural sheathing and 2"/12" fastener spacing (2" o.c. fastener spacing on the perimeter of each sheathing panel and 12" o.c. on the interior of the panel). Methods used to determine ISD values corresponding with damage states are illustrated in Section 3. Specifications for the wall specimens tested are as follows:

- Walls 8ft in height by either 2ft, 4ft or 8ft in length
- 1-1/2"x3-1/2" A446 33ksi steel top and bottom tracks with 33 mil thickness
- 1-1/2"x3-1/2" A446 33ksi steel studs spaced at 24" o.c.
- No. 8-1" sharp point flat head screws for panel to framing connection for wall specimens from the '96 and '97 reports.
- No. 8-1.5" self piercing bugle head screws for panel to framing connection for all other wall specimens.
- Wood structural panel sheathing attached with long dimension parallel to studs
- Spacing of sheathing to framing fasteners at 2" spacing on panel edges with 12" in field
- Seismic hold-downs at wall ends

### 3.6.1 Definition of Damage States

Damage states defined for walls with wood structural panel sheathing and 2"/12" fastener spacing are identical to $DS_1$ and $DS_3$ defined in Section 2. These damage states are defined here as $DS_1$ and $DS_2$. Walls with fastener spacing at 2"/12" were able to sustain higher loads yet typically failed quickly after reaching peak load. Therefore it was the judgment of the authors to report only two damage states for walls with 2"/12" fastener spacing. Refer to Figures 7 and 8 for photographs of damage states. Damage states for walls with 2"/12" fastener spacing are listed in Table 9

**Table 9 - Damage States for all Walls with WSP Sheathing and 2"/12" Fastener Spacing**

| Damage States ($DS_i$) | Description of Damage State |
|---|---|
| $DS_1$ | Fastener Pull through-Refasten structural panels |
| $DS_2$ | Failure of wall-Replace wall |

### 3.6.2 Development of Fragility Curves

Construction of the fragility curves for CFS walls with wood structural panel sheathing and 2"/12" fastener spacing was based cyclic test data from experiments conducted by Serette (1996 and 1997). Fragility curves for walls with 2"/12" fastener spacing are shown in Figure 13. Median and dispersion values for these fragility curves are shown in Table 10.

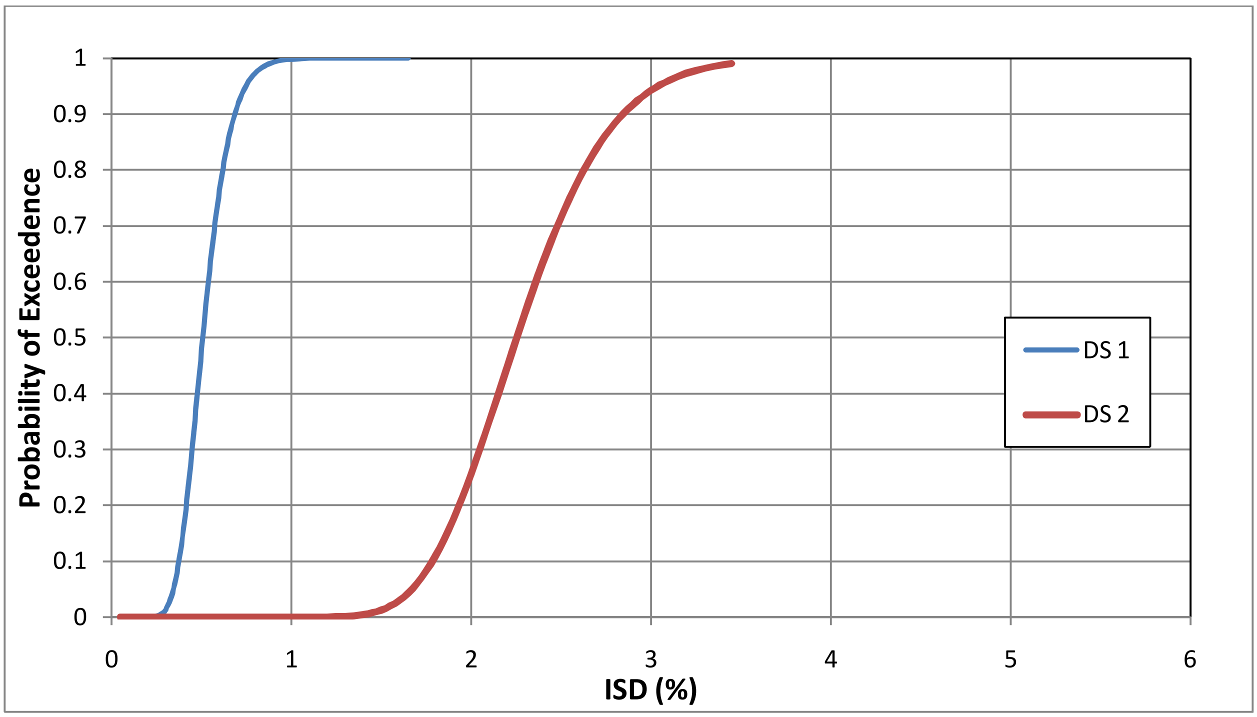


**Figure 13 - Fragility Curves for Walls with WSP Sheathing and 2"/12" Fastener Spacing**

**Table 10 - Medians and Dispersions for Walls with WSP Sheathing and 2"/12" Fastener Spacing**

| **Damage States** | **Demand Parameter (DP)** | **Median (θ)** | **Dispersion (β)** |
|---|---|---|---|
| **$DS_1$** | **Inter-Story Drift ISD (%)** | 0.51 | 0.24 |
| **$DS_2$** | | 2.25 | 0.18 |

### 3.7 Fragilities of Shear Walls with Flat Strap X-Bracing

This section addresses the development of fragility curves for shear walls with flat-strap diagonal bracing (X-bracing). There has been very little testing performed on shear walls with X-bracing. Although test data was limited for the development of fragility curves for walls with X-bracing due to the infrequency of this construction method being utilized in high wind or seismic zones, the authors believe the generation of these fragility curves to be important considering that X-bracing as a means of lateral reinforcement is deemed acceptable by AISI Section E8 (AISI 2001). Specifications for the wall specimens tested are as follows:

- Walls 8ft in height by 4ft in length
- 1-1/2"x3-1/2" A446 33ksi steel top and bottom tracks with 33 mil thickness
- 1-1/2"x3-1/2" A446 33ksi steel studs spaced at 24" o.c.
- 4-1/2" 8 mil or 23 mil flat strap X-bracing one side
- No 8-1/2in self drilling modified truss head screw (20 screws used to attach strap to gusset plate)
- Seismic tie-downs at wall ends

#### 3.7.1 Definition of Damage States

The damage states defined in this section are different than those defined in previous sections. Data was obtained for cyclic tests performed on walls with X-bracing (Serrette, 1997). Although no data from monotonic testing of X-brace walls was analyzed for development of these fragility curves, for assemblies with 4-1/2" X-bracing, failure of the specimens was identical to that observed during monotonic loading tests (Serrette, 1997). Based on the results from tests performed by Serrette, engineers must be cautious when designing with X-bracing in high wind and seismic zones since, when under high loads, straps attached on only one side of the shear wall result in eccentricity which can put both the chord stud and track in strong axis bending. The combination of these behaviors 'pulls' the track out of plane resulting in failure of the wall before the strap capacity is reached (Serrette, 1997). Therefore it is suggested that when designing walls with X-bracing on one side, designers should design the chord studs and tracks for 150% of the X-brace yield strength (Serrette, 1997). With these findings in mind, the authors have defined two damage states for walls with flat strap X-bracing. Since few observations were recorded throughout the loading phase, confident assertions regarding ISD values at which $DS_1$ and $DS_2$ occurred can only be made for values at peak load and wall failure respectively. Analysis of data to determine $DS_1$ and $DS_2$ was performed using the same methods highlighted in Section 3 of this document (see Figures 4 and 5). $DS_1$ is defined at the point of peak load. At this damage state, local buckling of the chord stud occurred. Buckling of the chord stud will result in removal of any cladding components (siding, GWB, etc.) and replacement of the buckled stud. $DS_2$ occurs at 80% of post peak loading. At this point, the wall has failed, either due to eccentricities resulting in strong axis bending of studs and tracks or due to yielding of the X-bracing. If $DS_2$ is reached, complete reconstruction of the wall is required. Damage states $DS_1$ and $DS_2$ are depicted in Figures 14 and 15 respectively.

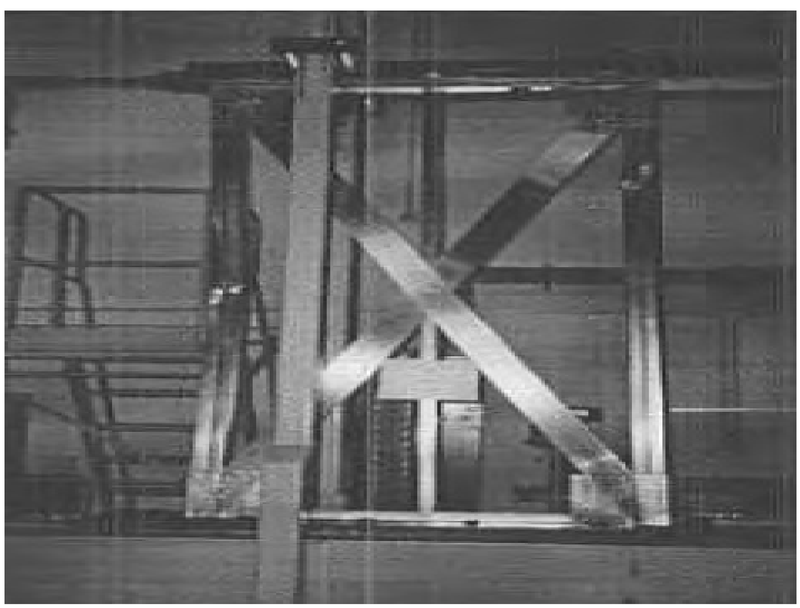

**Figure 14 - Buckling of chord stud ($DS_1$)**

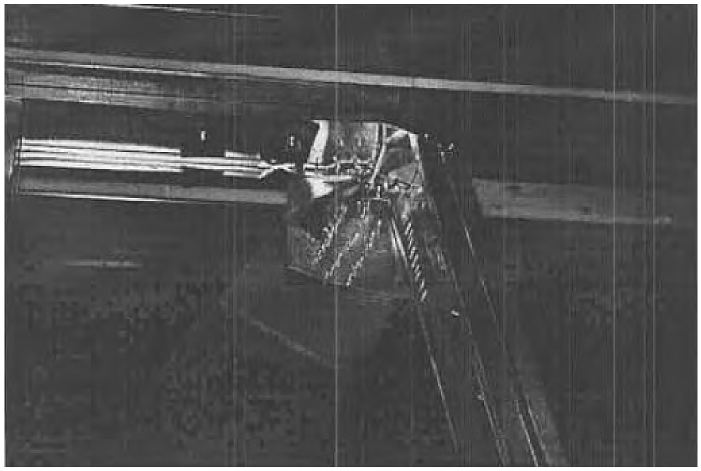

**Figure 15 - Bending yielding of track, X-bracing and Gusset ($DS_2$)**

### 3.7.2 Development of Fragility Curves

Construction of the fragility curves for shear walls with flat strap X-bracing was based on cyclic test data (Serrette, 1997). Only data pertaining to walls with 4-1/2" wide X-bracing was available to construct these fragility curves. Therefore, the authors advise that these fragility curves be used only when assessing damage to walls with 4-1/2" X-bracing since different failure modes were reported to exist with different strap specifications. Figure 16 displays $DS_1$ and $DS_2$ for walls with 4-1/2" flat strap X-bracing. Median and dispersion values for these fragility curves are shown in Table 11.

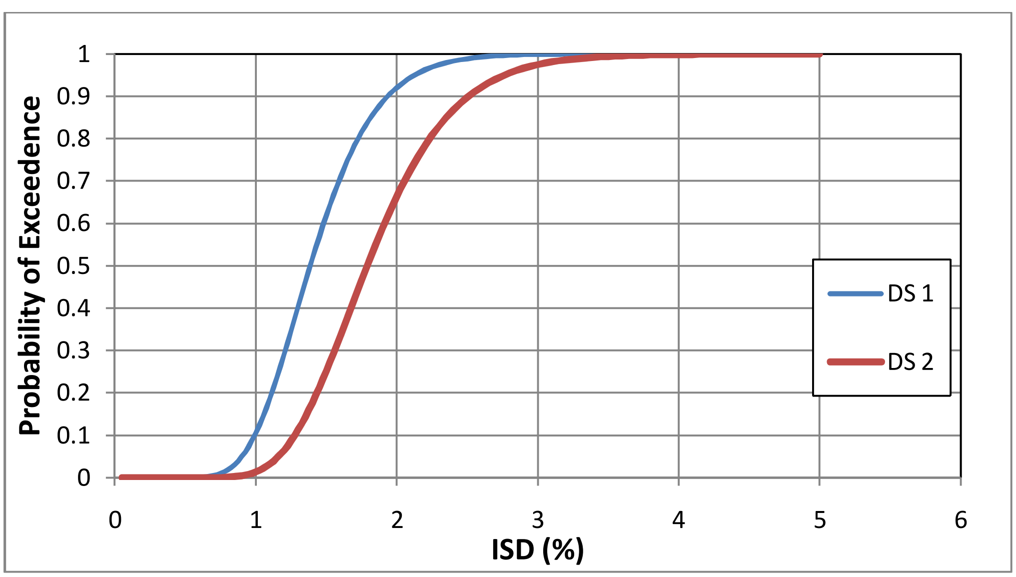


**Figure 16 - Fragilities of Walls with 4-1/2" Flat Strap X-Bracing.**

**Table 11 - Median and Dispersion Values for Walls with 4-1/2" Flat Strap X-Bracing**

| Damage States ($DS_i$) | Demand Parameter (DP) | Median (θ) | Dispersion (β) |
|---|---|---|---|
| $DS_1$ | Inter-Story Drift ISD (%) | 1.39 | .26 |
| $DS_2$ | | 1.79 | .26 |

### 3.8 Fragilities of Shear Walls with 8 mil or 23 mil Steel Sheathing

Construction of fragility curves for CFS walls with 8 mil or 23 mil steel sheathing was based on cyclic test data (Serrette, 1997). As reported by Serrette (1997) all walls with steel sheathing as the main lateral force resisting system performed quite well when subjected to cyclic loading. Serrette reported that using thicker gauge steel sheathing provides higher design capacities, yet the failure mode moves from rupture at the edge of the steel sheathing to sheathing screw pullout from wall studs (Serrette, 1997). Aspect ratios (height/width) of walls used to develop the fragility curves in this section ranged from 2:1 to a high aspect ratio of 4:1 (2ftx8ft wall) which is the maximum allowable aspect ratio shear walls (AISI 2001).

Specifications for the wall specimens tested are as follows:

- Walls 8ft in height by 2ft or 4ft length
- 1-1/2"x3-1/2" A446 33ksi steel top and bottom tracks with 33 mil thickness
- 1-1/2"x3-1/2" A446 33ksi steel studs spaced at 24" o.c.
- 8 mil or 23 mil steel sheathing
- No. 8-18x1/2in self-drilling modified truss head screws used to attach sheathing to studs
- Fastener pattern used to attach steel sheathing to studs ranged from 6"/12" to 2"/12"
- Seismic tie-downs at wall ends

### 3.8.1 Definition of Damage States

For walls with 8 mil or 23 mil steel sheathing, two damage states were defined. The first was determined based on the individual ISD drift of walls at peak load capacity. At this ISD, walls exhibited either pull out of the fastener from framing members or block shear rupture of the steel sheathing at panel edges. As was previously discussed, pull out of fasteners from framing members is more likely to be the governing failure mode with walls sheathed with thicker steel sheathing (48mil.). Additionally, it was reported by Serrette (1997) that walls with high aspect ratios (4:1) are capable of resisting high loads at fairly low displacements. However, after the seismic event, the wall will have zero initial stiffness and will therefore not resist further loading until brought back to the displacement at which the initial peak load occurred. This being said, the authors recommend complete replacement of steel sheathing at $DS_1$ in addition to the inspection of all framing members for rupture, global and local buckling. $DS_2$ occurs when the wall has sustained ISD corresponding to the point of 80% post peak loading. At this ISD the wall has failed and would need to be torn down and replaced as buckling of studs and tracks will most likely have occurred. Damage states $DS_1$ and $DS_2$ are depicted by Figures 17 and 18 respectively.

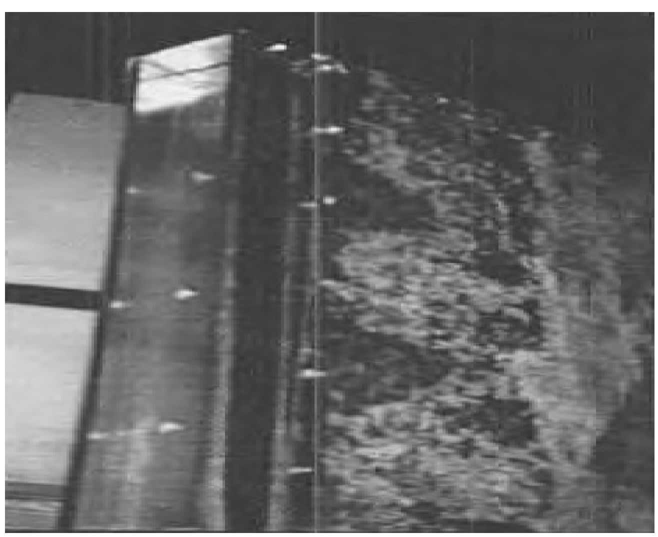

**Figure 17 – Pull Through of Fasteners from Studs ($DS_1$) (Serrette et al. 1997)**

**Figure 18 – Failed Wall Specimen ($DS_2$) (Serrette et al. 1997)**

### 3.8.2 Development of Fragility Curves

The fragility curves shown in Figure 19 are for shear walls with 8 mil or 23 mil steel sheathing. The close proximity of curve $DS_1$ to $DS_2$ accurately reflects the abrupt decrease in stiffness that was present in wall specimens after $DS_1$ initiated. This is due to the fact that once fasteners began to pull out of the wall studs or block shear rupture at panel edges began, an "unzipping" effect occurred where either of the two aforementioned failures moved from one fastener to the next causing relatively abrupt failure of the wall. Median and dispersion values for walls with steel sheathing are presented in Table 12.

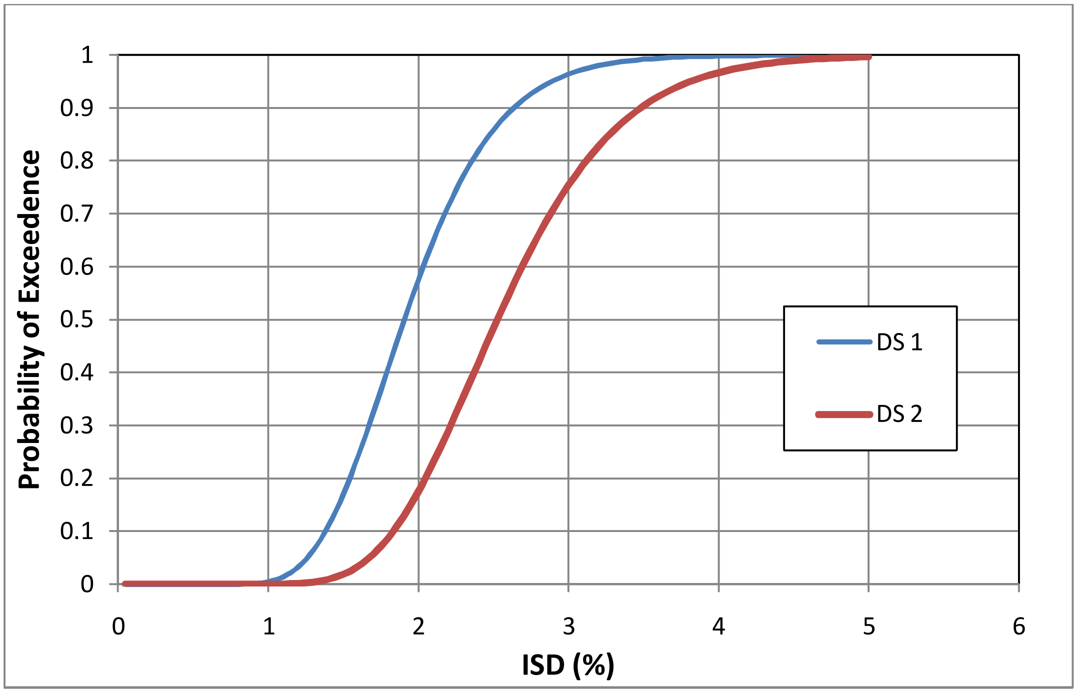


**Figure 19 – Fragilities for Shear Walls with 8 mil or 23 mil Steel Sheathing**

**Table 12 – Median and Dispersion Values for Walls with 8 mil or 23 mil Steel Sheathing**

| Damage States ($DS_i$) | Demand Parameter (DP) | Median (θ) | Dispersion (β) |
|---|---|---|---|
| $DS_1$ | Inter-Story Drift ISD (%) | 1.90 | .25 |
| $DS_2$ | | 2.53 | .25 |

## 3.9 Summary of Fragility Curves for CFS Light-Frame Shear Walls

Included in Table 13 is a summary of the demand parameters, medians and dispersions for the various CFS structural systems analyzed in this document. Also included in Table 13 is the ATC method used to calculate the fragility parameters θ and β. Descriptions of these methods are presented in Section 1.2.

**Table 13 – Summary of Demand Parameters and Fragility Parameters**

| System Type | Demand Parameter | Median (θ) | | | Dispersion (β) | | | Method Used* |
|---|---|---|---|---|---|---|---|---|
| | | $DS_1$ | $DS_2$ | $DS_3$ | $DS_1$ | $DS_2$ | $DS_3$ | |
| CFS sys#1-all walls | ISD (%) | 0.40 | 2.26 | 2.67 | 0.39 | 0.31 | 0.25 | A, E |
| CFS sys#1-6”/12” | | 0.34 | 2.06 | 2.65 | 0.30 | 0.32 | 0.23 | A, E |
| CFS sys#1-4”/12” | | 0.39 | 2.51 | 2.84 | 0.37 | 0.34 | 0.28 | A, E |
| CFS sys#1-3”/12” | | 0.48 | 2.23 | 2.60 | 0.32 | 0.36 | 0.34 | A, E |
| CFS sys#1-2”/12” | | 0.51 | 2.25 | N/A | 0.24 | 0.18 | N/A | A, E |
| CFS sys#2-steel sheathing | | 1.39 | 1.79 | N/A | 0.26 | 0.26 | N/A | A, E |
| CFS sys#3-X-bracing | | 1.90 | 2.53 | N/A | 0.25 | 0.25 | N/A | A, E |

*A-Parameters Derived from Actual Test Data (method A), E-Expert Judgment (method E)

### 3.9.1 Interaction Between Damage States

When assessing post earthquake damage to buildings, certain situations may arise in which a shear wall may consist of structural elements from numerous wall systems analyzed in this document. For example, a designer may specify that a wall be constructed using wood structural panel sheathing on the exterior of the wall and X-bracing on the wall interior or specify that some segments of a wall line are sheathed with gypsum wallboard while others are sheathed with wood structural panels. For situations such as these, interactions between various damage states for separate wall systems must be addressed. In this section, two states of interactions are defined.

The first interaction state between damage state conditions is defined as an Ordered Damage State. This means that for a shear wall, one damage state must transpire before another damage state is initiated. An example of this would be that for CFS System #1 (walls with wood structural panel sheathing), $DS_1$ must occur before $DS_2$ and $DS_2$ must occur before $DS_3$. That is a CFS System #1 wall will show damage to sheathing ($DS_1$) before reaching its peak load capacity and damage at peak load capacity ($DS_2$) will initiate before total failure of the wall ($DS_3$). Ordered damage states are abbreviated as $OS_{ij}$ with Subscripts i and j denoting which damage state must occur before the second damage state initiates.

The second interaction between damage state conditions is defined as Simultaneous Damage States (S). As the definition implies, this interaction means that two damage states can occur simultaneously. One example of this would be the wall consisting of both WSP's and X-bracing. After a seismic event, wood structural panel sheathing may have to be replaced ($DS_2$ for CFS System #1) while a buckled chord stud may also have to be replaced ($DS_2$ for CFS System #3). In such cases, the fragility curves developed for both wall systems may be used independently of one another.

Although no test data used to construct fragility curves for this document was available for CFS walls with gypsum wallboard, the reader is referred to "Fragility Curves for Wood Light-Frame Structural Systems" (Ekiert and Filiatrault 2008) for fragility data pertaining to damage states of walls constructed using gypsum wallboard. Since it has been shown that CFS shear walls distort in patterns similar to those of wood-frame shear walls for given ISD values, the damage to gypsum wallboard will be similar regardless of the framing system it is attached to. Therefore, gypsum wallboard damage states are included in the following table of damage state interactions (Table 14). CFS System #1 (walls with structural panel sheathing) is not subdivided into walls with wood structural panel sheathing and separate fastener schedules as they were to develop the original fragility curves. This is due to the fact that all damage state interactions remain similar for CFS System #1 walls regardless of the fastener spacing.

**Table 14 – Interactions of Damage States for CFS Wall Systems**

| | | Gypsum Wallboard | | CFS System #1 | | | CFS System #2 | | | CFS System #3 | |
|---|---|---|---|---|---|---|---|---|---|---|---|
| | | $DS_1$ | $DS_2$ | $DS_1$ | $DS_2$ | $DS_3$ | $DS_1$ | $DS_2$ | $DS_3$ | $DS_1$ | $DS_2$ |
| Gypsum Wallboard | $DS_1$ | | $OS_{12}$ | S | S | S | S | S | S | S | S |
| | $DS_2$ | | | S | S | S | S | S | S | S | S |
| CFS System #1 | $DS_1$ | | | | $OS_{12}$ | $OS_{13}$ | S | S | S | S | S |
| | $DS_2$ | | | | | $OS_{23}$ | S | S | S | S | S |
| | $DS_3$ | | | | | | S | S | S | S | S |
| CFS System #2 | $DS_1$ | | | | | | | $OS_{12}$ | $OS_{13}$ | S | S |
| | $DS_2$ | | | | | | | | $OS_{23}$ | S | S |
| | $DS_3$ | | | | | | | | | S | S |
| CFS System #3 | $DS_1$ | | | | | | | | | | S |
| | $DS_2$ | | | | | | | | | | |

**S-Damage States may Occur Simultaneously, $OS_{ij}$-($DS_i$ occurs before $DS_j$)**

### 3.9.2 Consequences of Damage States

This section of the document provides a table of consequences stemming from the various damage states reported throughout the document. The consequences of various damage states are categorized as follows:

C1-Damage state involves significant repair cost

C2-Damage state may cause injury or death

C3-Damage state threatens post-earthquake operability

C4-Damage state causes red-tagging of building

The authors acknowledge that certain consequences of damage states may differ depending on the configuration of the structure being assessed. For example a CFS wall which experienced $DS_3$ (failure of wall requiring complete replacement of wall) may or may not collapse depending on the magnitude of gravity loads above it. Likewise, a CFS wall which experiences $DS_1$ (fastener pull through requiring refastening of sheathing) may or may not involve significant repair cost depending on the finish cladding atop the structural sheathing and the length of the wall being assessed. Therefore, to err on the side of caution, all potential consequences of various damage states are reported in Table 15.

**Table 15 – Consequences Involving Various Damage States**

| Structural System | Damage State ($DS_i$) | Consequences of Various Damage States | | | |
|---|---|---|---|---|---|
| | | C1 | C2 | C3 | C4 |
| CFS Sys. #1 | $DS_1$ | Possibly | NO | NO | Not Likely |
| | $DS_2$ | YES | NO | YES | YES |
| | $DS_3$ | YES | YES | YES | YES |
| CFS Sys. #2 | $DS_1$ | YES | NO | NO | Possibly |
| | $DS_2$ | YES | NO | YES | YES |
| CFS Sys. #3 | $DS_1$ | YES | NO | YES | YES |
| | $DS_2$ | YES | YES | YES | YES |

# Chapter 4

# Development of Fragility Curves Using PGA as the EDP

## 4.1 Introduction to the Development of Fragility Curves Using PGA as the EDP

To increase the versatility of this document, fragility curves were developed using Peak Ground Acceleration (PGA) as the controlling Engineering Demand Parameter (EDP). To construct fragility curves of this type, experimental data was used in conjunction with various software programs to analyze the effect of earthquake ground acceleration on light-frame shear wall systems which were idealized as Single Degree of Freedom (SDOF) spring elements. The process by which this analysis was performed is outlined in the following paragraphs, and the resultant fragility curves are reported in this section.

Step 1: Scaling of Earthquake Records:

The process for scaling earthquake records is governed by the FEMA P695 document entitled "Quantification of Building Seismic Performance Factors." Within this document are specific methods for scaling existing earthquake data for use in evaluating the seismic performance of various structures. In order to perform the Incremental Dynamic Analysis (IDA) necessary to develop fragility curves of this type, each earthquake acceleration record had to be normalized to correspond with the fundamental period of the structure being analyzed. This process is necessary in order to "remove variability between earthquake acceleration records due to the differences in earthquake magnitude, the distance from the epicenter to the site where the earthquake acceleration was recorded and the site conditions at the location of recording" (FEMA P695). Additionally, it is required that only far-field earthquake records are used for IDA of CFS shear walls for which fragility curves are to be developed. The analysis of a structure based on far-field records sets insures that the structure is not subjected to any earthquake "pulse" as these pulses result in very high magnitude forces imposed on the structure and would therefore skew the results of the analysis. Table 16 lists the 22 record sets for use in performing an IDA. These 22 record sets were chosen based on the following criteria from FEMA P695:

- Source Magnitude-M≥6.5 Large magnitude earthquakes events pose the greatest risk of building collapse. Even though small magnitude events produce strong ground accelerations, the duration of shaking is relatively short. Large magnitude earthquakes, however, can generate strong and long lasting ground accelerations over a large region.
- Source Type-Strike Slip and Reverse Thrust Sources. Not only are few strong-motion record sets available for source mechanisms other than strike-slip or reverse thrust but additionally, these two source mechanisms are typical of shallow crustal earthquakes like those likely to occur in areas such as California.
- Site conditions-Soft Rock and Stiff Soil Sites. Record sets recorded on Class C and Class D sites as defined by ASCE-07, are used due to the fact that few earthquake records are available for Class B and Class A sites and Class E sites are susceptible to ground failure.
- Strongest Ground Motion Records-PGA greater than 0.2g and Peak Ground Velocity (PGV) greater than 15cm/sec. While these limits are arbitrary, they generally represent the threshold of structural damage for new buildings.

Table 16 – List of Far-Field Earthquake Record sets from FEMA P695

| ID No. | Earthquake | | | Recording Station | |
|---|---|---|---|---|---|
| | M | Year | Name | Name | Owner |
| 1 | 6.7 | 1994 | Northridge | Beverly Hills - Mulhol | USC |
| 2 | 6.7 | 1994 | Northridge | Canyon Country-WLC | USC |
| 3 | 7.1 | 1999 | Duzce, Turkey | Bolu | ERD |
| 4 | 7.1 | 1999 | Hector Mine | Hector | SCSN |
| 5 | 6.5 | 1979 | Imperial Valley | Delta | UNAMUCSD |
| 6 | 6.5 | 1979 | Imperial Valley | El Centro Array #11 | USGS |
| 7 | 6.9 | 1995 | Kobe, Japan | Nishi-Akashi | CUE |
| 8 | 6.9 | 1995 | Kobe, Japan | Shin-Osaka | CUE |
| 9 | 7.5 | 1999 | Kocaeli, Turkey | Duzce | ERD |
| 10 | 7.5 | 1999 | Kocaeli, Turkey | Arcelik | KOERI |
| 11 | 7.3 | 1992 | Landers | Yermo Fire Station | CDMG |
| 12 | 7.3 | 1992 | Landers | Coolwater | SCE |
| 13 | 6.9 | 1989 | Loma Prieta | Capitola | CDMG |
| 14 | 6.9 | 1989 | Loma Prieta | Gilroy Array #3 | CDMG |
| 15 | 7.4 | 1990 | Manjil, Iran | Abbar | BHRC |
| 16 | 6.5 | 1987 | Superstition Hills | El Centro Imp. Co. | CDMG |
| 17 | 6.5 | 1987 | Superstition Hills | Poe Road (temp) | USGS |
| 18 | 7.0 | 1992 | Cape Mendocino | Rio Dell Overpass | CDMG |
| 19 | 7.6 | 1999 | Chi-Chi, Taiwan | CHY101 | CWB |
| 20 | 7.6 | 1999 | Chi-Chi, Taiwan | TCU045 | CWB |
| 21 | 6.6 | 1971 | San Fernando | LA - Hollywood Stor | CDMG |
| 22 | 6.5 | 1976 | Friuli, Italy | Tolmezzo | -- |

Of the 22 earthquake records listed in Table16, 10 sets of earthquake records (both horizontal components of acceleration) were used to develop fragility curves as a function of PGA. Table 17 lists the earthquake used, their ID Numbers, recorded PGA's, filenames for both horizontal acceleration record sets, lowest frequencies and the source mechanism.

**Table 17 – Earthquake Records used to Develop Fragility Curves with PGA as the EDP (FEMA P695)**

| ID No. | PEER-NGA Record Information | | | | Record Motions | | Source Mechanism |
|---|---|---|---|---|---|---|---|
| | Record No. | Lowest Freq. (Hz.) | File name: Horiz. Comp. #1 | File name: Horiz. Comp. #2 | $PGA_{max}$ (g) | $PGV_{max}$ (cm/sec.) | Strike Slip or Reverse Thrust |
| 1 | 953 | 0.25 | NORTHR/MUL009 | NORTHR/MUL279 | 0.52 | 63 | THRUST |
| 2 | 960 | 0.13 | NORTHR/LOS000 | NORTHR/LOS270 | 0.48 | 45 | THRUST |
| 5 | 169 | 0.06 | IMPVALL/H-DLT262 | IMPVALL/H-DLT352 | 0.35 | 33 | STRIKE-SLIP |
| 6 | 174 | 0.25 | IMPVALL/H-E11140 | IMPVALL/H-E111230 | 0.38 | 42 | STRIKE-SLIP |
| 7 | 1111 | 0.13 | KOBE/NIS000 | KOBE/NIS090 | 0.51 | 37 | STRIKE-SLIP |
| 8 | 1116 | 0.13 | KOBE/SHI000 | KOBE/SHI090 | 0.24 | 38 | STRIKE-SLIP |
| 9 | 1158 | 0.24 | KOCAELI/DZC180 | KOCAELI/DZC270 | 0.36 | 59 | STRIKE-SLIP |
| 10 | 1148 | 0.09 | KOCAELI/ARC000 | KOCAELI/ARC090 | 0.22 | 40 | STRIKE-SLIP |
| 13 | 752 | 0.13 | LOMAP/CAP000 | LOMAP/CAP090 | 0.53 | 35 | STRIKE-SLIP |
| 14 | 767 | 0.13 | LOMAP/G03000 | LOMAP/G03090 | 0.56 | 45 | STRIKE-SLIP |

All earthquake records were obtained from the PEER Strong Motion Database at http://peer.berkeley.edu/smcat/. Prior to running the earthquake records for analysis, each earthquake record had to be scaled according to the ratio between Spectral Acceleration (Sa) of the earthquake at the natural period of the structure to be analyzed and the Spectral Acceleration at the structure's natural period as calculated in ASCE-07. The natural period of the structure was determined using ASCE (2005) Equation 12.8-7:

$$T_a = C_t h_n^x$$

where:

$T_a$=the approximate fundamental period of the structure

$C_t$=Approximate Period Parameter (ASCE (2005) Table 12.8-2) =0.02

X=Approximate Period Parameter (ASCE (2005) Table 12.802) =0.75

$h_n$=the height in feet from the base of the structure to the structures highest point=30ft

Therefore, the calculated $T_a$ value of 0.25 was used. Construction of the Design Response Spectrum in accordance with ASCE-07 Section 11.4.5 yielded a Spectral Acceleration value of 1.0g at the calculated fundamental period of 0.25sec. NONLIN was then used to develop plots of Spectral Acceleration vs. T for each earthquake ground acceleration record. Spectral Acceleration values from these plots were then taken at the fundamental period of 0.25. Finally, the calculated Sa of 1.0g was divided by each Spectral Acceleration value from the earthquake records. These ratios were used to scale the respective earthquake acceleration record from which they were developed. An example output from the program NONLIN is presented in Figure 20, the dashed yellow lines indicate the value of Sa taken at a corresponding period of 0.25sec the red lines indicate the ASCE design spectrum. A list of determined factors used to scale the various earthquake records is presented in Table 18.

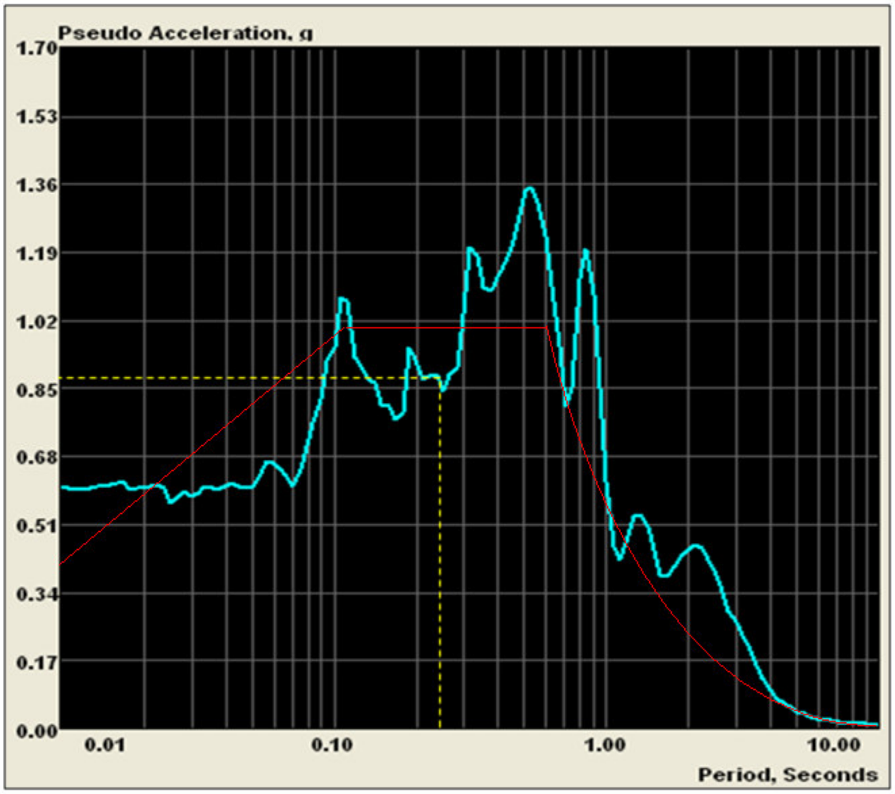


**Figure 20 – Example Output of Spectral Acceleration (Sa) Vs. Period (T) From NONLIN**

**Table 18 – Scaling Factors for Earthquake Records**

| Earthquake ID No. | Scaling Factor (Horiz. Comp. #1) | Scaling Factor (Horiz. Comp. #2) |
|---|---|---|
| 1 | 0.90 | 0.77 |
| 2 | 0.80 | 0.73 |
| 5 | 1.64 | 0.96 |
| 6 | 0.48 | 0.56 |
| 7 | 0.59 | 0.70 |
| 8 | 1.99 | 2.48 |
| 9 | 1.52 | 0.84 |
| 10 | 2.73 | 2.07 |
| 13 | 0.49 | 1.08 |
| 14 | 0.52 | 1.05 |

Step 2: Determination of Hysteretic Parameters

For each wall type to be analyzed, hysteretic parameters were necessary to model the performance of the wall when modeled as a SDOF spring element. The program SAPWood, written by Shiling Pei and Jon Van de Lindt, was used to visually fit the hysteretic parameters used to characterize each wall specimen as a SDOF spring element. This was done by inputting the same hysteretic data used to determine backbone curves shown in Section 3, into SAPWood's hysteresis manual fitting tool. The manual fitting tool allows the user to choose between two non-linear response systems. Either the CUREE hysteretic model (a ten parameter mathematical model used to predict the performance of shear walls) or the Evolutionary Parameter Hysteretic Model (EPHM) (a sixteen parameter mathematical model) can be used to model the hysteretic behavior of various wall specimens. The ten parameter CUREE hysteretic model (SAPWood Users Manual) is illustrated in Figure 21. Refer to Table 19 for a description of each parameter.

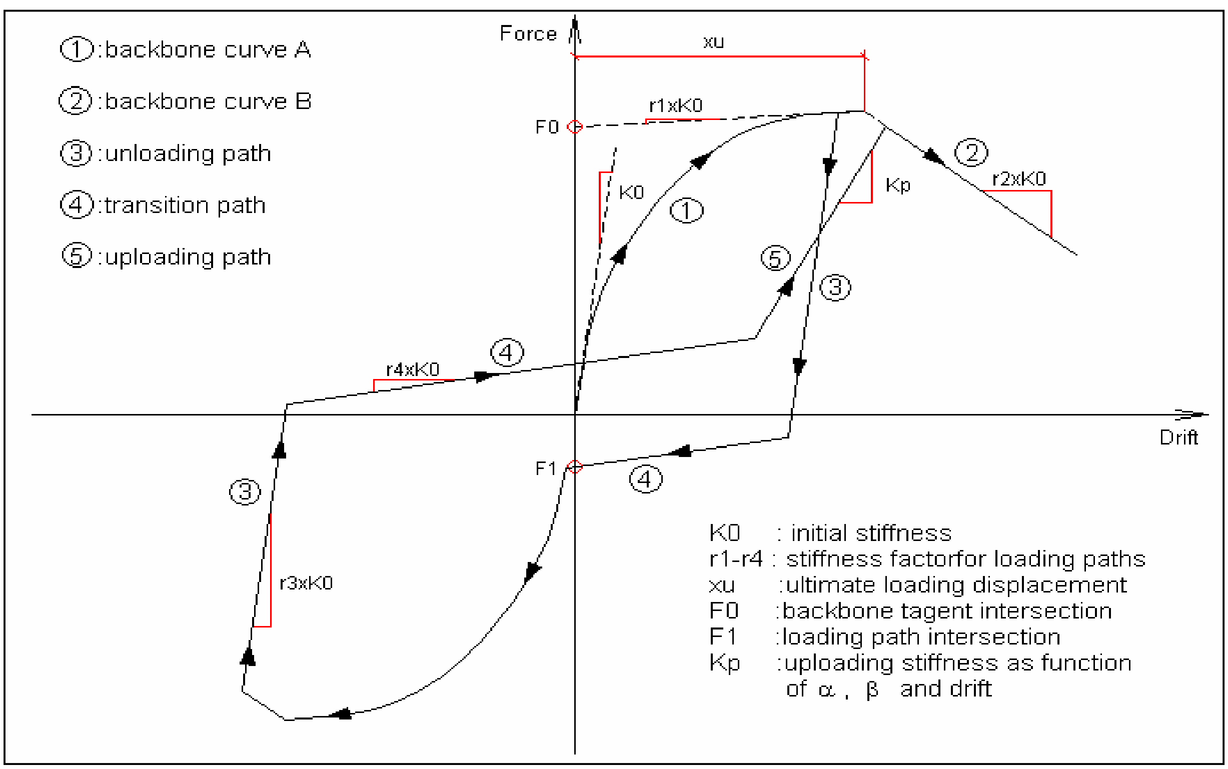


**Figure 21 – CUREE 10 Parameter Hysteretic Model (SAPWood Users manual**

**Table 19 – Description of CUREE Hysteretic Model Parameters (SAPWood Users Manual)**

| Hysteretic Parameter | Description |
|---|---|
| K0 | Initial stiffness |
| F0 | The resistance force parameter of the backbone |
| F1 | Pinching residual resistance force |
| R1 | The stiffness ratio parameter of the backbone |
| R2 | The ratio of degrading backbone stiffness to K0 |
| R3 | The ratio of the unloading path stiffness to K0 |
| R4 | The ratio of the pinching load path stiffness to K0 |
| Xu | The drift corresponding to the maximum restoring force of the backbone curve |
| Alpha | Stiffness degradation parameter |
| Beta | Stiffness degradation parameter |

Additionally, the 16 parameter EPHM model (SAPWood Users Manual) is illustrated in Figures 22 and 23. Refer to Table 20 for a description of the EPHM parameters.

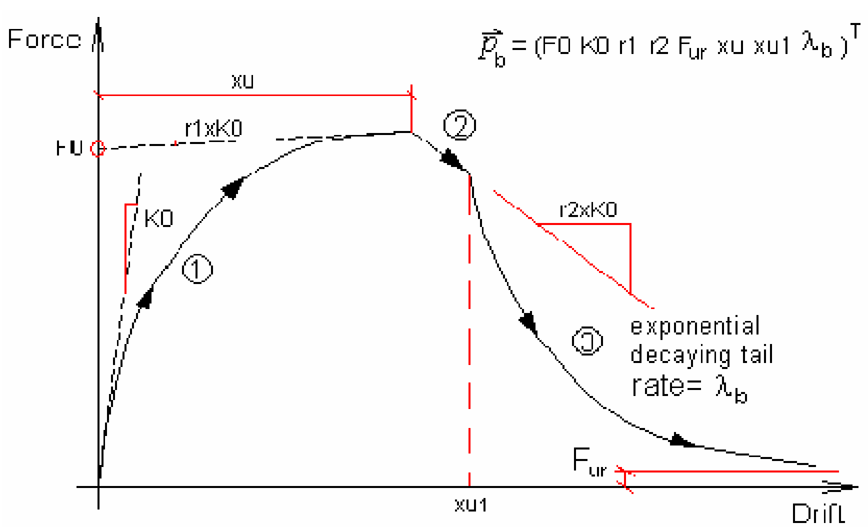


**Figure 22 – Backbone Curve for EPHM Hysteresis (SAPWood Users Manual)**

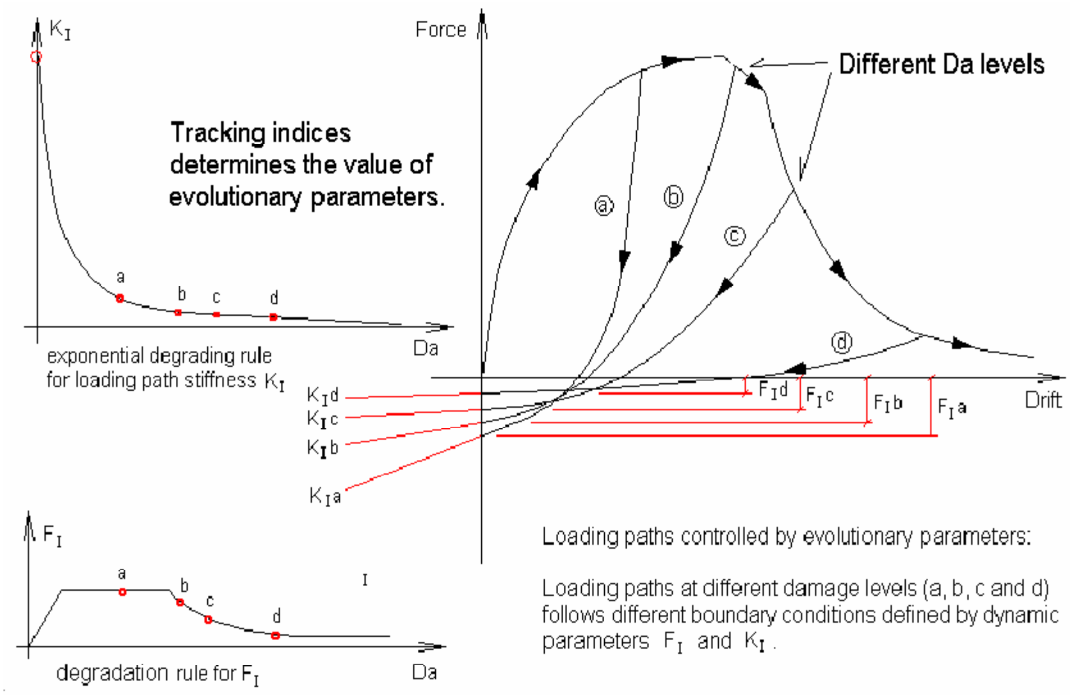


**Figure 23 – Degradation of Loading Paths for EPHM Hysteretic Model (SAPWood Users Manual**

**Table 20 – Description of Hysteretic Parameters for EPHM Hysteretic Model (SAPWood Users Manual)**

| Hysteretic Parameter | Description |
|---|---|
| K0 | Initial stiffness |
| F0 | The resistance force parameter of the backbone |
| R1 | The stiffness ratio parameter of the backbone |
| Xu | The drift corresponding to the maximum restoring force of the backbone curve |
| R2 | The ratio of the degrading backbone stiffness (linear portion) to K0 |
| Xu1 | The drift corresponding to the point where linear degradation ends and exponential degradation begins |
| P1 | The exponentially degrading rate parameter of the backbone |
| F1m | Maximum value that the residual pinching force can reach |
| F1r | Minimum value of the residual pinching force in severe damage stage |
| DF1a | Tracking damage index corresponding to the starting point of the plateau portion of the FI degrading function |
| DF1b | Tracking damage index corresponding to the ending point of the plateau portion of the FI degrading function |
| pF1 | The exponential degrading rate parameter of the FI degrading function |
| Pr4 | The exponential degrading rate parameter of the KI (the tangent stiffness point where loading paths intersect with Y-axis) degradation function |
| r4r | Ratio of the residual KI value to initial stiffness |
| Beta | Strength degradation parameter |
| Fur | Residual resistance force of the backbone in severe damage stage |

Using SAPWood's manual fitting tool, hysteretic parameters were determined for a number of wall specimens. Data from Serrette et. al (1996 and 1997) was used as inputs to SAPWood. Refer to Figure 24 for an example screenshot of the hysteresis manual fitting tool. The input hysteretic data is shown in red while the white graph is the 10 parameter idealized hysteresis. Note the accuracy of the ten parameter

CUREE hysteretic model in determining the hysteretic performance of Wall Specimen E3. A list of wall specimens, and corresponding component info for each wall analyzed in this section is provided in Table 21. Although the SAPWood model can accurately predict shear wall performance, it does not account for P-Δ effects or the effects of overturning forces.

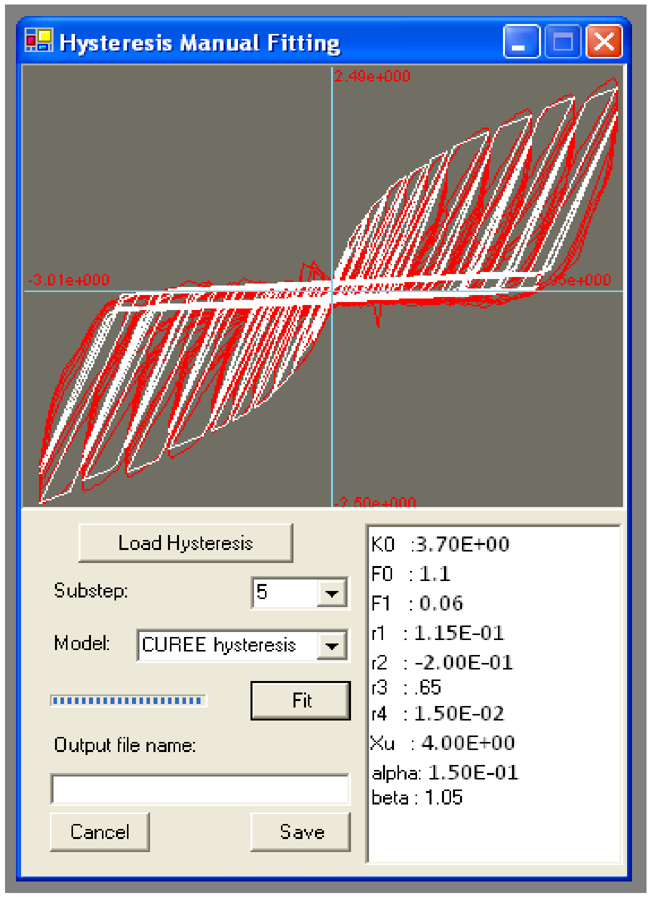


**Figure 24 – Example Output from SAPWood Hysteresis Manual Fitting Tool**

**Table 21 – Wall Specimens Idealized as SDOF Systems and Hysteretic Model Used**

| Specimen ID | Hysteretic Model Used | Structural Component Info | Wall Length |
|---|---|---|---|
| Ply 1 | CUREE | 15/32" plywood w/ 6"/12" fastener schedule | 4'x8' |
| Ply 2 | CUREE | 15/32" plywood w/ 6"/12" fastener schedule | 4'x8' |
| E1 | CUREE | 15/32" plywood w/ 6"/12" fastener schedule | 2'x8' |
| E2 | CUREE | 15/32" plywood w/ 6"/12" fastener schedule | 2'x8' |
| OSB 3 | CUREE | 15/32" plywood w/ 4"/12" fastener schedule | 4'x8' |
| OSB 4 | CUREE | 15/32" plywood w/ 4"/12" fastener schedule | 4'x8' |
| PLY 3 | CUREE | 15/32" plywood w/ 4"/12" fastener schedule | 4'x8' |
| PLY 4 | CUREE | 15/32" plywood w/ 4"/12" fastener schedule | 4'x8' |
| PLY 5 | CUREE | 15/32" plywood w/ 3"/12" fastener schedule | 4'x8' |
| PLY 6 | CUREE | 15/32" plywood w/ 3"/12" fastener schedule | 4'x8' |
| A1 | CUREE | 15/32" plywood w/ 3"/12" fastener schedule | 4'x8' |
| C1 | EPHM | Flat strap X-Brace | 4'x8' |
| C2 | EPHM | Flat strap X-Brace | 4'x8' |
| C3 | EPHM | Flat strap X-Brace | 4'x8' |
| C4 | CUREE | Flat strap X-Brace | 4'x8' |
| D1 | CUREE | Steel Sheathing | 4'x8' |
| D2 | CUREE | Steel Sheathing | 4'x8' |
| F1 | EPHM | Steel Sheathing | 2'x8' |
| F2 | EPHM | Steel Sheathing | 2'x8' |

Step 3: SAPWood Output

Once the aforementioned wall specimens were idealized as SDOF spring elements via CUREE or EPHM hysteretic models, each wall specimen was subject to the scaled earthquake records listed in Table 17.

SAPWood allows the user to build an SDOF shear wall using hysteretic parameters and then to input various earthquake records which can be scaled using PGA as the scaling factor. Earthquake records were scaled from PGA of 0.1g to a PGA of 5.0g in increments of 0.1g. The resultant output from SAPWood included maximum drift corresponding to each PGA for each earthquake record used. For walls with WSP sheathing, empirical data from testing of each wall specimen was averaged to determine the value at which damage states $DS_1$ and $DS_2$ occurred. $DS_3$ for walls with WSP sheathing was defined as the point in which the PGA vs. Displacement graph took an abrupt "jump" in displacement. This jump signified instability in the wall model caused by excessive loading. Damage states descriptions are identical to those presented in Section 3.2.1. Please refer to Section 3.2.1 for pictures and descriptions of various damage states. The empirically determined average horizontal displacements corresponding to various damage states for each wall type analyzed are presented in Table 22.

**Table 22 – Average Horizontal Displacements Corresponding to $DS_1$, $DS_2$, and $DS_3$ Determined from Envelope Curves**

| | Average Horizontal Displacements at Damage States (in) | | |
|---|---|---|---|
| Wall Type | $DS_1$ | $DS_2$ | $DS_3$ |
| 6"/12" fastener Schedule sheathed with WSP | 0.33 | 2.31 | N/A |
| 4"/12" fastener schedule sheathed with WSP | 0.44 | 2.43 | 2.57 |
| 3"/12" fastener Schedule sheathed with WSP | 0.5 | 2.58 | 2.86 |
| X-Brace | 1.36 | 1.77 | N/A |
| Steel Sheathing | 1.83 | 2.39 | N/A |

For walls with X-Bracing, PGA values for $DS_1$ were taken at the average horizontal displacement value calculated from test data. PGA values for $DS_2$ were taken at the point where instability in the wall model was present. The PGA values corresponding to horizontal displacements could then be found by graphing PGA vs. Horizontal displacement for each wall type using all 10 earthquake records (two files per earthquake record to account for both components of ground acceleration.) Refer to Figure 25 for example output of PGA vs. Horizontal Displacement for wall Specimen PLY5 when subject to scaled earthquake records identified in the legend. Data from SAPWood outputs of PGA vs. Horizontal Displacement was used to construct the fragility curves shown in the next section.

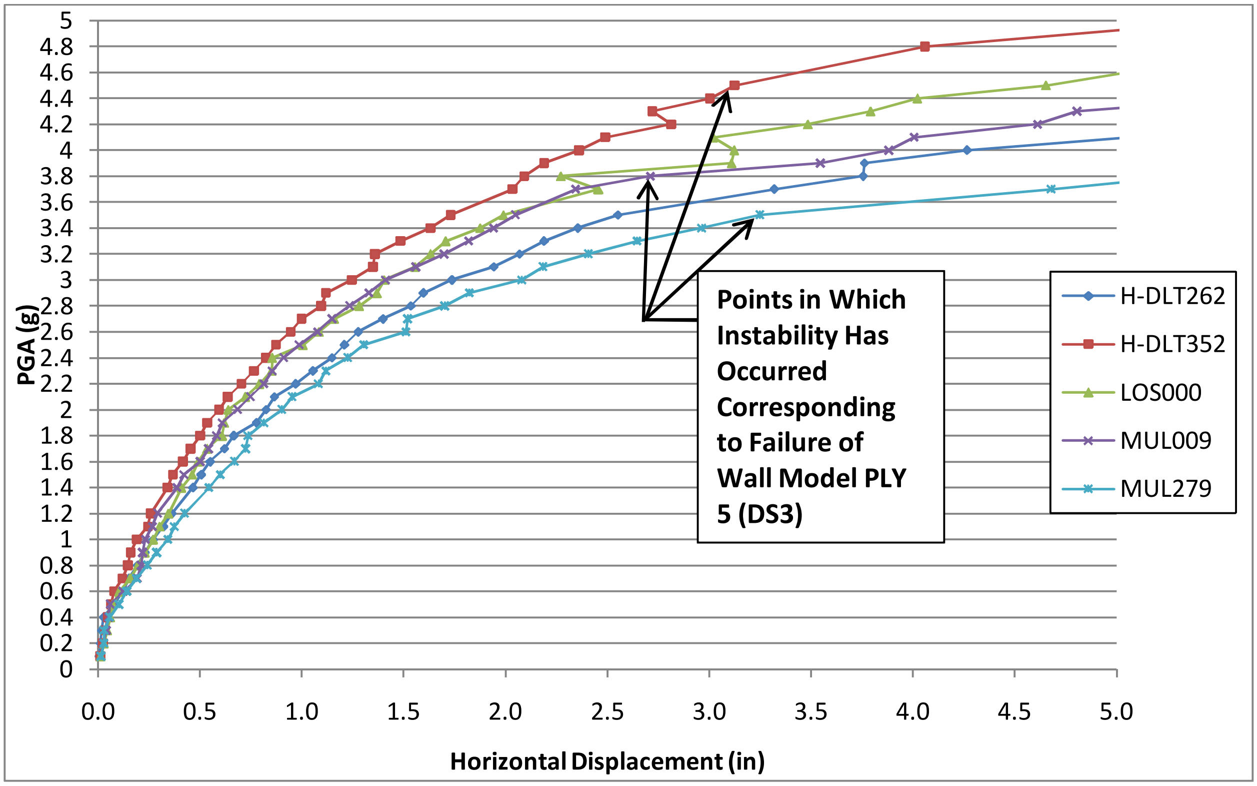


**Figure 25 – Example Output of PGA Vs. Horizontal Displacement from SAPWood**

## 4.2 Fragilities of Walls with WSP Sheathing and 6"/12" Fastener Spacing

In this section fragility curves are provided for walls with WSP sheathing that is fastened with screws which are spaced at 6"o.c. on panel edges and 12"o.c. on the interior of the panel (6"/12"). These fragility curves were constructed following the methodology described in Section 4.1. SAPWood was used to fit hysteretic parameters to data sets provided by Serrette *et al.* (1996) and Serrette *et al.* (1997). Specifications for the walls tested are as follows:

- Walls 8ft in height by either 4ft in length
- 1-1/2”x3-1/2”  A446 33ksi steel top and bottom tracks with 33 mil thickness
- 1-1/2”x3-1/2” A446 33ksi steel studs spaced at 24” o.c.
- No. 8-1” sharp point flat head screws for panel to framing connection
- Wood structural panel sheathing attached with long dimension parallel to studs
- Spacing of sheathing to framing fasteners at 6” on panel edges with 12” in field
- Seismic hold-downs at wall ends

### 4.2.1 Definition of Damage States

For detailed description of damage states refer to Section 3.2.1.  Specific damage state definitions are listed in Table 23.

**Table 23 – Description of Damage States for walls with 6”/12” Fastener Spacing**

| Damage States ($DS_i$) | Description of Damage State |
|---|---|
| $DS_1$ | Fastener Pull through-Refasten structural panels |
| $DS_2$ | Failure of structural panels-replace panels and inspect studs and tracks |
| $DS_3$ | Failure of wall-Replace wall |

### 4.2.2 Development of Fragility Curves

Displayed in Figure 26 are the fragility curves for walls with WSP sheathing and 6”/12” fastener spacing. Each of the four walls used to construct these fragility curves were subject to the 10 earthquake ground acceleration records provided in Table 17. The fragility parameters for walls with sheathing attached using 6”/12” fastener spacing are provided in Table 24.

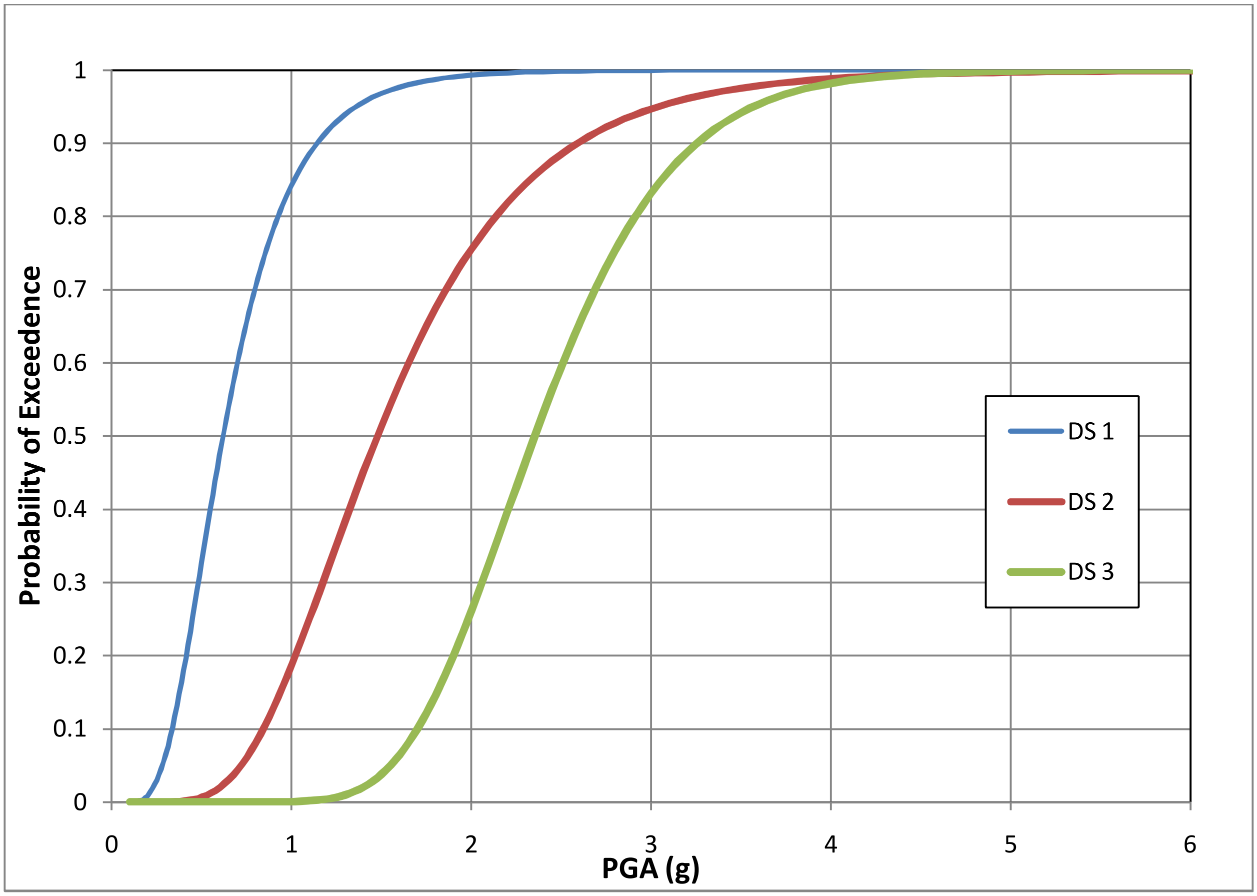


**Figure 26 – Fragility Curves for Walls with WSP Sheathing and 6”/12” Fastener Spacing**

**Table 24 – Median and Dispersion Values for Walls with WSP Sheathing and 6”/12” Fastener Spacing**

| Damage States | Demand Parameter (DP) | Median (θ) | Dispersion (β) |
|---|---|---|---|
| $DS_1$ | Peak Ground Acceleration PGA (g) | 0.62 | 0.48 |
| $DS_2$ | | 1.47 | 0.44 |
| $DS_3$ | | 2.36 | 0.25 |

## 4.3 Fragilities of Shear Walls with WSP Sheathing and 4”/12” Fastener Spacing

This section includes the development of fragility curves from all monotonic and cyclic test specimens with structural sheathing and 4”/12” fastener spacing (4” o.c. fastener spacing on the perimeter of each sheathing panel and 12” o.c. on the interior of the panel). Methods used to determine PGA values at drifts corresponding to DS1-DS3 are outlined in Section 4.1 . SAPWood was used to fit hysteretic parameters to data sets provided by Serrette *et al.* (1996) and Serrette *et al.* (1997). Specifications for the wall specimens tested are as follows:

- Walls 8ft in height by 4ft in length
- 1-1/2"x3-1/2" A446 33ksi steel top and bottom tracks with 33 mil thickness
- 1-1/2"x3-1/2" A446 33ksi steel studs spaced at 24" o.c.
- No. 8-1" sharp point flat head screws for panel to framing connection
- Wood structural panel sheathing attached with long dimension of panel parallel to studs
- Spacing of sheathing to framing fasteners at 4" spacing on panel edges with 12" spacing in field
- Seismic hold-downs at wall ends

### 4.3.1 Definition of Damage States

Damage states defined for walls with structural sheathing and 4"/12" fastener spacing are identical to those defined in Section 3.2.1. Refer to Figures 6, 7 and 8 for photographs of damage states. The damage states for CFS walls with wood structural panel sheathing attached with 4"/12" fastener spacing are provided in Table 25.

**Table 25 – Damage States for Walls with WSP Sheathing and 4"/12" Fastener Spacing**

| Damage States ($DS_i$) | Description of Damage State |
|---|---|
| $DS_1$ | Fastener Pull through-Refasten structural panels |
| $DS_2$ | Failure of structural panels-replace panels and inspect studs and tracks |
| $DS_3$ | Failure of wall-Replace wall |

### 4.3.2 Development of Fragility Curves

Construction of the fragility curves for walls with WSP sheathing and 4"/12" fastener spacing was based on cyclic data from research conducted by Nguyen, Hall and Serette *et al.* (1996) and Serette *et al.* (1997). The process for developing these fragility curves is outlined in Section 4.1. Fragility curves for walls with 4"/12" fastener spacing are shown in Figure 27. The median and dispersion values for these fragility curves are provided in Table 26.

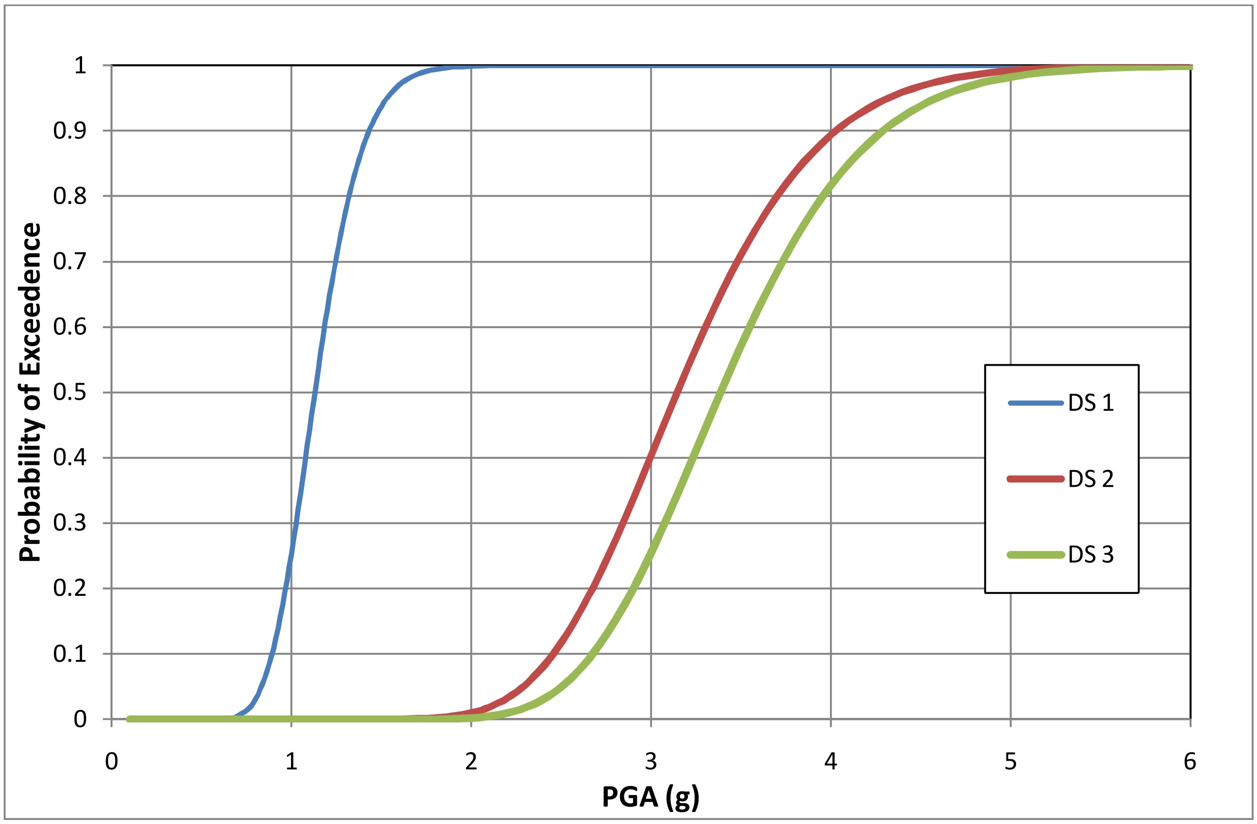


**Figure 27 - Fragility Curves for Walls with WSP Sheathing and 4"/12" Fastener Spacing**

**Table 26 – Median and Dispersion Values for Walls with WSP Sheathing and 4"/12" Fastener Spacing**

| Damage States | Demand Parameter (DP) | Median (θ) | Dispersion (β) |
|---|---|---|---|
| **$DS_1$** | **Peak Ground Acceleration PGA (g)** | 1.13 | 0.18 |
| **$DS_2$** | | 3.14 | 0.19 |
| **$DS_3$** | | 3.39 | 0.18 |

## 4.4 Fragilities of Shear Walls with WSP Sheathing and 3"/12" Fastener Spacing

In this section fragility curves are provided for walls with WSP sheathing that is fastened with screws which are spaced at 4"o.c. on panel edges and 12"o.c. on the interior of the panel (3"/12"). These fragility curves were constructed following the methodology described in Section 4.1. SAPWood was used to fit hysteretic parameters to data sets provided by Serrette *et al.* (1996) and Serrette *et al.* (1997). Specifications for the walls tested are as follows:

- Walls 8ft in height by either 4ft in length
- 1-1/2"x3-1/2" A446 33ksi steel top and bottom tracks with 33 mil thickness
- 1-1/2"x3-1/2" A446 33ksi steel studs spaced at 24" o.c.
- No. 8-1" sharp point flat head screws for panel to framing connection
- Wood structural panel sheathing attached with long dimension parallel to studs
- Spacing of sheathing to framing fasteners at 3" on panel edges with 12" in field
- Seismic hold-downs at wall ends

### 4.4.1 Definition of Damage States

Damage states defined for walls with structural sheathing and 3"/12" fastener spacing are identical to those defined in Section 3.2.1. Refer to Figures 6, 7 and 8 for photographs of damage states. The damage states for CFS walls with wood structural panel sheathing attached with 3"/12" fastener spacing are provided in Table 27.

**Table 27 – Damage States for Walls with WSP Sheathing and 3"/12" Fastener Spacing**

| Damage States ($DS_i$) | Description of Damage State |
|---|---|
| $DS_1$ | Fastener Pull through-Refasten structural panels |
| $DS_2$ | Failure of structural panels-replace panels and inspect studs and tracks |
| $DS_3$ | Failure of wall-Replace wall |

### 4.4.2 Development of Fragility Curves

Construction of the fragility curves for walls with WSP sheathing and 3"/12" fastener spacing was based on cyclic data from research conducted by Nguyen, Hall and Serette *et al.* (1996) and Serette *et al.* (1997). The process for developing these fragility curves is outlined in Section 4.1. Fragility curves for walls with 3"/12" fastener spacing are shown in Figure 28. The median and dispersion values for these fragility curves are provided in Table 28.

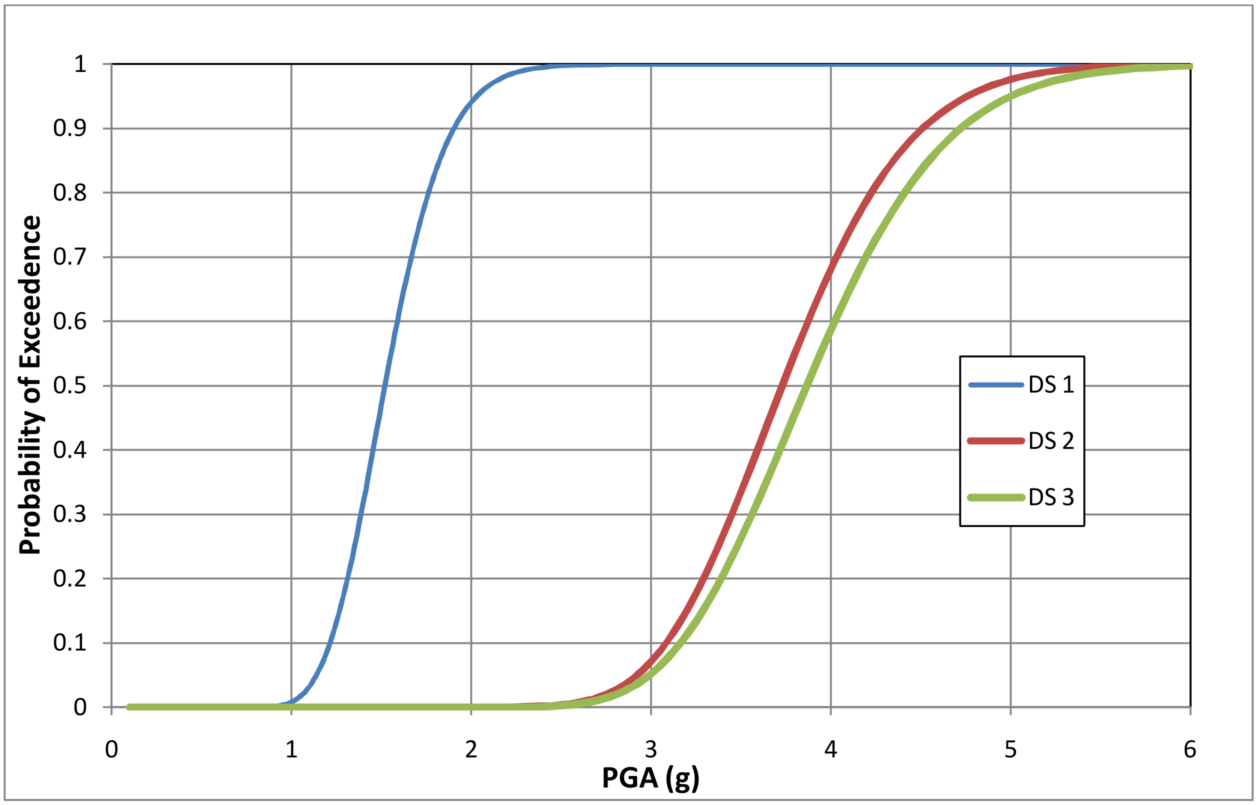


**Figure 28 - Fragility Curves for Walls with WSP Sheathing and 3"/12" Fastener Spacing**

**Table 28 – Median and Dispersion Values for Walls with WSP Sheathing and 3"/12" Fastener Spacing**

| Damage States ($DS_i$) | Demand Parameter (DP) | Median ($\theta$) | Dispersion ($\beta$) |
|---|---|---|---|
| $DS_1$ | PGA (g) | 1.52 | 0.18 |
| $DS_2$ | | 3.73 | 0.15 |
| $DS_3$ | | 3.86 | 0.16 |

## 4.5 Fragilities of Shear Walls with Flat Strap X-Bracing

This section addresses the development of fragility curves for walls with flat strap X-bracing as the main structural component to resist lateral force. Development of fragility curves for this section are based on hysteretic parameters determined from test data by Serette *et al.*(1996) and Serette *et al.* (1997). Specifications for the wall specimens are as follows:

- Walls 8ft in height by 4ft in length
- 1-1/2"x3-1/2" A446 33ksi steel top and bottom tracks with 33 mil thickness
- 1-1/2"x3-1/2" A446 33ksi steel studs spaced at 24" o.c.
- 4-1/2" 8 mil or 23 mil flat strap X-bracing one side
- No 8-1/2in self drilling modified truss head screw (20 screws used to attach strap to gusset plate)
- Seismic tie-downs at wall ends

### 4.5.1 Definition of Damage States

Damage states for walls with flat strap X-bracing are identical to those in Section 3.7.1. Please refer to Section 3.7.1 for a detailed description and illustrations of damage states. $DS_1$ and $DS_2$ are listed in Table 29.

**Table 29 - Damage States for Walls with 4-1/2" Flat Strap X-Bracing**

| Damage States ($DS_i$) | Description of Damage State |
|---|---|
| $DS_1$ | Local buckling of chord stud-remove cladding and replace stud |
| $DS_2$ | Failure of wall via strong axis bending or yielding of X-brace-rebuild wall |

### 4.5.2 Development of Fragility Curves

Data from Serrette (1997) was used to develop hysteretic parameters for use in the construction of fragility curves for this section. $DS_1$ and $DS_2$ for walls with 4-1/2" flat strap X-bracing are presented in Figure 29. Median and dispersion values for these fragility curves are shown in Table 30.

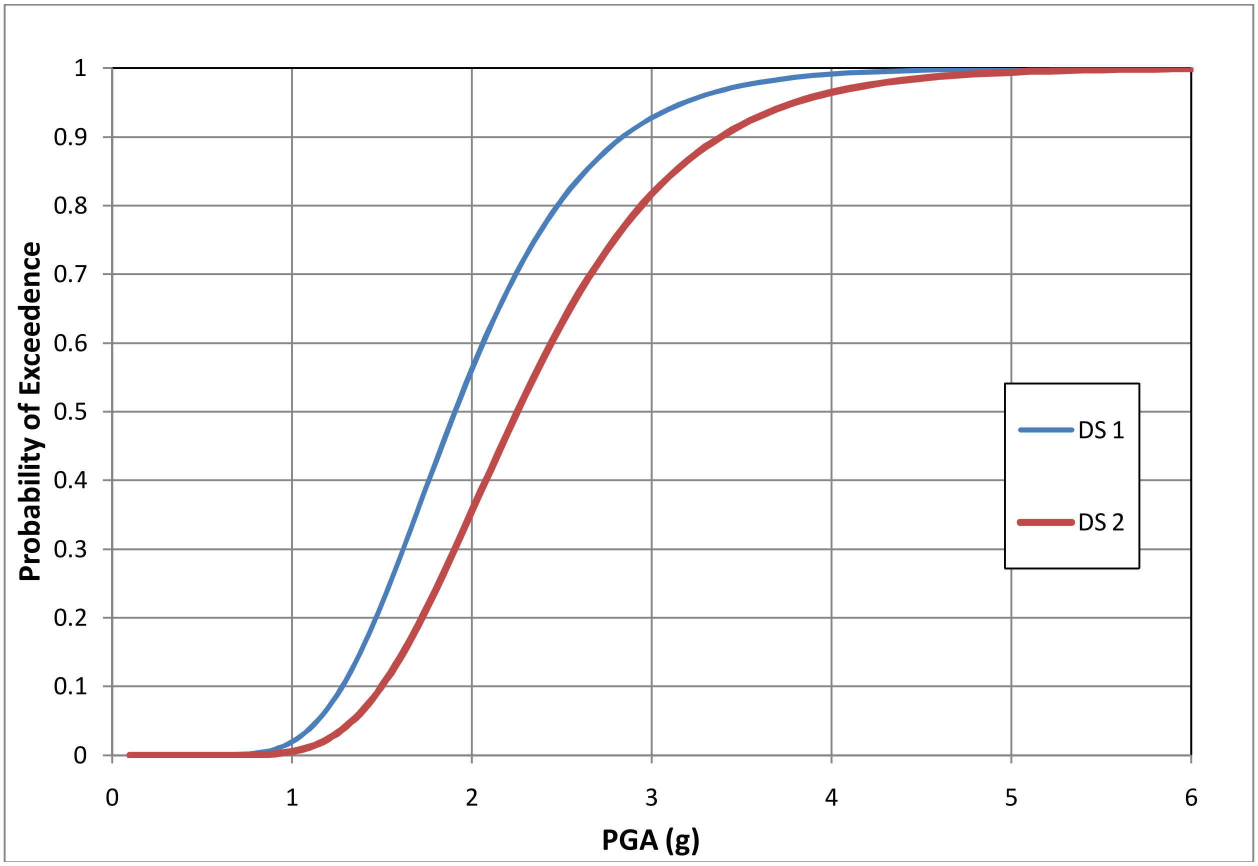


**Figure 29 – Fragility Curves for Walls with 4-1/2" Flat Strap X-Bracing**

**Table 30 - Median and Dispersion Values for Walls with 4-1/2" Flat Strap X-Bracing**

| Damage States ($DS_i$) | Demand Parameter (DP) | Median (θ) | Dispersion (β) |
|---|---|---|---|
| $DS_1$ | PGA (g) | 1.91 | 0.31 |
| $DS_2$ | | 2.25 | 0.32 |

## 4.6 Fragilities of Shear Walls with Steel Sheathing

Construction of fragility curves for CFS walls with 8 mil or 23 mil steel sheathing was based on hysteretic parameters determined from cyclic test data Serrette (1997). Specifications for the wall specimens tested are as follows:

- Walls 8ft in height by 2ft or 4ft length
- 1-1/2"x3-1/2" A446 33ksi steel top and bottom tracks with 33 mil thickness
- 1-1/2"x3-1/2" A446 33ksi steel studs spaced at 24" o.c.
- 8 mil or 23 mil steel sheathing
- No. 8-18x1/2in self-drilling modified truss head screws used to attach sheathing to studs
- Fastener pattern used to attach steel sheathing to studs ranged from 6"/12" to 2"/12"
- Seismic tie-downs at wall ends

### 4.6.1 Definition of Damage States

Damage states for walls with steel sheathing are identical to those in Section 3.8.1. Please refer to Section 3.8.1 for a detailed description and illustrations of damage states. $DS_1$ and $DS_2$ are listed in Table 31.

**Table 31 – Description of Damage States for Walls with Steel Sheathing**

| Damage States ($DS_i$) | Description of Damage State |
|---|---|
| $DS_1$ | Pull through of fasteners or block shear rupture at panel edges |
| $DS_2$ | Buckling of studs and tracks |

### 4.6.2 Development of Fragility Curves

Hysteretic parameters for input to SAPWood to construct fragility curves for this section were developed from test data from Serrette (1997). Fragility curves for $DS_1$ and $DS_2$ are shown in Figure 30. Median and dispersion values for these fragility curves are shown in Table 32

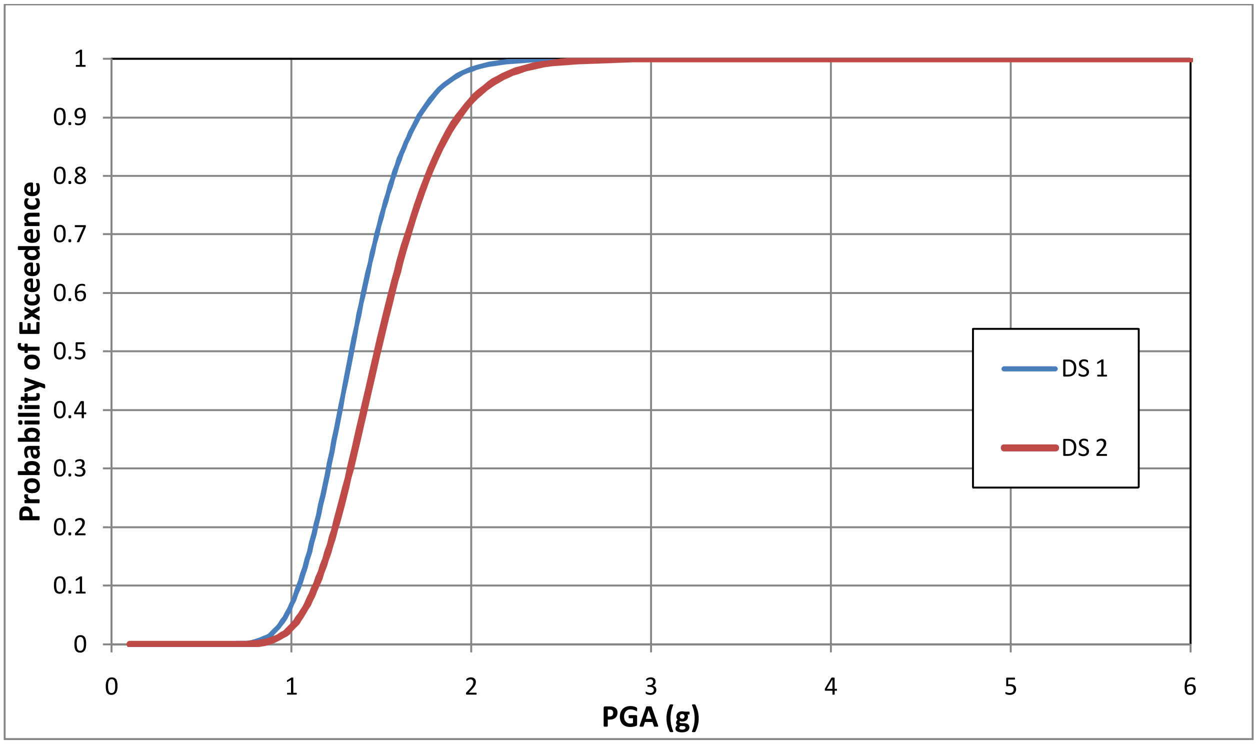


**Figure 30 – Fragility Curves for Walls with 8 mil or 23 mil Steel Sheathing**

.

**Table 32 – Median and Dispersion Values for Walls with 8 mil or 23 mil Steel Sheathing**

| Damage States ($DS_i$) | Demand Parameter (DP) | Median (θ) | Dispersion (β) |
|---|---|---|---|
| **$DS_1$** | **Inter-Story Drift (ISD) (%)** | **1.33** | **0.19** |
| **$DS_2$** | | **1.48** | **0.21** |

## 4.7 Summary of Fragility Curves for CFS Light-Frame Shear Walls using PGA as the EDP

A summary of the median and dispersion values are presented in Table 33, as well as the method used to calculate fragility parameters (θ and β) for all walls used to construct fragility curves with PGA as the EDP.

**Table 33- Summary of Median and Dispersion Values for Fragility Curves Constructed Using PGA as the EDP**

| System Type | Demand Parameter | Median (θ) | | | Dispersion (β) | | | Method Used* |
|---|---|---|---|---|---|---|---|---|
| | | $DS_1$ | $DS_2$ | $DS_3$ | $DS_1$ | $DS_2$ | $DS_3$ | |
| CFS sys#1-6"/12" | PGA (g) | 0.62 | 1.47 | 2.36 | 0.48 | 0.44 | 0.25 | A, E |
| CFS sys#1-4"/12" | | 1.13 | 3.14 | 3.39 | 0.18 | 0.19 | 0.18 | A, E |
| CFS sys#1-3"/12" | | 1.52 | 3.73 | 3.86 | 0.18 | 0.15 | 0.16 | A, E |
| CFS sys#2-steel sheathing | | 1.33 | 1.48 | N/A | 0.19 | 0.21 | N/A | A, E |
| CFS sys#3-X-bracing | | 1.91 | 2.25 | N/A | 0.31 | 0.32 | N/A | A, E |

*A-Parameters Derived from Actual Test Data (method A), E-Expert Judgment (method E)

# Chapter 5

# Interpretation of Data

## 5.1 Interpretation of Fragility Curves Developed from Test Data

As was previously mentioned, the fragility curves presented in Section 3 of this document were developed for a report which has been submitted to the ATC. Review of the report has determined that the fragility curves presented in Section 3 are acceptable for use in evaluating the seismic performance of CFS structures. However, as mentioned previously, some fragility curves developed in Section 3 were developed using test data from high aspect ratio walls (4:1 aspect ratio). High aspect ratio walls are known to have less peak load capacity since flexural bending of the wall dominates shear/fastener deformation. In total, there were ten test specimens with 4:1 aspect ratios. These ten specimens included all means of lateral force resisting systems described earlier except flat strap X-bracing (i.e. two walls with steel sheathing, two walls with WSP sheathing and 6"/12" fastener spacing, etc.). For fragility curves developed with many test specimens such as fragility curves for walls with WSP sheathing, data from two high aspect ratio test specimens produced a negligible effect on fragility parameters. However, for walls with steel sheathing, two of the six test specimens used to develop fragility curves consisted of walls with high aspect ratios. Although inclusion of high aspect ratio test specimens does produce a conservative calculation of fragility parameters, it was the decision of the author not to censor this test data. This was due to the fact that many construction applications include the use of high aspect ratio shear walls. Therefore, inclusion of high aspect ratio test specimens does provide for more robust, widely applicable fragility curves.

Consideration must also be given to the differences between wall construction in a laboratory setting and construction of walls on a building site. In a laboratory setting, great care is taken insure quality construction of shear walls. This involves making sure that fasteners are not overdriven. Overdriving of the sheathing screws will result in lower strength, stiffness and ductility of a shear wall compared with values obtained from testing (Rokas, 2006). This and other common quality issues can affect the performance of shear walls, they are as follows:

**1)** Fasteners attaching WSP sheathing to framing studs (either wood or CFS) are overdriven: Overdriving of fasteners can cause a significant reduction in shear strength of a wall. For example FEMA 232 *Homebuilders Guide to Earthquake Resistant Design and Construction* states that " if 3/8 inch wood structural panel sheathing is used and the nails are overdriven 1/8 inch, the strength of the wall is reduced as much as 40 to 50 percent." This is directly relatable to CFS walls with WSP shear wall construction as it has been shown that wood-frame shear walls behave similarly to CFS shear walls (Dolan and Easterling 1999.)

**2)** Improper installation of hold-down anchors: While it is commonly required on larger commercial construction projects that a certified building inspector be present during the installation of hold-down anchors, inspection of hold-down installation is not required on small residential construction projects. Lack of inspection increases the probability that a hold-down anchor will be installed with concrete debris still present in the hold-down hole. Failure to adequately remove this debris can result in weak bonding between the epoxy and the hold-down anchor. In extreme cases, this poor bonding will cause failure of the connection far below the connection design capacity. In the case of premature failure, lateral load will be abruptly transferred to perimeter WSP fasteners which can cause an "unzipping effect" of the framing to sheathing fasteners.

**3)** Inconsistent fastener spacing: Often times fastener patterns may greatly deviate from the specified patterns. This can lead to an imbalance of screws fastening the WSP to the framing studs. In the event of seismic loading, this imbalance of fasters can produce torsional irregularities, as the center of resistance of the sheet has moved from the center of the sheet due to asymmetrical fastener patterns. Torsional irregularities result in higher loads to individual fasteners which can degrade the performance of the shear wall.

Although these numerous factors may negatively affect the performance of CFS walls, they are accounted for by design provisions present in codebooks such as the AISI Design Standard and the Standard for Cold-Formed Steel Framing – Prescriptive Method for One and Two Family Dwellings. Additionally, it is impractical and far too costly to test the capacities of shear walls when constructed with numerous combinations of flaws. This being said, the fragility curves developed in Chapter 3 may be used as a basis for analyzing the seismic performance of CFS shear walls. However, additional investigation is needed to determine the effect of construction tolerances on fragility parameters.

Finally, although these fragility curves were developed to analyze seismic performance of CFS shear walls used in the construction of low-rise structures, these fragility curves may also be used in the evaluation of taller structures. This is possible since damage states corresponding to different values of ISD are not dependent on overall building height.

## 5.2 Interpretation of Fragility Curves Developed Using PGA as the EDP

Although the development of fragility curves using PGA as the EDP was based on hysteretic parameters from test data, the idealized wall models had to be checked for vulnerability to certain earthquake records. To investigate the vulnerability of shear wall models to certain earthquake records, fundamental aspects of structural dynamics had to be examined. Firstly, every structural component has a certain fundamental frequency and corresponding fundamental period. When a component is subject to a cyclic force at this same fundamental period, resonance is reached. As was evidenced by the Tacoma Narrows bridge collapse, when resonance frequency is reached, structures incur large deformations which lead to failure. Considering this, it was necessary to examine individual “problematic” earthquake records to determine whether the excitation frequency was the cause of wall model instability. One efficient way of performing such an analysis makes use of the Fast Fourier Transform. The Fast Fourier Transform is based on the idea any regular periodic function and certain non periodic functions with finite integrals can be expressed as a sum of trigonometric functions in an infinite time framework (Boggs, and Narcowich, 2001). A Fast Fourier Transform is thus an efficient way to determine the most prevalent frequencies within an earthquake. Code was written in MATLAB to perform the aforementioned Fast Fourier Transform. The output is referred to as a power spectrum (Power vs. frequency.) as it illustrates how the power of a signal is distributed for given frequencies. Shown in Figure 31 is an example output of Power vs. Frequency for earthquake record H-DLT352.

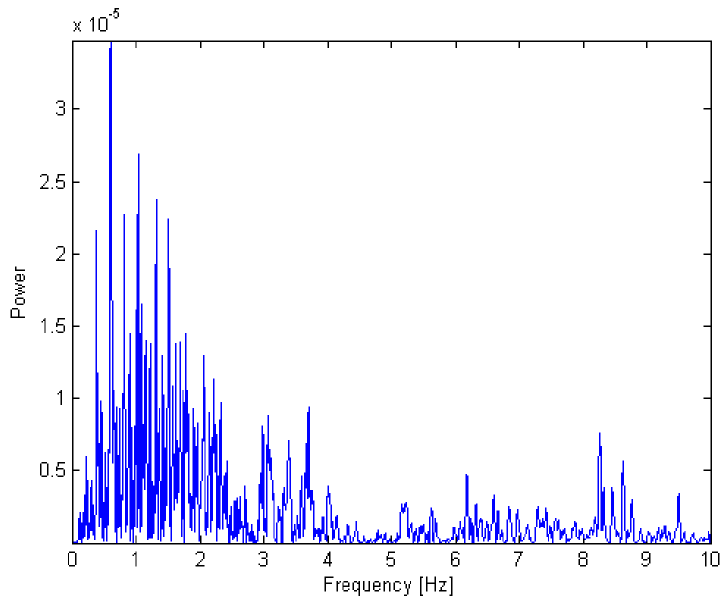


**Figure 31 – FFT vs. Frequency Output for Earthquake Record H-DLT352**

As evidenced from this power spectrum, the acceleration record H-DLT352 will produce the most damage to structures having a fundamental frequency around in the range of 0.7-1.5Hz. Since the fundament frequency ($\omega_n=1/T_n$) is approximately 4Hz for the wall models analyzed, this will not result in idealized wall model instability since all earthquake records show a majority of frequencies occurring around 1Hz. It is however noteworthy to mention that the fundamental frequency of a structure is subject to change as the structure is damaged. In terms of mass and effective spring stiffness, the fundamental frequency of a structure can be written as:

$$\omega_n = \sqrt{\frac{K_{eff}}{m}}$$

where:

m=mass of the structure, for all wall models analyzed this mass is taken to be $\frac{800lb}{g}$ as calculated based on weights of typical 2-story building components with a tributary area of 24ft$^2$.

and, $K_{eff}$=effective spring stiffness of the structure

Considering that the effective spring stiffness of each wall model degrades with time when subject to seismic loading (as illustrated in Figures 21, 22 and 23), the fundamental frequency, given by the above equation will decrease as the structure is damaged. Although the natural frequency of the structure will decrease as damage is incurred, thus making the structure more susceptible to low frequency earthquake excitation, this does not amount to structural instabilities at low PGA values as evidenced by PGA vs. Horizontal displacement graphs (see Appendix D for graphs).

As was previously mentioned, earthquake normalization was performed using a fundamental period of 0.25sec. Although this approximate period pertains to a structure with a height of 33ft., the fragility curves developed using PGA as the EDP may still be used for structures exceeding this height. This can be done if PGA is taken to be the relative acceleration between the shear wall being analyzed and the acceleration of the floor below.

## 5.3 Comparison of Fragility Curves

A two-pronged approach to the development of fragility curves for CFS shear walls would not have been complete without a comparison between fragility curves developed using ISD as the EDP, and those developed using PGA as the EDP. This comparison between fragility curves is done for a number of reasons. Firstly, values obtained using SAPWood to perform the IDA necessary to develop fragility curves using PGA, must be compared with test data to insure that SAPWood outputs are realistic.

Secondly, a comparison of fragility curves is necessary to prove that PGA fragility curves developed based on IDA can be used in place of fragility curves developed directly from test data.

Validation of SAPWood output could be determined by relating ISD fragility curves (from test data) to PGA fragility curves via peak load values. To compare peak load values used to develop fragility curves using PGA as the EDP with those obtained from test data, the following procedure was used:

1. Horizontal displacement values were recorded at the point of peak load for various test specimens.
2. PGA values from SAPWood corresponding to the horizontal displacement values were averaged to determine the average PGA at which peak load occurred.
3. SAPWood outputs of maximum force in idealized wall models were recorded and compared with maximum capacities of test specimens.

A comparison of maximum capacities of test specimens and maximum capacities of idealized wall models is presented in Table 34.

**Table 34 – Comparison of Test Data to SAPWood Output**

| Specimen ID | Specimen Info. | Test Data (kip) | SAPWood Output (kip) | % Difference |
|---|---|---|---|---|
| PLY 1 | WSP 6"/12" | 4.05 | 3.67 | 9.4 |
| PLY 2 | WSP 6"/12" | 3.88 | 3.77 | 2.8 |
| E1 | WSP 6"/12" | 1.54 | 1.35 | 12.3 |
| E2 | WSP 6"/12" | 1.66 | 1.52 | 8.4 |
| OSB 3 | WSP 4"/12" | 5.18 | 4.98 | 3.9 |
| OSB 4 | WSP 4"/12" | 4.96 | 4.77 | 3.8 |
| PLY 3 | WSP 4"/12" | 4.8 | 4.74 | 1.2 |
| PLY 4 | WSP 4"/12" | 5.68 | 5.29 | 6.9 |
| PLY 5 | WSP 3"/12" | 6.95 | 6.21 | 10.6 |
| PLY 6 | WSP 3"/12" | 5.1 | 5.77 | 13.1 |
| A1 | WSP 3"/12" | 7.8 | 7.3 | 6.4 |
| C1 | X-Brace | 3.79 | 3.57 | 5.8 |
| C2 | X-Brace | 3.76 | 3.52 | 6.4 |
| C3 | X-Brace | 3.75 | 3.99 | 6.4 |
| C4 | X-Brace | 4.16 | 3.87 | 7.0 |
| D1 | Steel Sheathing | 1.58 | 1.64 | 3.8 |
| D2 | Steel Sheathing | 1.71 | 1.74 | 1.8 |
| F1 | Steel Sheathing | 2.14 | 1.89 | 11.7 |
| F2 | Steel Sheathing | 2.13 | 1.87 | 12.2 |

A comparison of peak load values for test specimens and SAPWood outputs illustrates the accuracy of the IDA. In general, SAPWood predicted peak load values within 10% of those determined from testing. In most cases, SAPWood under predicted shear wall capacity with the exception of predictions for test specimens PLY 6, C3, D1 and D2 (highlighted in Table 34). This comparison of peak load output validates the accuracy of fragility curves developed using PGA as the EDP, however it should be noted that given the under prediction of wall capacities, the fragility curves are somewhat conservative. Accuracy of PGA fragility curves can be further validated by examining the similarity in trends between PGA fragility curves and ISD fragility curves for CFS shear walls with WSP sheathing. Test data signified that the load capacity of a CFS shear wall with WSP's increased with decreased fastener spacing (e.g. 6"/12" spacing compared to 4"/12" spacing). Although decreasing the fastener spacing did increase the load capacity of the wall, the difference between horizontal displacements at $DS_2$ and $DS_3$ also decreased. This trend in test data is accurately reflected by fragility curves for walls with WSP sheathing using ISD as the EDP and those using PGA as the EDP. Since the probability that $DS_2$ will not be exceeded for a given EDP is taken to be the difference in probabilities read from fragility curves for $DS_2$ and $DS_3$ (refer to Figure 2 for details) it becomes apparent that as the fastener spacing of a WSP shear wall decreases, the probability that $DS_2$ will not be exceeded decreases as well. This trend is apparent in both fragility curves developed using ISD as the EDP and curves using PGA as the EDP and accurately reflects trends in test data.

# Chapter 6

# Conclusions and Recommendations

Fragility curves developed based on test data and based on SAPWood outputs are deemed acceptable for use in determining the seismic performance of CFS shear walls for a number of reasons. Firstly when developing fragility curves based on test data, careful attention was given to the analysis of test data. Empirical data was excluded from data sets used to develop fragility curves by the methods specified in ATC-58 (see Section 3.1 for details). Secondly, when developing fragility curves using PGA as the EDP, SAPWood outputs were carefully scrutinized for skewed results. Each set of output data generated by SAPWood was compared with empirical data to insure that the resultant output was reasonable. Additionally, although fragility curves developed in this document were based on test data from walls no longer than 8ft in length (most of which were 4ft in length), fragility curves developed in this document may be used to evaluate the performance of CFS shear walls regardless of wall length. This is due to the fact that research has shown that the performance of shear walls sheathed with WSP's is contingent on the behavior of individual 4ft by 8ft sheets. As lateral loading of a WSP shear wall utilizing hold-downs increases, the individual sheets rotate independently and thus the wall segment behaves as a series of independent 4ft by 8ft rigid elements regardless of length, not as one collective rigid body.

Lastly, the user of these fragility curves must keep conservatism in mind when evaluating the seismic performance of CFS shear walls built with high construction tolerances or built to carry large gravity loads. This is due to the fact that fragility curves developed in this document were constructed using test data from specimens built with minimal construction tolerances. Additionally, the fragility curves developed using PGA as the EDP were based on SAPWood output which does not account for P-$\Delta$ effects or effects of shear wall overturning.

# References


American Society for Testing and Materials (ASTM) (2010), *Annual Book of Standards*. ASTM. West Conshohocken, PA.

ANSI/AISI (2001) "*Standard for Cold-Formed Steel Framing – Prescriptive Method for One and Two Family Dwellings,"* American Iron and Steel Institute, Washington DC, 36 p.

Applied Technology Council – ATC (2007) *Guidelines for Seismic Performance Assessment of Buildings* – ATC -58 35% Draft., Applied Technology Council, Redwood City, CA.

American Society of Civil Engineers, 2006, (ASCE). 2006, *Minimum Design Loads for Buildings and Other Structures.* ASCE Standard ASCE/SEI 7-02, American Society of Civil Engineers, Washington, D.C.

Blais, C. (2006). *Testing and analysis of light gauge steel frame /9 mm OSB wood panel shear walls*. Thesis (M. Eng.)--McGill University.

Boggess A, Narcowich FJ (2001): *A First Course in Wavelets with Fourier Analysis.* Prentice Hall. Upper Saddle River, NJ.

Boudreault, Felix-Antoine (2005). *Seismic Analysis of Steel Frame/ Wood Panel Shear Walls*. Thesis (M. Eng.)--McGill University.

Branston, A. E. (2004). *Development of a Design Methodology for Steel Frame / Wood Panel Shear Walls*. Thesis (M. Eng.)--McGill University.

Branston, A., Chen, C., Boudreault, F., & Rogers, C. (2006). Testing of Light-Gauge Steel-Frame - Wood structural panel shear walls. *Canadian Journal of Civil Engineering. Vol.*33, 561-572.

Chen, C. Y. (2004). *Testing and Performance of Steel Frame / Wood Panel Shear Walls*. Thesis (M. Eng.)--McGill University.

COMEAU, G. (2008). *Inelastic performance of welded cold-formed steel strap braced walls*. McGill theses. Thesis (M. Eng.)--McGill University, 2008.

Ekiert, C., Filiatrault, A. (2008) *"Fragility Curves for Wood Light-Frame Structural Systems for ATC-58,"* Department of Civil, Structural and Environmental Engineering University at Buffalo, State University of New York, Buffalo, NY.

Federal Emergency Management Agency. *Homebuilders'Guide to Earthquake Resistant Design and Constructio,* FEMA P232. FEMA, Washington, D.C.

Federal Emergency Management Agency. *Quantification of Building Seismic Performance Factors* ,FEMA P695. FEMA, Washington, D.C.

Filiatrault, A., and Folz, B. (2002). “Performance-based seismic design of wood framed buildings.” *J. Struct. Eng.*, 128(1), pp.39–47.

Folz, B., and Filiatrault, A. (2002). *A computer program for seismic analysis of woodframe structures*, CUREE Publication No. W-21, Richmond, Calif.

Folz, B., and Filiatrault, A. (2004a). “Seismic analysis of woodframe structures. I: Model formulation.” *J. Struct. Eng.*, 130(9), pp.1353–1360.

Folz, B., and Filiatrault, A. (2004b). “Seismic analysis of woodframe structures. II: Model implementation and verification.” *J. Struct. Eng.*,130(9), pp.1361–1370.

Hikita, K. (2006). *Combined Gravity and Lateral Loading of Light Gauge Steel Frame/Wood Panel Shear Walls*. Thesis (M. Eng.)--McGill University.

Lilliefors, H. W. (1967) “On the Kolmogorov-Smirnov Test for Normality with Mean and Variance Unknown,” *Journal of the American Statistical Association*, 62, pp.399-402.

Pei, Shiling. *Loss Analysis and Loss Based Seismic Design for Woodframe Structures*. , 2007. Print.
Porter, K. (2007) *“Fragility Testing and Reporting for ATC-58 – Version 06,”* Applied Technology Council, Redwood City, CA.

Rokas, D. (2006). *Testing and Evaluation of Light Gauge Steel Frame / 9.5 mm CSP Wood Panel Shear Walls*. Montreal: Dept. of Civil Engineering and Applied Mechanics, McGill University.

Salenikovich, A.J., Dolan, J.D., Easterling, W.S. (1999). *Monotonic and Cyclic Tests of Long Steel-Frame Shear Walls with Openings* Report No. TE-1999-001. Submitted to the American Iron and Steel Institute, Virginia Polytechnic Institute and State University Department of Wood Science and Forests Products Brooks Forest Products Research Center and Timber Engineering Center, Blacksburg, VA.

Serrette, R., Hoang N., and Hall, G. (1996). *Shear Wall Values for Light Weight Steel Framing*. Light Gauge Steel Research Group Report No. LGSRG-3-96, Department of Civil Engineering Santa Clara University, Santa Clara, CA.

Serrette, Reynaud (1997). *Additional Shear Wall Values for Light Weight Steel Framing*. Light Gauge Steel Research Group Report No. LGSRG-1-97, Department of Civil Engineering Santa Clara University, Santa Clara, CA.

Vagh, S., Dolan, J.D., Easterling, W.S. (2000). *Effect of Anchorage and Sheathing Configuration on the Cyclic Response of Long Steel-Frame Shear Walls.* Report No. TE-2000-002. Submitted to the American Iron and Steel Institute, Virginia Polytechnic Institute and State University Department of Wood Science and Forests Products Brooks Forest Products Research Center and Timber Engineering Center, Blacksburg, VA.

Velchev, K. (2008). *Inelastic performance of screw connected cold-formed steel strap braced walls*. McGill theses. Thesis (M. Eng.)--McGill University, 2008.

## Appendix A – Lognormal Fragility Functions from Test Data

This appendix contains fragility curves developed from test data, plotted with log normally distributed data points.

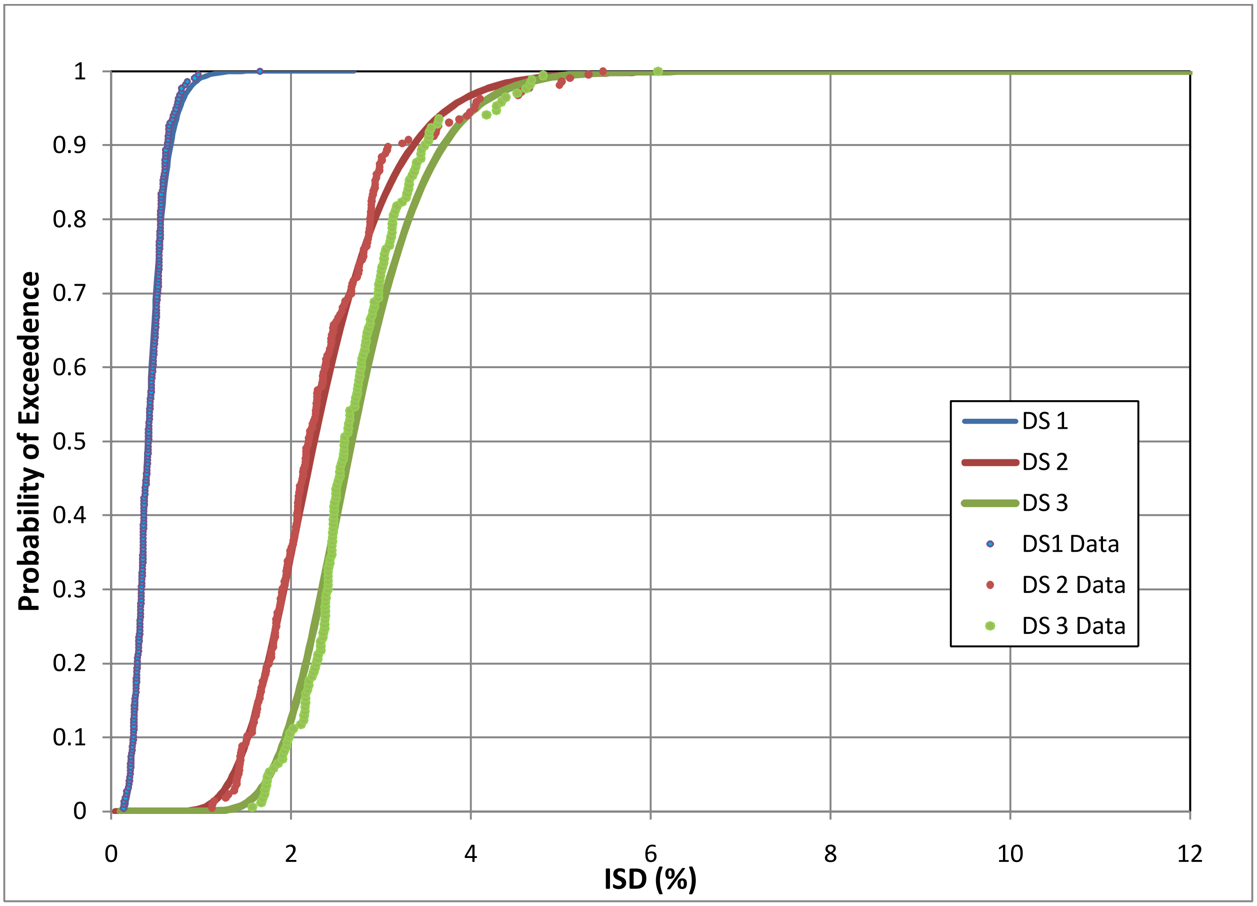


**Figure A 1 – Fragility Curves for all Walls with Structural Sheathing**

**Table A 1 – Medians and Dispersions for all Walls with Structural Sheathing**

| $DS_i$ | Median θ | Dispersion β | # of specimens | Lilliefors Test @ 5% significance |
|---|---|---|---|---|
| DS1 | 0.4 | 0.39 | 217 | Passes |
| DS2 | 2.26 | 0.31 | 216 | Passes |
| DS3 | 2.67 | 0.25 | 170 | Fails |

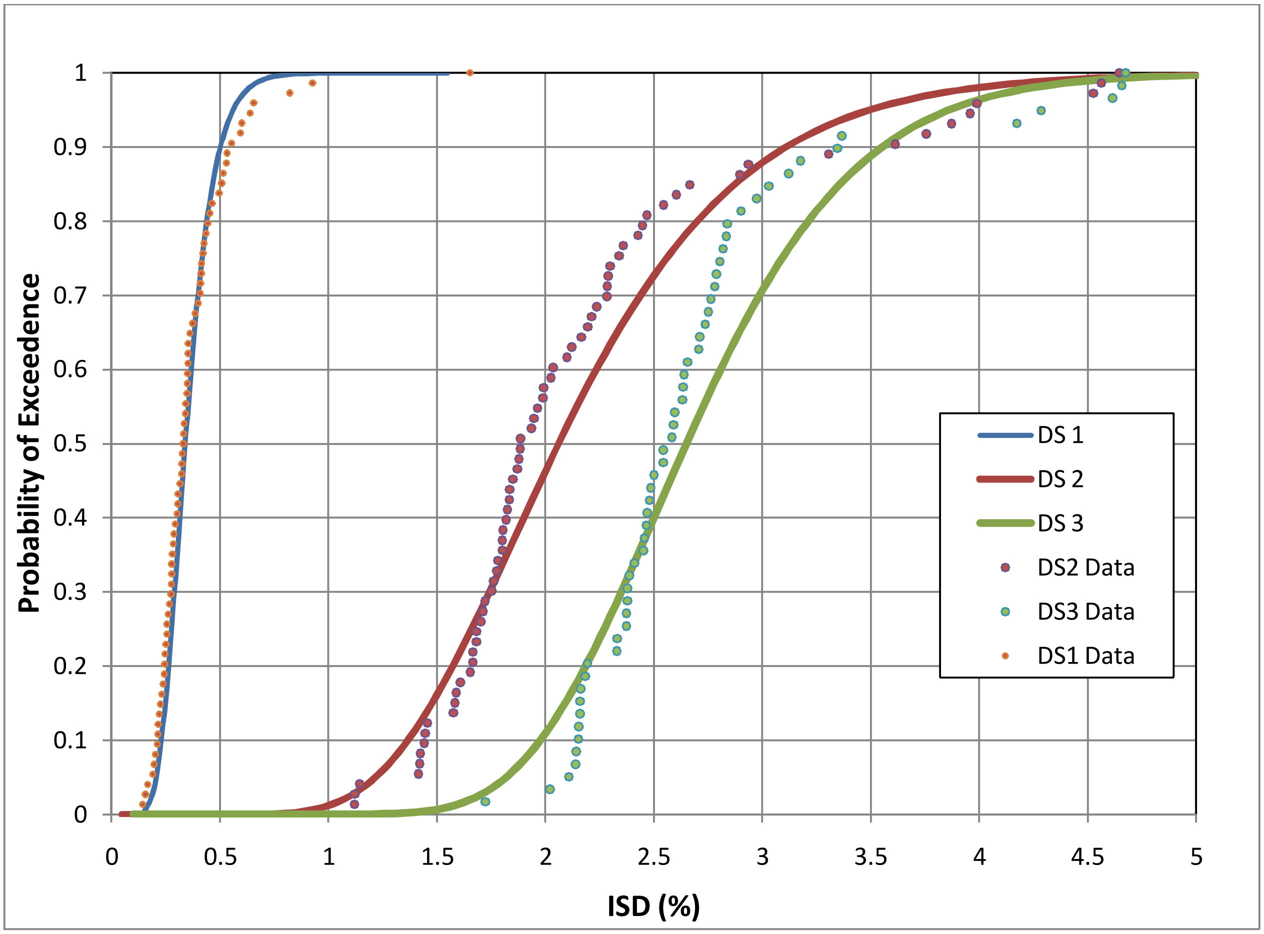


**Figure A 2 - Fragility Curves for Walls with Structural Sheathing and 6”/12” Fastener Spacing**

**Table A 2 - Medians and Dispersions for Walls with Structural Sheathing and 6"/12" Fastener Spacing**

| $DS_i$ | Median θ | Dispersion β | # of specimens | Lilliefors Test @ 5% significance |
|---|---|---|---|---|
| DS1 | 0.34 | 0.3 | 74 | Passes |
| DS2 | 2.06 | 0.32 | 73 | Fails |
| DS3 | 2.65 | 0.23 | 59 | Fails |

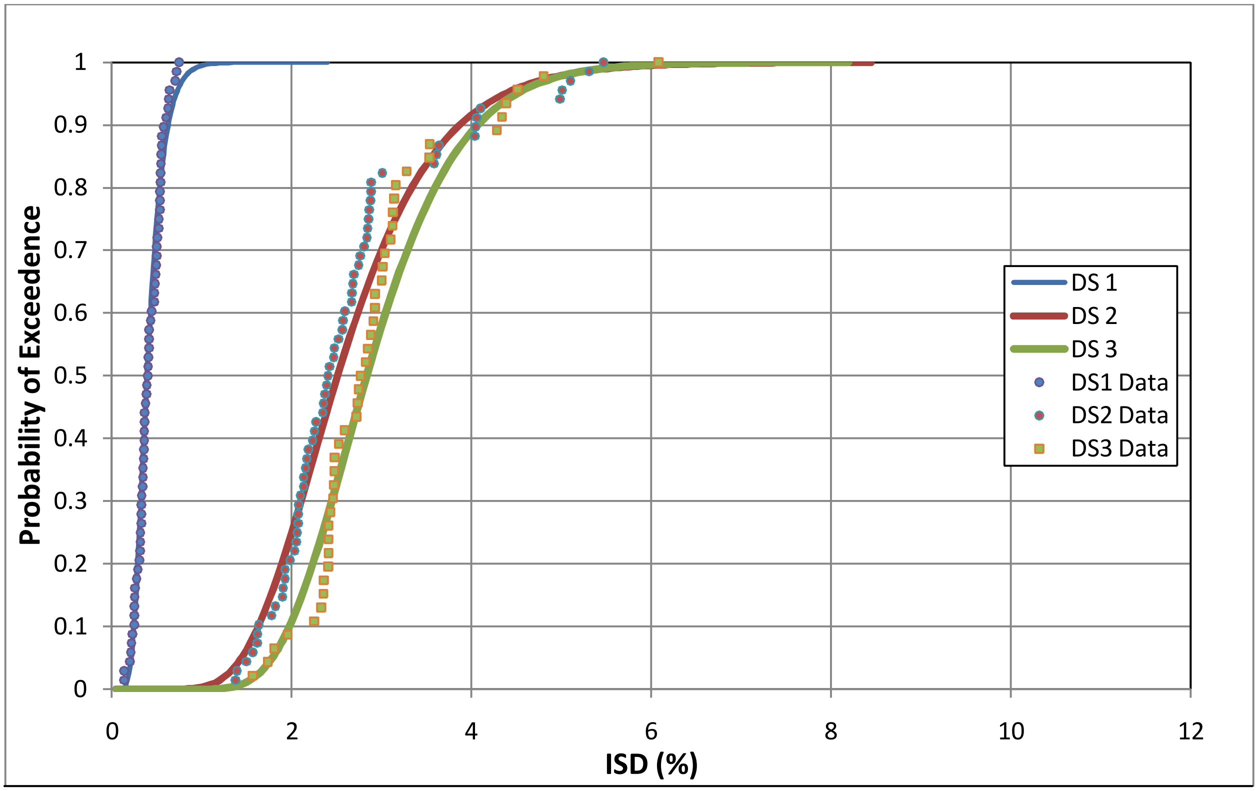


**Figure A 3 – Fragility Curves for Walls with Structural Sheathing and 4"/12" Fastener Spacing**

**Table A 3 - Medians and Dispersions for Walls w;ith Structural Sheathing and 4"/12" Fastener Spacing**

| $DS_i$ | Median θ | Dispersion β | # of specimens | Lilliefors Test @ 5% significance |
|---|---|---|---|---|
| DS1 | 0.39 | 0.37 | 68 | Passes |
| DS2 | 2.51 | 0.34 | 68 | Fails |
| DS3 | 2.84 | 0.28 | 46 | Passes |

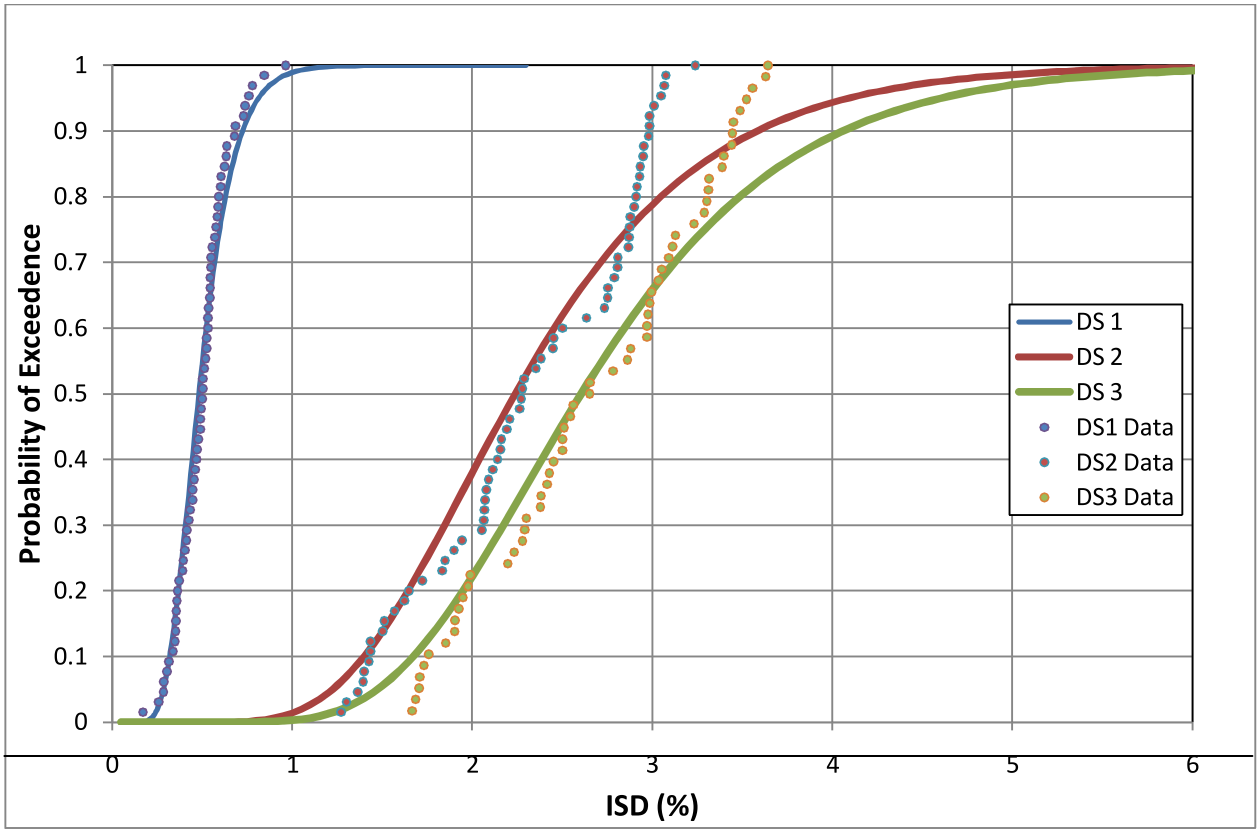


**Figure A 4 - Fragility Curves for Walls with Structural Sheathing and 3"/12" Fastener Spacing**

**Table A4 - Medians and Dispersions for Walls with Structural Sheathing and 3''/12'' Fastener Spacing**

| $DS_i$ | Median θ | Dispersion β | # of specimens | Lilliefors Test @ 5% significance |
|---|---|---|---|---|
| DS1 | 0.48 | 0.32 | 65 | Passes |
| DS2 | 2.23 | 0.36 | 65 | Fails |
| DS3 | 2.6 | 0.34 | 65 | Fails |

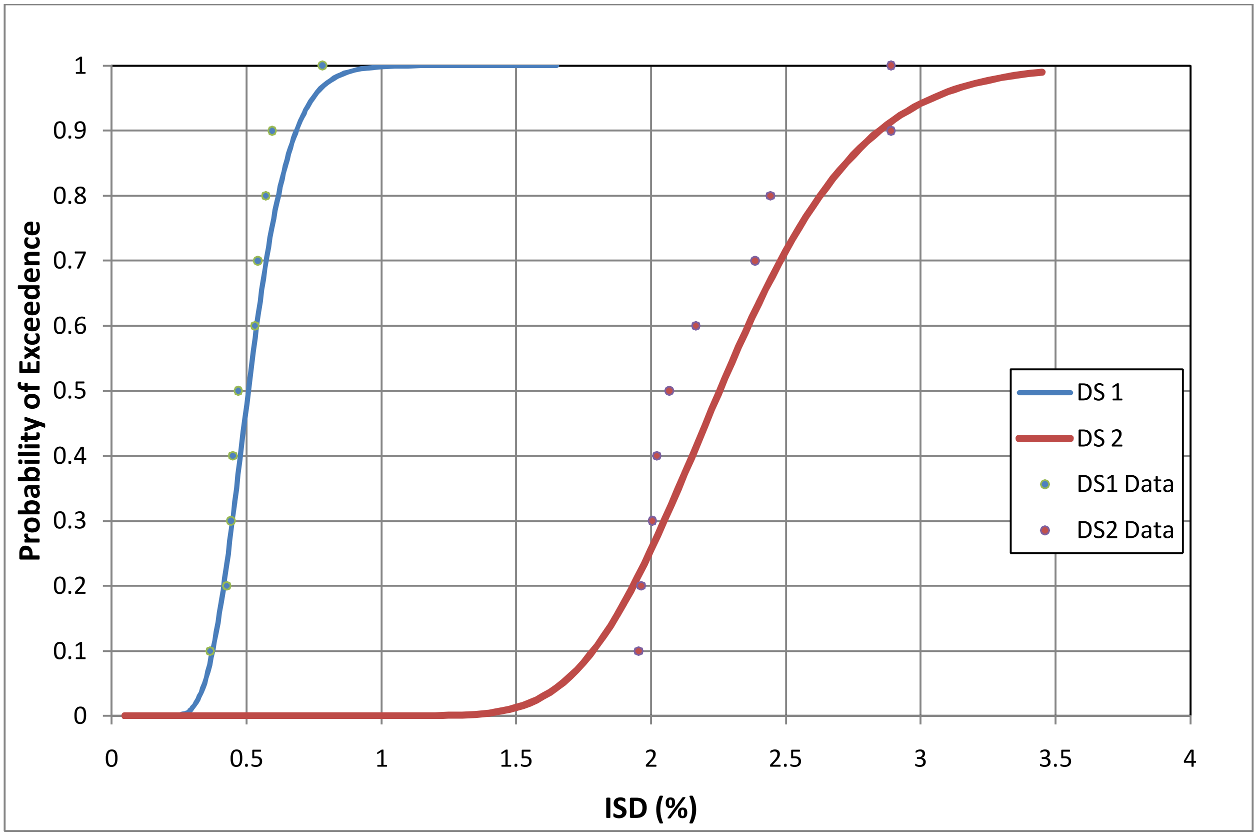


**Figure A5 – Fragility Curves for Walls with Structural Sheathing and 2"/12" Fastener Spacing**

**Table A5 - Medians and Dispersions for Walls with Structural Sheathing and 2"/12" Fastener Spacing**

| $DS_i$ | Median θ | Dispersion β | # of specimens | Lilliefors Test @ 5% significance |
|---|---|---|---|---|
| DS1 | 0.51 | 0.24 | 10 | Passes |
| DS2 | 2.25 | 0.18 | 10 | Passes |

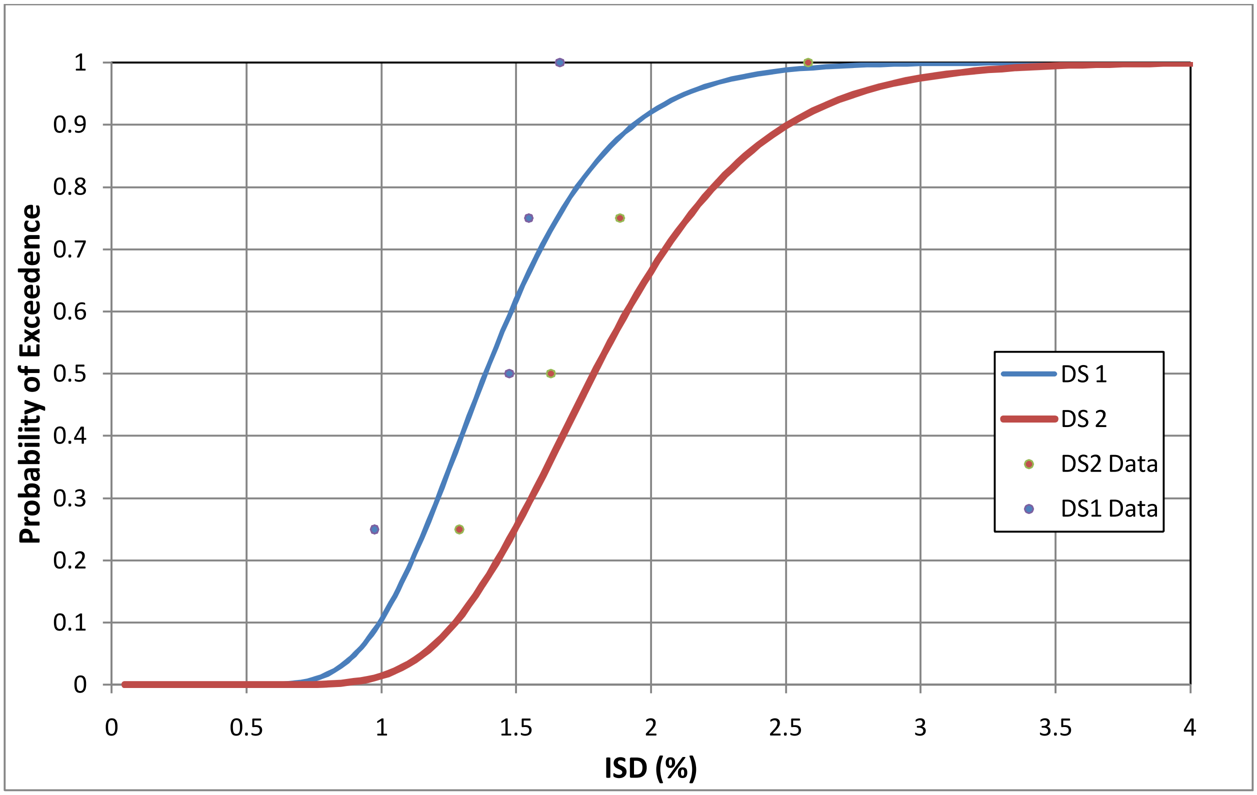


**Table A6 – Fragility Curves for Walls with Flat Strap X-Bracing**

**Table A6 - Medians and Dispersions for Walls with Flat Strap X-Bracing**

| $DS_i$ | Median θ | Dispersion β | # of specimens | Lilliefors Test @ 5% significance |
|---|---|---|---|---|
| DS1 | 1.39 | 0.26 | 4 | Passes |
| DS2 | 1.79 | 0.26 | 4 | Passes |

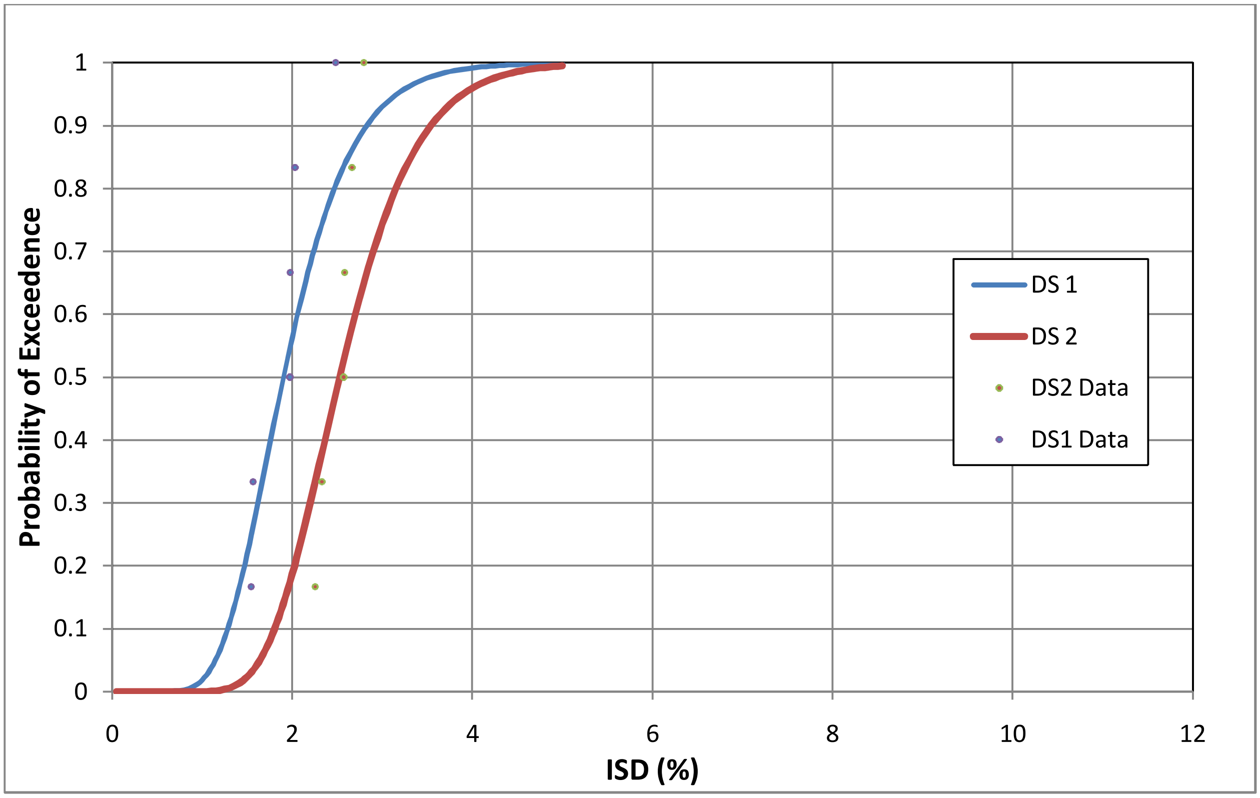

**Figure A7 – Fragility Curves for Walls with 8 mil or 23 mil Steel Sheathing**

**Table A7 - Medians and Dispersions for Walls with 8 mil Or 23 mil Steel Sheathing**

| $DS_i$ | Median θ | Dispersion β | # of specimens | Lilliefors Test @ 5% significance |
|---|---|---|---|---|
| DS1 | 1.9 | 0.25 | 6 | Passes |
| DS2 | 2.53 | 0.25 | 6 | Fails |

## Appendix B- Test Data and Field Observations

This appendix contains test data and field observations which were recorded and observed from various tests from which data was used to develop fragility curves using ISD as the EDP.

**Table B1- Monotonic Test Data from Boudreault (2005)**

| Test | Panel Type | Fastener Schedule (mm) | Displ. at 0.4 $S_u$ ($\Delta_{net,0.4u}$) mm | Yield Load ($S_y$) kN/m | Displ. at $S_y$ ($\Delta_{net,y}$) mm |
|---|---|---|---|---|---|
| 1A | CSP | 102 / 305 | 9.14 | 13.43 | 19.25 |
| 1B | CSP | 102 / 305 | 9.39 | 14.77 | 20.27 |
| 1C | CSP | 102 / 305 | 8.13 | 14.41 | 17.47 |
| **AVERAGE** | **CSP** | **102 / 305** | **8.89** | **14.20** | **19.00** |
| 1D | CSP Richply | 102 / 305 | 9.39 | 22.46 | 19.24 |
| 1E | CSP Richply | 102 / 305 | 9.32 | 18.59 | 19.68 |
| 1F | CSP Richply | 102 / 305 | 8.33 | 18.78 | 17.92 |
| **AVERAGE** | **CSP Richply** | **102 / 305** | **9.01** | **19.94** | **18.95** |
| 5A | DFP | 102 / 305 | 7.83 | 17.51 | 16.24 |
| 5B | DFP | 102 / 305 | 9.26 | 21.58 | 19.46 |
| 5C | DFP | 102 / 305 | 10.55 | 19.73 | 21.76 |
| 5D | DFP | 102 / 305 | 9.91 | 21.08 | 21.34 |
| **AVERAGE** | **DFP** | **102 / 305** | **9.39** | **19.98** | **19.70** |

**Table B2-Cyclic Test Data for Positive Cycles from Boudreault (2005)**

| Test | Panel Type | Fastener Schedule (mm) | Yield Load ($S_{y+}$) kN/m | Displ. at $S_{y+}$ ($\Delta_{net,y+}$) mm |
|---|---|---|---|---|
| 3A | CSP | 102 / 305 | 15.09 | 9.34 |
| 3B | CSP | 102 / 305 | 15.84 | 9.72 |
| 3C | CSP | 102 / 305 | 15.08 | 13.62 |
| **AVERAGE** | **CSP** | **102 / 305** | **15.34** | **10.89** |
| 4A | CSP | 102 / 305 | 14.63 | 16.55 |
| 4B | CSP | 102 / 305 | 15.61 | 13.29 |
| 4C | CSP | 102 / 305 | 16.19 | 14.75 |
| **AVERAGE** | **CSP** | **102 / 305** | **15.48** | **14.86** |
| 6A | DFP | 102 / 305 | 18.79 | 16.88 |
| 6B | DFP | 102 / 305 | 19.37 | 16.67 |
| 6C | DFP | 102 / 305 | 19.23 | 15.11 |
| **AVERAGE** | **DFP** | **102 / 305** | **19.13** | **16.22** |

Table B3- Cyclic Test Data for Negative Cycles from Boudreault (2005)

| Test | Panel Type | Fastener Schedule (mm) | Yield Load ($S_{y-}$) kN/m | Displ. at $S_{y-}$ ($\Delta_{net,y-}$) mm |
|---|---|---|---|---|
| 3A | CSP | 102 / 305 | -15.89 | -11.54 |
| 3B | CSP | 102 / 305 | -15.81 | -10.79 |
| 3C | CSP | 102 / 305 | -15.16 | -10.11 |
| **AVERAGE** | **CSP** | **102 / 305** | **-15.62** | **-10.81** |
| 4A | CSP | 102 / 305 | -13.12 | -15.82 |
| 4B | CSP | 102 / 305 | -13.64 | -18.67 |
| 4C | CSP | 102 / 305 | -14.19 | -14.18 |
| **AVERAGE** | **CSP** | **102 / 305** | **-13.65** | **-16.22** |
| 6A | DFP | 102 / 305 | -17.56 | -15.66 |
| 6B | DFP | 102 / 305 | -16.60 | -14.82 |
| 6C | DFP | 102 / 305 | -17.55 | -15.90 |
| **AVERAGE** | **DFP** | **102 / 305** | **-17.24** | **-15.46** |

Table B4 – Monotonic Test Data From Hikita (2006)

| Test | Panel Type | Fastener Schedule | Maximum Wall Resistance ($S_u$) kN/m | Displ. @ 0.4$S_u$ ($\Delta_{net,0.4u}$) mm | Displ. @ $S_u$ ($\Delta_{net,u}$) mm | Displ. @ 0.8 $S_u$ ($\Delta_{net,0.8u}$) |
|---|---|---|---|---|---|---|
| 47A | DFP | 75/305 | 31.11 | 10.83 | 70.98 | 80.77 |
| 47B | DFP | 75/305 | 28.98 | 10.63 | 72.80 | 82.83 |
| 47C[1] | DFP | 75/305 | 32.40 | 11.25 | 70.12 | 74.43 |
| Average | | | 30.83 | 10.90 | 71.30 | 79.34 |
| 49A | OSB | 152/305 | 10.92 | 3.31 | 38.41 | 60.12 |
| 49B[1] | OSB | 152/305 | 11.75 | 4.13 | 40.61 | 52.67 |
| 49C | OSB | 152/305 | 13.32 | 4.28 | 45.96 | 64.17 |
| 49D | OSB | 152/305 | 12.13 | 3.71 | 40.32 | 52.16 |
| Average | | | 12.03 | 3.86 | 41.33 | 57.28 |
| 51A | OSB | 75/305 | 22.17 | 4.88 | 42.01 | 54.47 |
| 51B[1] | OSB | 75/305 | 23.11 | 4.69 | 36.66 | 41.12 |
| 51C | OSB | 75/305 | 22.35 | 4.02 | 36.86 | 48.5 |
| Average | | | 22.54 | 4.53 | 38.51 | 48.03 |
| 53A | CSP | 152/305 | 13.39 | 6.67 | 57.06 | 77.44 |
| 53B | CSP | 152/305 | 12.41 | 9.25 | 55.71 | 81.58 |
| 53C[1] | CSP | 152/305 | 13.15 | 5.71 | 55.84 | 76.12 |
| Average | | | 12.98 | 7.21 | 56.20 | 78.38 |
| 55A | CSP | 152/305 | 25.68 | 11.01 | 70.19 | 88.80 |
| 55B[1] | CSP | 75/305 | 28.36 | 11.31 | 69.91 | 75.91 |
| 55C | CSP | 75/305 | 24.70 | 11.56 | 68.44 | 83.94 |
| 55D | CSP | 75/305 | 27.08 | 12.26 | 71.94 | 84.14 |
| Average | | | 26.46 | 11.54 | 70.12 | 83.20 |

**Table B5 – Test Results For Reversed Cyclic Tests (Positive Cycles) from Hikita (2006)**

| Test | Panel Type | Fastener Schedule | Maximum Wall Resistance ($S_{u'+}$) (positive cycle) kN/m | Displacement as Su'+ ($\Delta_{net, u+}$) mm | $\Delta$net, 0.8u+ (mm) |
|---|---|---|---|---|---|
| 48A | DFP | 75/305 | 29.26 | 65.39 | 69.67 |
| 48B | DFP | 75/305 | 29.14 | 66.44 | 69.05 |
| 48C[1] | DFP | 75/305 | 28.35 | 50.05 | 74.47 |
| AVERAGE | | | 28.92 | 60.63 | 71.06 |
| 50A | OSB | 152/305 | 10.77 | 33.24 | 51.68 |
| 50B | OSB | 152/305 | 10.49 | 30.84 | 48.83 |
| 50C[1] | OSB | 152/305 | 11.11 | 46.66 | 48.51 |
| AVERAGE | | | 10.79 | 36.91 | 49.67 |
| 52A | OSB | 75/305 | 22.18 | 26.79 | 39.94 |
| 52B | OSB | 75/305 | 22.12 | 37.11 | 39.34 |
| 52C[1] | OSB | 75/305 | 25.64 | 41.25 | 42.21 |
| AVERAGE | | | 23.31 | 35.05 | 40.50 |
| 54A | CSP | 152/305 | 11.95 | 56.06 | 65.12 |
| 54B | CSP | 152/305 | 12.16 | 58.66 | 66.4 |
| 54C[1] | CSP | 152/305 | 12.96 | 41.29 | 65.2 |
| AVERAGE | | | 12.36 | 52.00 | 65.57 |
| 56A[1] | CSP | 75/305 | 26.90 | 57.13 | 58.05 |
| 56B | CSP | 75/305 | 25.56 | 60.29 | 63.78 |
| 56C | CSP | 75/305 | 25.85 | 57.6 | 59.52 |
| AVERAGE | | | 26.10 | 58.34 | 60.45 |

**Table B6 - Test Results For Reversed Cyclic Tests (Negative Cycles) from Hikita (2006)**

| Test | Panel Type | Fastener Schedule | Maximum Wall Resistance ($S_{u'-}$) (negative cycle) kN/m | Displacement as Su'- ($\Delta_{net, u-}$) mm |
|---|---|---|---|---|
| 48A | DFP | 75/305 | -27.99 | -49.09 |
| 48B | DFP | 75/305 | -27.20 | -47.25 |
| 48C[1] | DFP | 75/305 | -27.85 | -41.68 |
| AVERAGE | | | -27.68 | -46.01 |
| 50A | OSB | 152/305 | -10.70 | -33.01 |
| 50B | OSB | 152/305 | -10.06 | -34.26 |
| 50C[1] | OSB | 152/305 | -10.79 | -31.22 |
| AVERAGE | | | -10.52 | -32.83 |
| 52A | OSB | 75/305 | -20.83 | -30.82 |
| 52B | OSB | 75/305 | -22.23 | -27.1 |
| 52C[1] | OSB | 75/305 | -22.99 | -29.58 |
| AVERAGE | | | -22.01 | -29.17 |
| 54A | CSP | 152/305 | -10.93 | -43.43 |
| 54B | CSP | 152/305 | -11.56 | -40.49 |
| 54C[1] | CSP | 152/305 | -11.59 | -39.97 |
| AVERAGE | | | -11.36 | -41.30 |
| 56A[1] | CSP | 75/305 | -21.47 | -45.98 |
| 56B | CSP | 75/305 | -22.60 | -39.975 |
| 56C | CSP | 75/305 | -20.22 | -39.13 |
| AVERAGE | | | -21.43 | -41.70 |

**Table B7 – Test Data from Nguyen, Hall and Serrette (1996)**

| Test Specimen | Maximum Load Capacity (lb/ft) | Displacement at max Load (in) |
|---|---|---|
| A6 | 1038 | 2.41 |
| A7 | 1087 | 2.43 |
| A2 | 931 | 1.50 |
| A3 | 891 | 1.47 |
| A5 | 1033 | 2.19 |
| A6 | 989 | 1.94 |
| E1 | 990 | 2.38 |
| E2 | 1061 | 2.77 |
| D1 | 846 | 1.50 |
| D2 | 875 | 1.50 |
| D3 | 1473 | 2.36 |
| D4 | 1350 | 2.30 |
| D5 | 1763 | 2.30 |
| D6 | 1709 | 1.86 |
| D7 | 1933 | 1.84 |
| D8 | 1891 | 2.10 |
| F1 | 1190 | 2.25 |
| F2 | 1243 | 2.23 |
| F3 | 1516 | 2.37 |
| F4 | 1604 | 2.52 |
| F5 | 1918 | 1.84 |
| F6 | 1850 | 1.73 |
| A1 | 545 | 0.77 |
| A3 | 621 | 0.96 |
| A2 | 915 | 0.95 |

**Table B8– Test Observations from Serrette and Research Assistants (1997)**

| Test Specimen | Behavior of Wall Assembly |
|---|---|
| A1 | Screws pull through plywood sheathing at the bottom corners |
| A2 | Screw pull through sheathing along bottom edge |
| A3 | Buckling of bottom track after screws pulled through sheathing. Buckling in chord studs approx. 2ft above track. |
| A4 | Screws pull through plywood sheathing at bottom corners. Buckling in bottom track at shear anchor. |
| A5 | Screws break vertical edges of OSB. Screws pull through OSB along bottom edge. |
| A6 | Screws break vertical edges of OSB. Screws pull through OSB along bottom edge. |
| A7 | Screws pull through OSB sheathing along bottom edge and both sides. Local buckling in the lip of all studs. |
| A8 | Screws pulled through plywood along top and vertical edges. |
| B1 | Screw shear along bottom track. Screws pulled out of sheathing along vertical edges. |
| B2 | Screws pulled through panel along vertical edges and along bottom track. |
| B3 | Screw shear along entire vertical edge (load side). Screws pull through panel at top and bottom track. |
| B4 | Screw pull through panel along vertical edge and bottom track. Some screws sheared. |
| C1 | Buckling in both chord studs (at web knockouts) |
| C2 | Buckling in both chord studs (at web knockouts) |
| C3 | Top and bottom track pulled out of plane of the wall. Buckling in chord stud at loaded end. |
| C4 | Top and bottom track pulled out of plane of the wall. Buckling in chord stud occurred after bending in top and bottom track. |
| D1 | Screws pulled out of studs. Screws rupture edge of sheathing. Many screws loose after test is stopped. |
| D2 | Screws pulled out of stud along top track and at vertical edges adjacent to top track. Screws pulled out interior stud close to top track. |

**Table B9 – Average Max Loads and Displacements for Similar Test Specimens from Serrette (1997)**

| Test Specimen | Average Maximum Load (lb/ft) | Displacement at Max Load (in) |
|---|---|---|
| A1 | 1775 | 2.2 |
| A2 | | |
| A3 | 2190 | 2.7 |
| A4 | | |
| A5 | 1523 | 1.6 |
| A6 | | |
| A7 | 2058 | 2.0 |
| A8 | | |
| B1 | 892 | 1.8 |
| B2 | | |
| B3 | 904 | 1.2 |
| B4 | | |
| C1 | 821 | 1.2 |
| C2 | | |
| C3 | 839 | 0.8 |
| C4 | | |
| D1 | 392 | 1.0 |
| D2 | | |

## Table B10- Test Observations from Branston (2004)

| Specimen ID | Test Protocol | Pullout withdrawl (Po) | Fatigue Fracture Shear (FF) | Pull Through Sheathing (PT) | Partial Pull-through (PPT) | Tearout of Sheathing (TO) | Wood bearing Failure (WB) |
|---|---|---|---|---|---|---|---|
| 7A | MONO | X | X | X | | X | |
| 7B | MONO | | X | X | X | X | X |
| 7C | MONO | X | X | X | X | X | X |
| 8A | CYCLIC | | X | X | X | X | X |
| 8B | CYCLIC | X | X | X | | | X |
| 8C | CYCLIC | X | X | X | X | | X |
| 9A | MONO | | X | X | | X | |
| 9B | MONO | | X | X | X | X | |
| 9C | MONO | | | X | X | X | |
| 10A | CYCLIC | | X | X | | X | X |
| 10B | CYCLIC | X | X | X | | X | |
| 10C | CYCLIC | | X | X | | X | X |
| 11A | MONO | | | | X | X | |
| 11B | MONO | | X | X | X | | X |
| 11C | MONO | | X | X | X | X | X |
| 12A | CYCLIC | | X | X | X | X | |
| 12B | CYCLIC | | X | X | X | X | X |
| 12C | CYCLIC | | X | X | X | X | X |
| 13A | MONO | | X | X | X | X | X |
| 13B | MONO | | | X | X | | X |
| 13C | MONO | | | X | X | X | X |
| 14A | CYCLIC | | X | X | X | X | X |
| 14B | CYCLIC | | X | X | X | X | X |
| 14C | CYCLIC | X | X | X | X | X | X |
| 14D | CYCLIC | | | X | X | X | X |
| 21A | MONO | | | X | X | X | |
| 21B | MONO | | X | X | X | X | |
| 21C | MONO | | X | X | X | | |
| 22A | CYCLIC | | X | X | X | X | X |
| 22B | CYCLIC | | X | X | X | X | X |
| 22C | CYCLIC | | X | X | X | X | X |
| 23A | MONO | | | X | X | X | |
| 23B | MONO | | | X | X | X | |
| 23C | MONO | | X | X | X | | |
| 24A | CYCLIC | | | X | X | X | X |
| 24B | CYCLIC | | X | X | X | X | X |
| 24C | CYCLIC | X | X | X | X | X | X |
| 25A | MONO | | | X | X | X | |
| 25B | MONO | | | X | X | X | |
| 25C | MONO | | | X | X | X | |
| 26A | CYCLIC | X | | X | X | X | X |
| 26B | CYCLIC | | X | X | X | X | X |
| 26C | CYCLIC | X | X | X | X | | X |

**Table B11 - Test Observations from Boudreault (2004)**

| Specimen ID | Panel Type | Test Protocol | Pullout withdrawl (Po) | Fatigue Fracture Shear (FF) | Pull Through Sheathing (PT) | Partial Pull-through (PPT) | Tearout of Sheathing (TO) | Wood bearing Failure (WB) |
|---|---|---|---|---|---|---|---|---|
| 1A | | MONO | | | X | X | X | X |
| 1B | | MONO | | | X | | X | |
| 1C | | MONO | | X | X | | X | X |
| 1D | | MONO | | | X | X | X | |
| 1E | | MONO | | | X | | X | X |
| 1F | | MONO | | | X | X | | X |
| 3A | | CYCLIC | | X | X | X | | X |
| 3B | | CYCLIC | X | X | X | X | | X |
| 3C | | CYCLIC | X | X | X | | X | |
| 4A | | CUREE | | X | X | X | | X |
| 4B | | CUREE | | X | X | | X | X |
| 4C | | CUREE | | X | X | X | X | X |
| 5A | | MONO | | | X | | X | X |
| 5B | | MONO | | | X | X | X | X |
| 5C | | MONO | | | X | X | X | X |
| 5D | | MONO | | | X | | X | X |
| 6A | | CYCLIC | | X | X | X | X | X |
| 6B | | CYCLIC | | X | X | X | X | X |
| 6C | | CYCLIC | | X | X | X | X | |

**Table B12- Test Observations from Chen (2004)**

| Specimen ID | Panel Type | Test Protocol | Pullout withdrawl (Po) | Fatigue Fracture Shear (FF) | Pull Through Sheathing (PT) | Partial Pull-through (PPT) | Tearout of Sheathing (TO) | Wood bearing Failure (WB) |
|---|---|---|---|---|---|---|---|---|
| 15A | | MONO | | | | | X | |
| 15B | | MONO | | | X | X | X | |
| 15C | | MONO | | | X | X | X | |
| 16A | | CYCLIC | | | X | X | X | |
| 16B | | CYCLIC | | | | X | X | |
| 16C | | CYCLIC | | | | | X | X |
| 17A | | MONO | | | X | X | X | |
| 17B | | MONO | | | X | | X | |
| 17C | | MONO | | | X | X | X | |
| 18A | | CYCLIC | | | X | X | X | |
| 18B | | CYCLIC | | | | X | X | |
| 18C | | CYCLIC | | | X | X | X | X |
| 19A | | MONO | | | X | X | X | X |
| 19B | | MONO | | | X | X | X | X |
| 19C | | MONO | | | X | X | X | |
| 20A | | CYCLIC | | | X | X | X | X |
| 20B | | CYCLIC | | | X | | X | |
| 20C | | CYCLIC | | | X | X | X | |
| 27A | | MONO | | | X | X | X | |
| 27B | | MONO | | | X | X | X | X |
| 27C | | MONO | | | X | X | X | X |
| 28A | | CYCLIC | | | X | X | X | |
| 28B | | CYCLIC | | | | X | X | |
| 28C | | CYCLIC | | | | X | X | |
| 29A | | MONO | | X | X | X | X | X |
| 29B | | MONO | | X | X | X | X | X |
| 29C | | MONO | | X | X | X | X | X |
| 30A | | CYCLIC | | | X | X | X | X |
| 30B | | CYCLIC | | | X | X | X | X |
| 30C | | CYCLIC | | | X | X | X | X |
| 31A | | MONO | | | X | X | X | X |
| 31B | | MONO | | | X | X | X | X |
| 31C | | MONO | | | X | X | X | X |
| 31D | | MONO | | | X | X | X | X |
| 31E | | MONO | | | X | X | X | X |
| 31F | | MONO | | | X | X | X | X |
| 32A | | CYCLIC | | | X | X | X | X |
| 32B | | CYCLIC | | | X | X | X | X |
| 32C | | CYCLIC | | | X | X | X | X |
| 33A | | MONO | | | | X | X | X |
| 33B | | MONO | | | | X | X | X |
| 33C | | MONO | | | | X | X | X |
| 34A | | CYCLIC | | | X | X | X | X |
| 34B | | CYCLIC | | | X | X | X | X |
| 34C | | CYCLIC | | | X | X | X | X |
| 34D | | CYCLIC | | | X | X | X | X |

**Table B13-Test Observations from Rokas (2006)**

| Specimen ID | Panel Type | Test Protocol | Pullout withdrawl (Po) | Fatigue Fracture Shear (FF) | Pull Through Sheathing (PT) | Partial Pull-through (PPT) | Tearout of Sheathing (TO) | Wood bearing Failure (WB) |
|---|---|---|---|---|---|---|---|---|
| 36A | CSP | CUREE | | | X | | | X |
| 36B | CSP | CUREE | | | X | | | X |
| 36C | CSP | CUREE | | | X | | | X |
| 38A | CSP | CUREE | | | X | X | | X |
| 38B | CSP | CUREE | | | X | X | | X |
| 38C | CSP | CUREE | | | X | X | | X |
| 40A | CSP | CUREE | | | X | X | | X |
| 40B | CSP | CUREE | | | X | X | | X |
| 40C | CSP | CUREE | | | X | X | | X |

**Table 14 - Test Observations from Blais (2006)**

| Specimen ID | Test Protocol | Pullout withdrawl (Po) | Fatigue Fracture Shear (FF) | Pull Through Sheathing (PT) | Partial Pull-through (PPT) | Tearout of Sheathing (TO) | Wood bearing Failure (WB) |
|---|---|---|---|---|---|---|---|
| 41A | MONO | | | X | X | | X |
| 41B | MONO | | X | X | X | | X |
| 41C | MONO | | | X | X | | X |
| 43A | MONO | | x | x | x | | x |
| 43B | MONO | | | X | X | | X |
| 43C | MONO | | | X | X | | X |
| 45A | MONO | | | X | X | | X |
| 45B | MONO | | | X | X | | X |
| 45C | MONO | | | X | X | | X |
| 42A | CYCLIC | | | X | X | | X |
| 42B | CYCLIC | | X | X | X | | X |
| 42C | CYCLIC | | X | X | X | | X |
| 44A | CYCLIC | | | X | X | | X |
| 44B | CYCLIC | | | X | X | | X |
| 44C | CYCLIC | | | X | X | | X |
| 46A | CYCLIC | | X | X | X | | X |
| 46B | CYCLIC | | X | X | X | | X |
| 46C | CYCLIC | | X | X | X | | X |

**Table B15 - Test Observations from Hikita (2006)**

| Specimen ID | Test Protocol | Pullout withdrawl (Po) | Fatigue Fracture Shear (FF) | Pull Through Sheathing (PT) | Partial Pull-through (PPT) | Tearout of Sheathing (TO) | Wood bearing Failure (WB) |
|---|---|---|---|---|---|---|---|
| 47A | MONO | | | X | X | X | X |
| 47B | MONO | | | X | X | | X |
| 47C | MONO | | | X | X | X | X |
| 48A | CYCLIC | X | | X | X | | X |
| 48B | CYCLIC | | | X | X | | X |
| 48C | CYCLIC | X | | X | X | | X |
| 49A | MONO | | | X | X | X | |
| 49B | MONO | | | X | X | X | |
| 49C | MONO | | | X | X | X | |
| 49D | MONO | | | X | X | X | X |
| 50A | CYCLIC | | | X | X | X | |
| 50B | CYCLIC | | | X | X | X | X |
| 50C | CYCLIC | | | X | X | X | X |
| 51A | MONO | | | X | X | | X |
| 51B | MONO | | | X | X | | X |
| 51C | MONO | | | X | X | X | X |
| 52A | CYCLIC | | | X | | | X |
| 52B | CYCLIC | | | X | X | | |
| 52C | CYCLIC | | | X | X | X | X |
| 53A | MONO | X | | X | | X | |
| 53B | MONO | | | X | X | X | X |
| 53C | MONO | | | X | X | X | X |
| 54A | CYCLIC | | X | X | X | X | X |
| 54B | CYCLIC | | | X | X | X | X |
| 54C | CYCLIC | | | X | X | X | X |
| 55A | MONO | | | X | X | X | X |
| 55B | MONO | | | X | X | X | X |
| 55C | MONO | | | X | X | X | X |
| 55D | MONO | | | X | X | X | X |
| 56A | CYCLIC | | | X | X | | X |
| 56B | CYCLIC | | | X | X | | X |
| 56C | CYCLIC | | | X | X | | X |

## Appendix C - Lognormal Fragility Functions using PGA as the EDP

This appendix contains fragility curves developed from SAPWood output, plotted with log normally distributed data points.

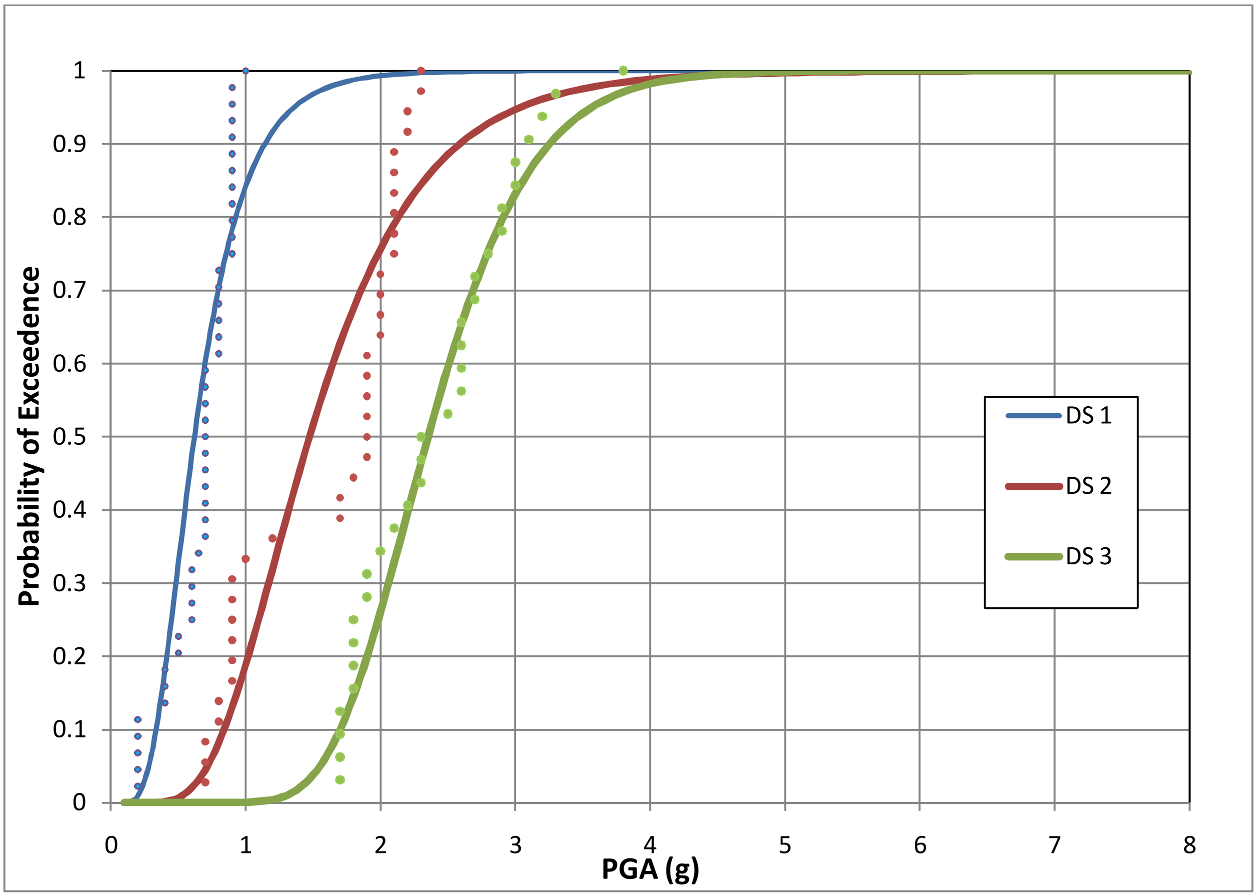


**Figure C1 – Fragility Curves for Walls with WSP Sheathing and 6"/12" Fastener Spacing**

**Table A 4 – Medians and Dispersions for all Walls with WSP Sheathing and 6"/12" Fastener Spacing**

| $DS_i$ | Median θ | Dispersion β | # of specimens | Lilliefors Test @ 5% significance |
|---|---|---|---|---|
| DS1 | 062 | 0.48 | 44 | Fails |
| DS2 | 1.47 | 0.44 | 38 | Fails |
| DS3 | 2.36 | 0.25 | 32 | Passes |

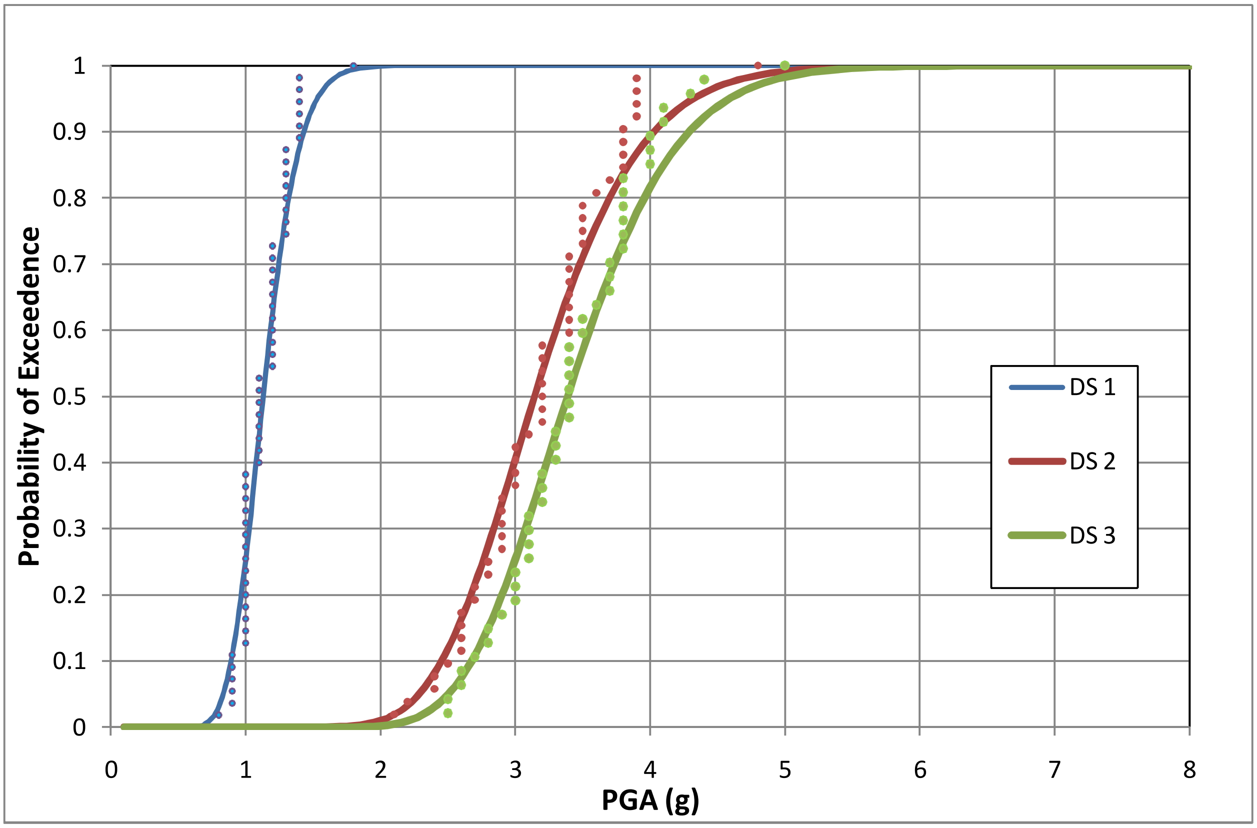


**Figure C2 - Fragility Curves for Walls with WSP Sheathing and 4"/12" Fastener Spacing**

**Table C2 - Medians and Dispersions for Walls with WSP Sheathing and 4''/12'' Fastener Spacing**

| $DS_i$ | Median $\theta$ | Dispersion $\beta$ | # of specimens | Lilliefors Test @ 5% significance |
|---|---|---|---|---|
| DS1 | 1.13 | 0.18 | 55 | Fails |
| DS2 | 3.14 | 0.19 | 52 | Passes |
| DS3 | 3.39 | 0.18 | 47 | Passes |

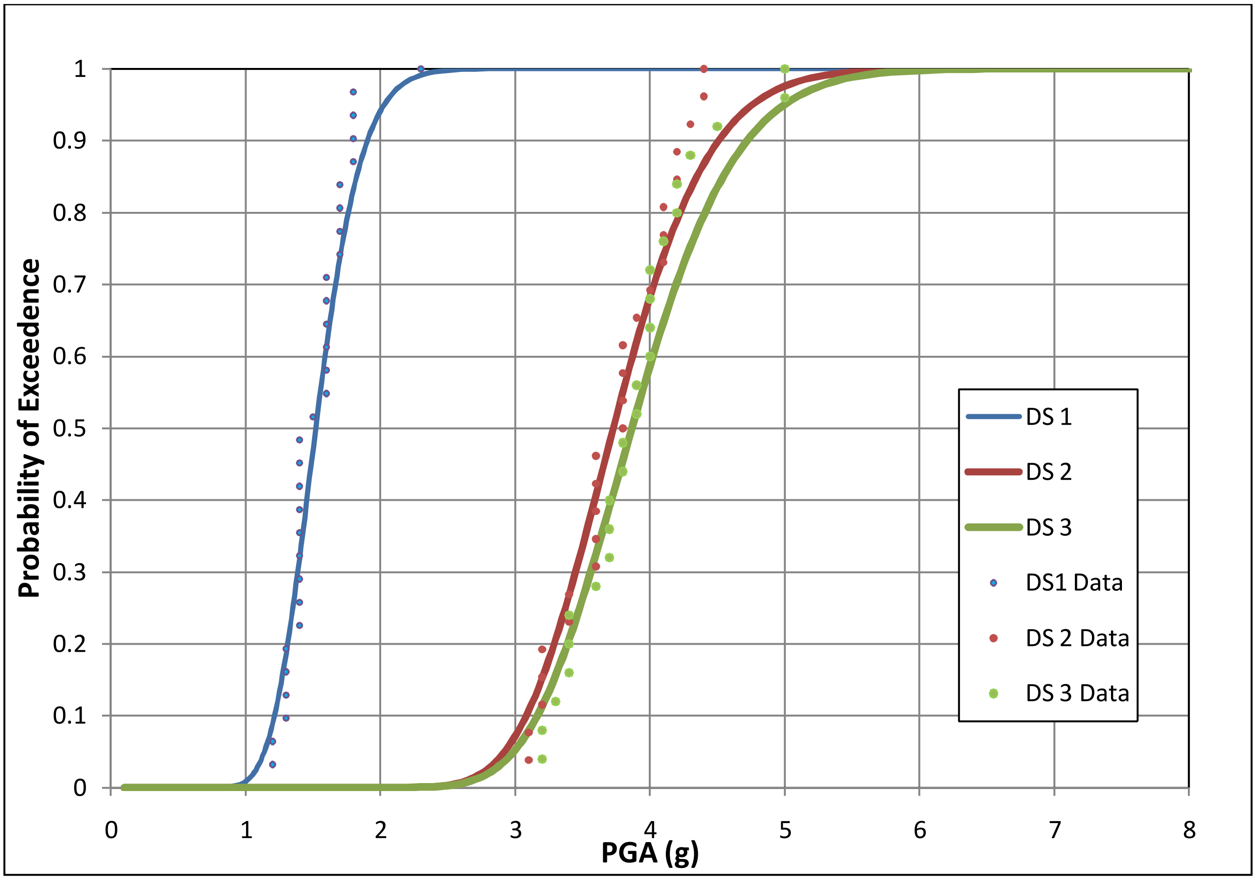


**Figure C3 – Fragility Curves for Walls with WSP Sheathing and 3"/12" Fastener Spacing**

**Table C3 - Medians and Dispersions for Walls w;ith WSP Sheathing and 3"/12" Fastener Spacing**

| $DS_i$ | Median θ | Dispersion β | # of specimens | Lilliefors Test @ 5% significance |
|---|---|---|---|---|
| DS1 | 1.52 | 0.18 | 31 | Passes |
| DS2 | 3.73 | 0.15 | 26 | Passes |
| DS3 | 3.86 | 0.16 | 25 | Passes |

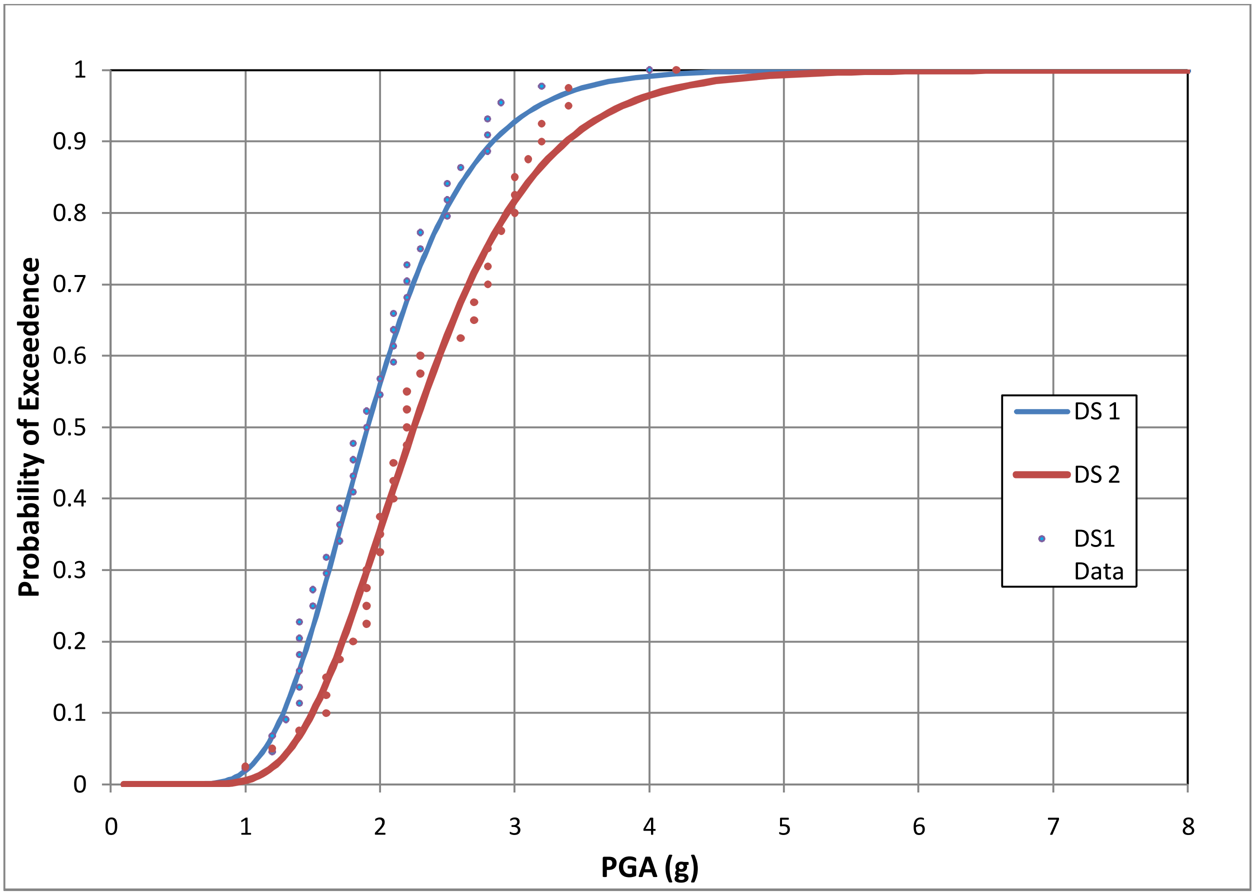


**Figure C4 - Fragility Curves for Walls with X-Bracing**

**Table C4 - Medians and Dispersions for Walls with X-Bracing**

| $DS_i$ | Median θ | Dispersion β | # of specimens | Lilliefors Test @ 5% significance |
|---|---|---|---|---|
| DS1 | 1.91 | 0.31 | 44 | Passes |
| DS2 | 2.25 | 0.32 | 40 | Passes |

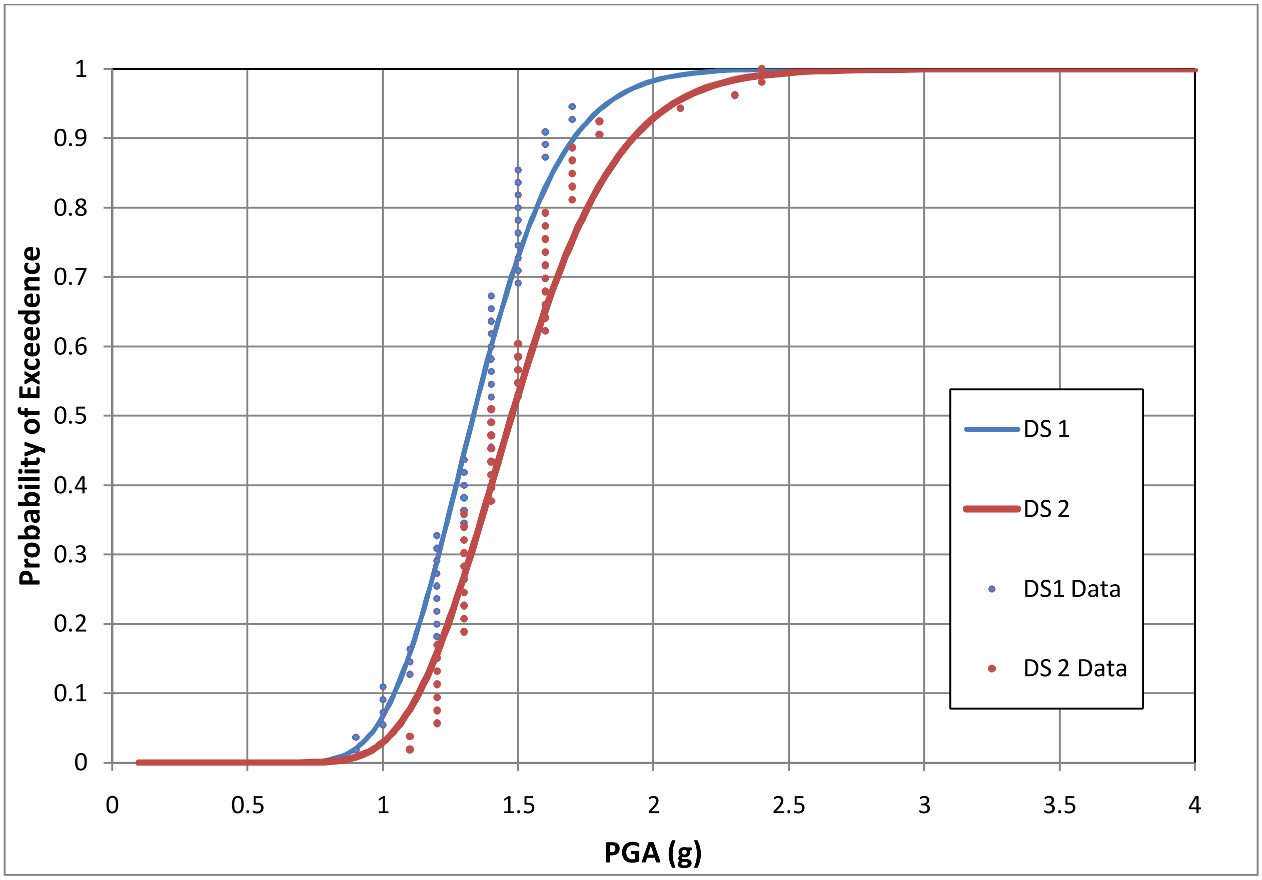


**Figure C5 – Fragility Curves for Walls with Steel Sheathing**

**Table C5 - Medians and Dispersions for Walls with Steel Sheathing**

| $DS_i$ | Median θ | Dispersion β | # of specimens | Lilliefors Test @ 5% significance |
|---|---|---|---|---|
| DS1 | 1.33 | 0.19 | 55 | Passes |
| DS2 | 1.48 | 0.21 | 53 | Passes |

## Appendix D – PGA vs. Horizontal Displacement Plots From SAPWood

**Note to reader: Each** PGA vs. Horizontal Displacement graph shown in this appendix contains values for each of the 10 earthquake records presented in Table 17. The record ID numbers are shown in the legend of Figure D1. Legends for other PGA vs. Horizontal Displacement graphs are identical to that seen in Figure D1. Legends are omitted from other graphs in this section for brevity.

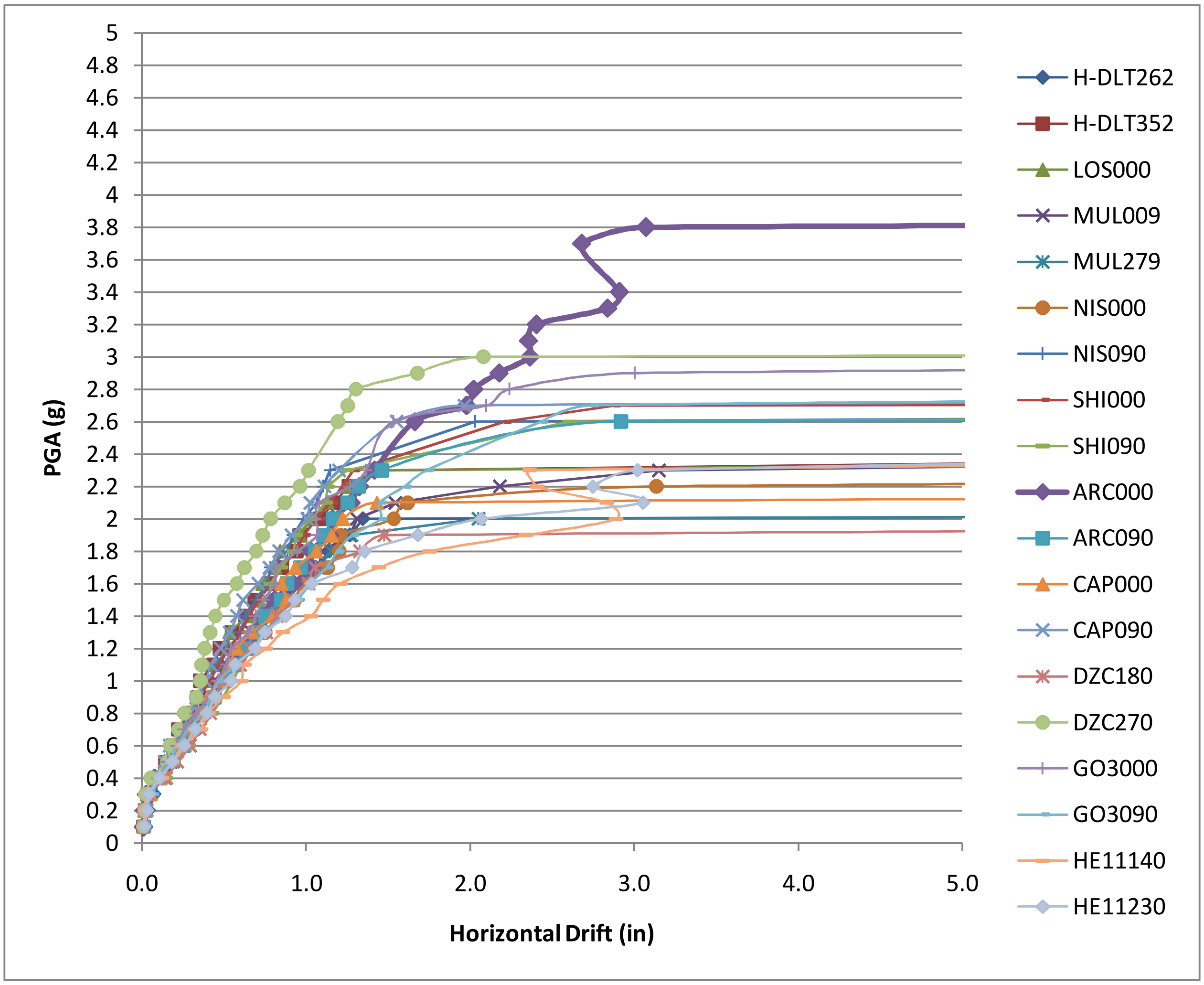


**Figure D 1 – PGA vs. Horizontal Displacement Graph for Model Ply1 (6"/12" Fastener Spacing)**

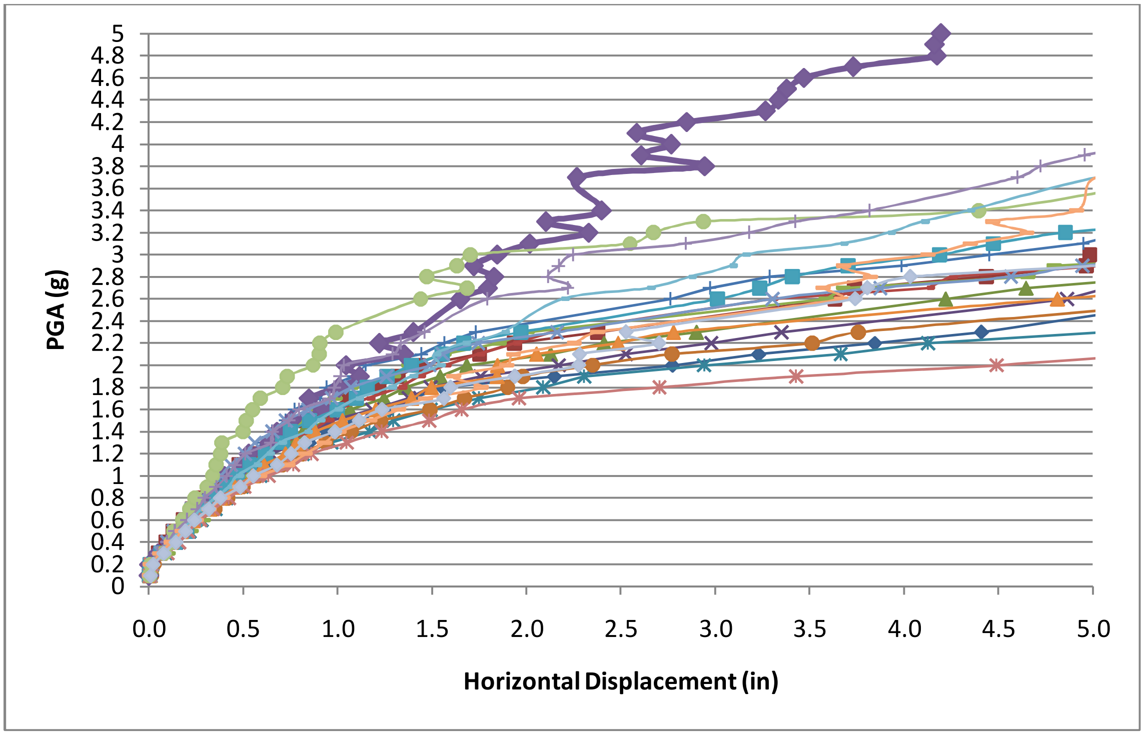


**Figure D 2 - PGA vs. Horizontal Displacement Graph for Model Ply2 (6"/12" Fastener Spacing)**

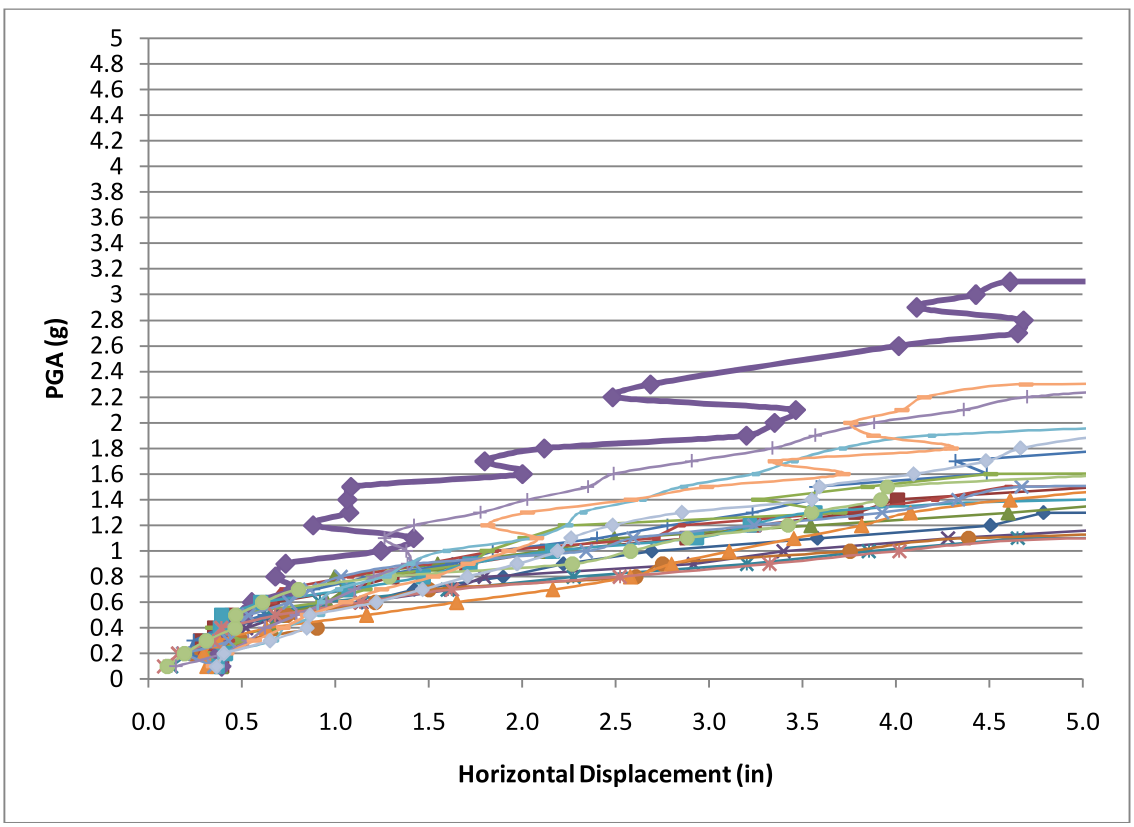


**Figure D 3 - PGA vs. Horizontal Displacement Graph for Model E1 (6"/12" Fastener Spacing)**

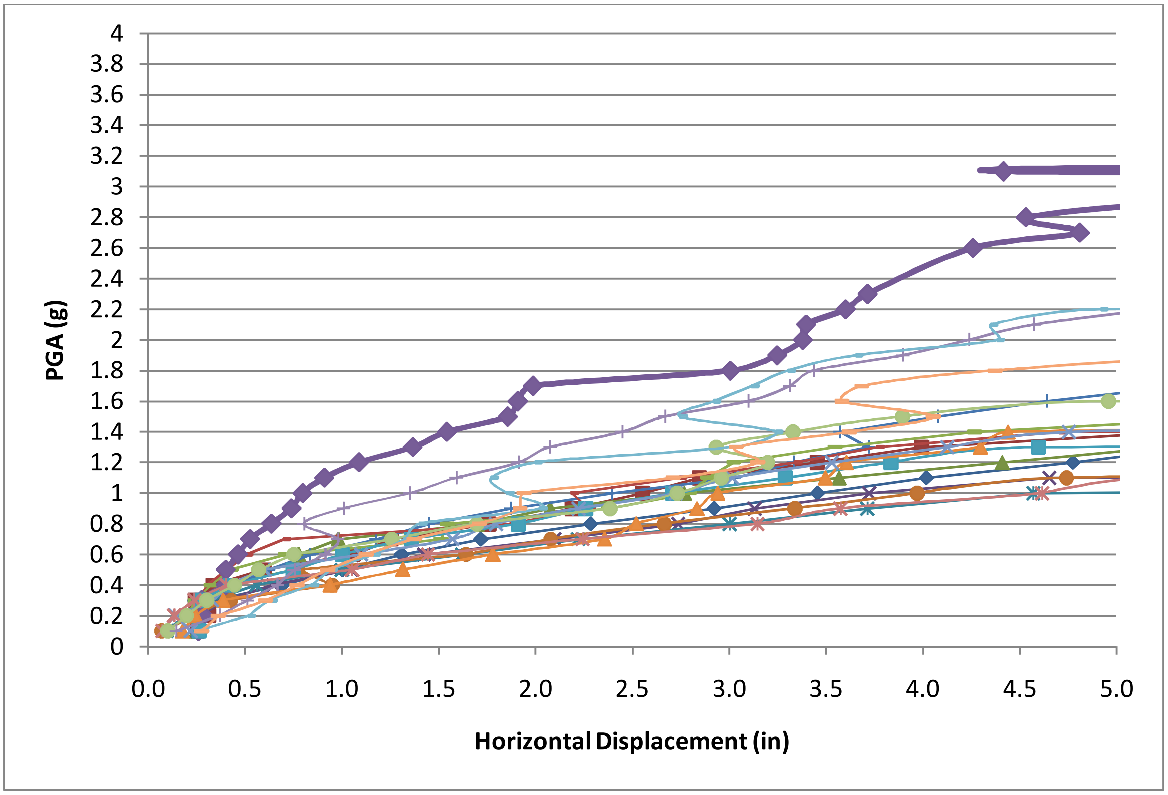


**Figure D 4 - PGA vs. Horizontal Displacement Graph for Model E2(6"/12" Fastener Spacing)**

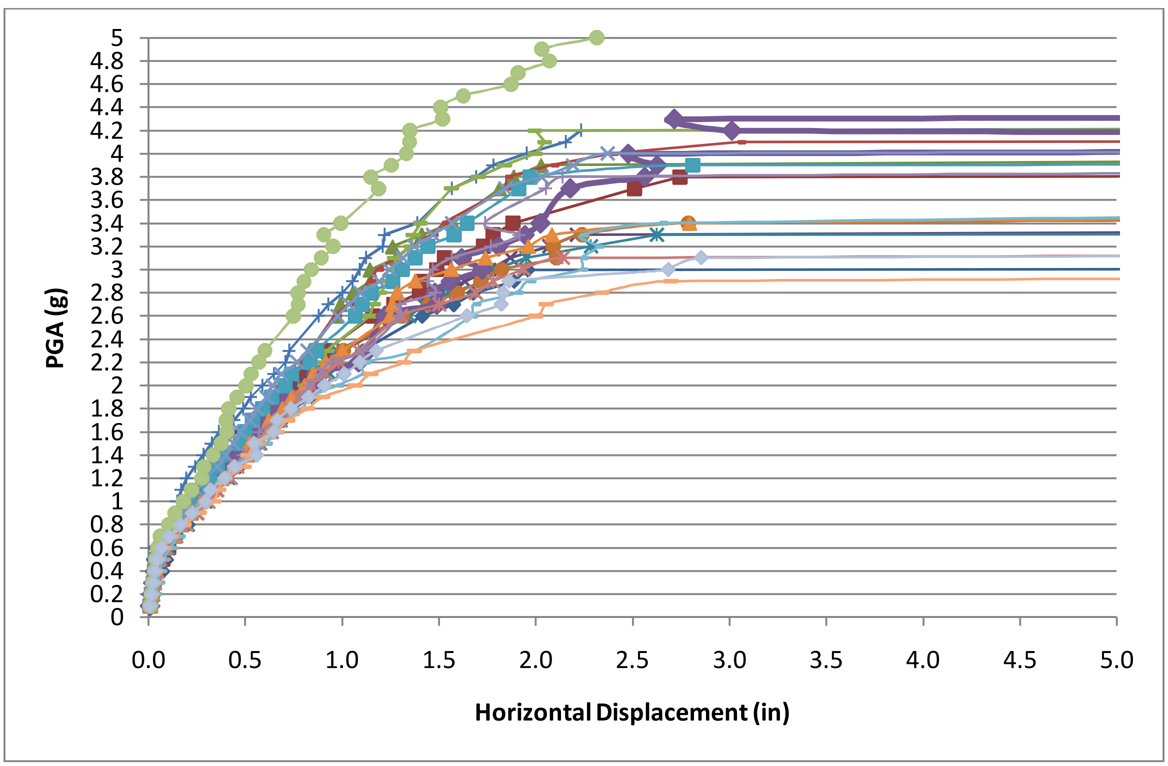


**Figure D 5 – PGA vs. Horizontal Displacement Graph for Model OSB3 (4"/12" Fastener Spacing)**

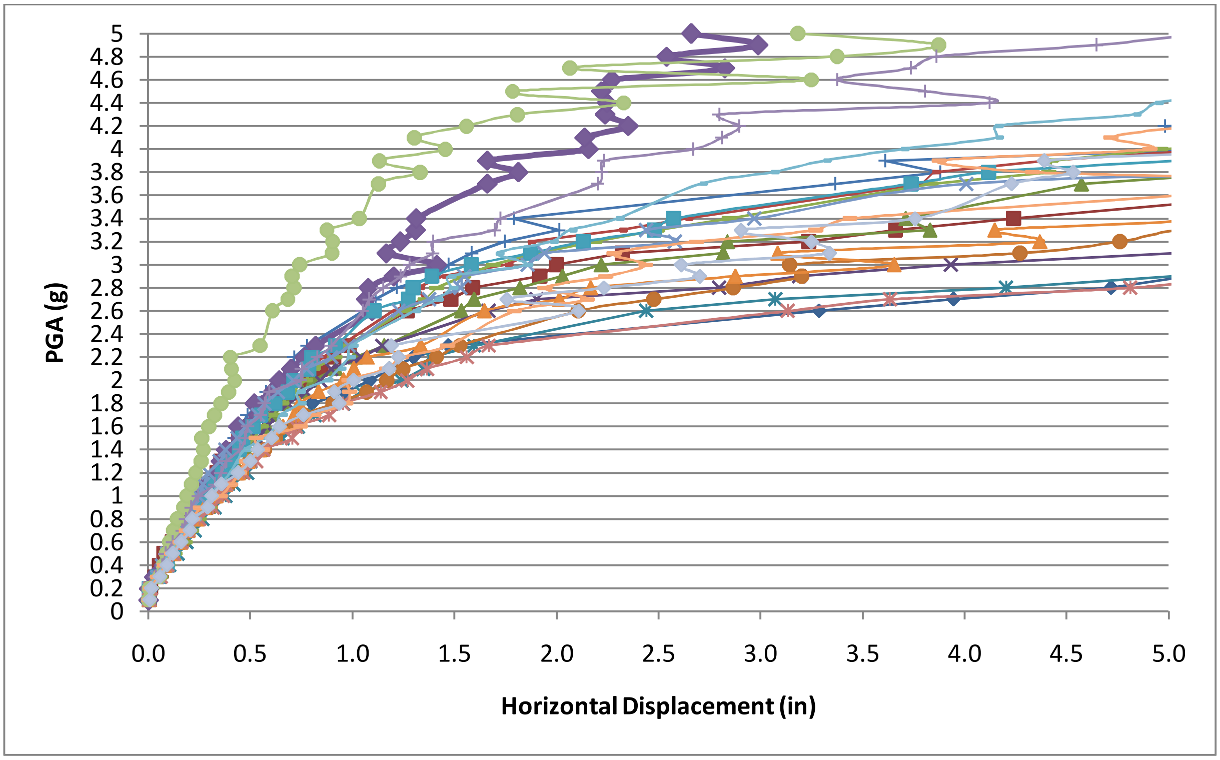


**Figure D 6 - PGA vs. Horizontal Displacement Graph for Model OSB4 (4"/12" Fastener Spacing)**

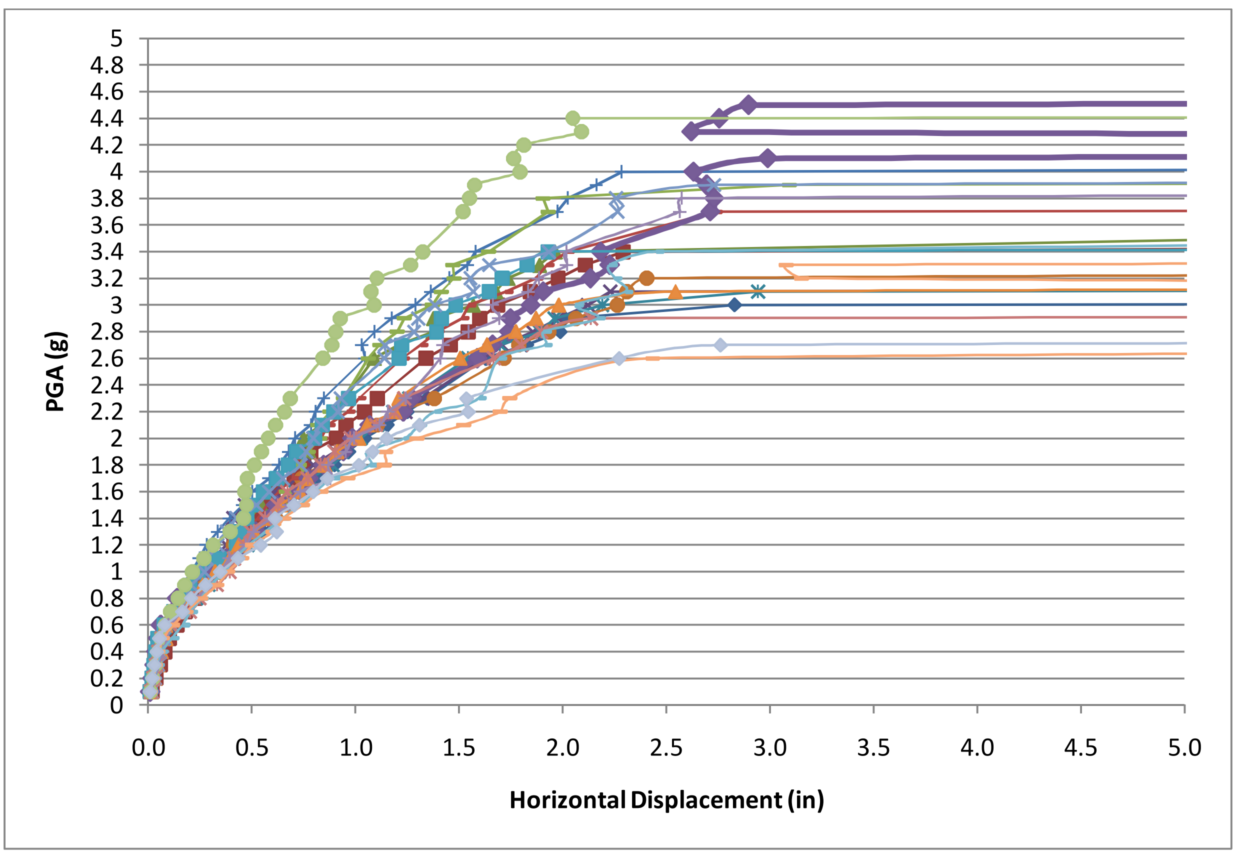


**Figure D 7 - PGA vs. Horizontal Displacement Graph for Model PLY3 (4"/12" Fastener Spacing**

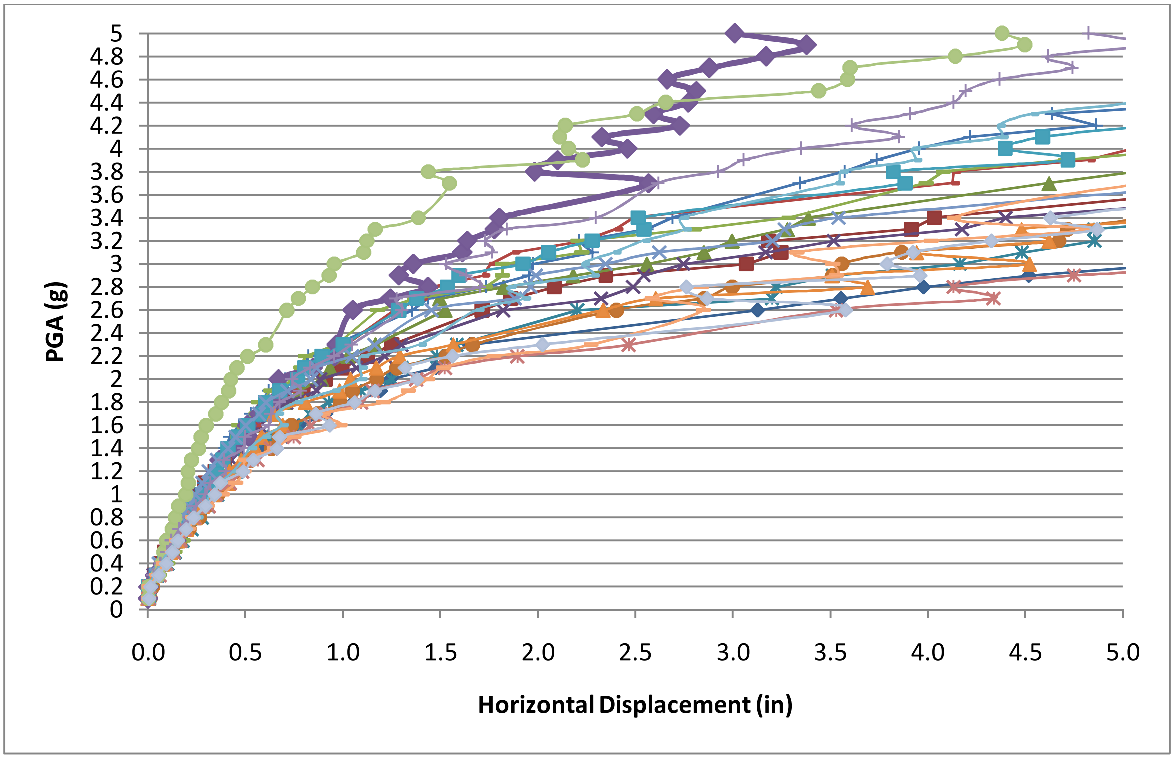


**Figure D 8 - PGA vs. Horizontal Displacement Graph for Model PLY4 (4"/12" Fastener Spacing)**

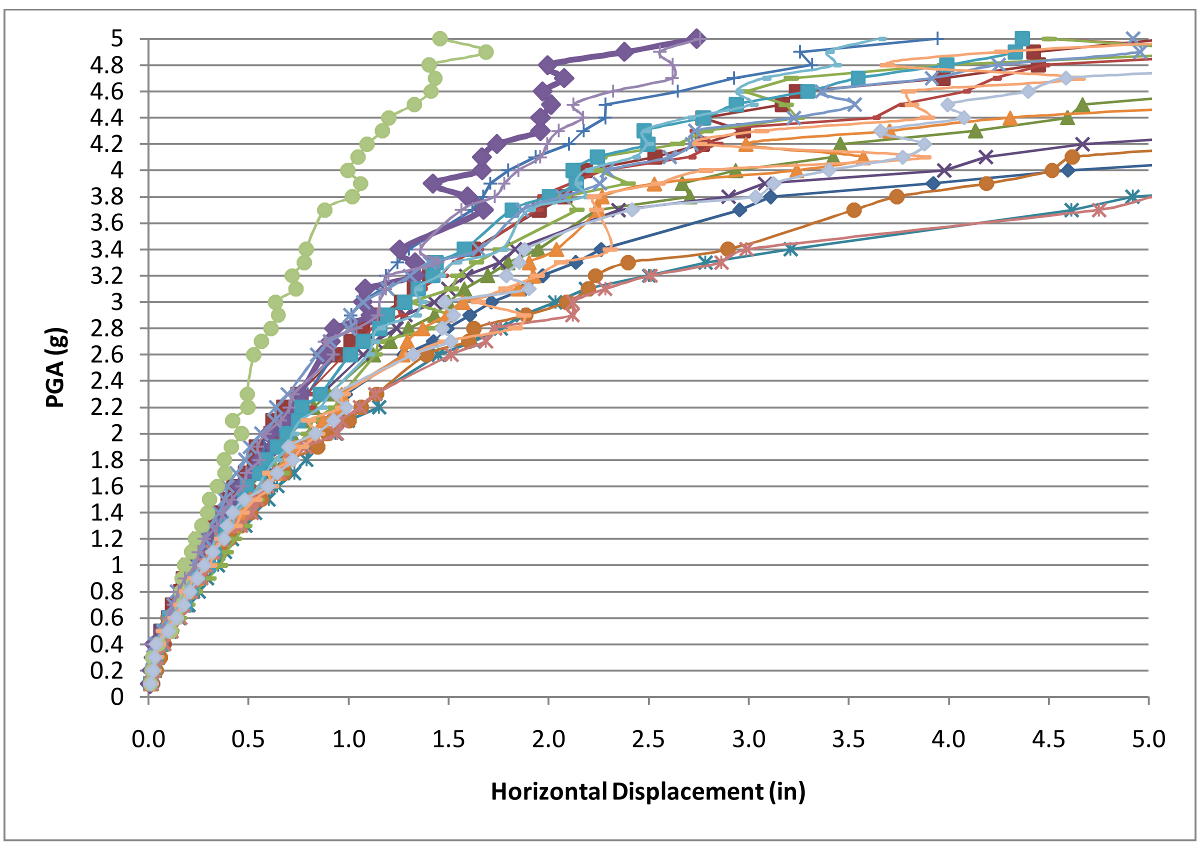


**Figure D 9 – PGA vs. Horizontal Displacement Graph for Model PLY 5 (3"/12" Fastener Spacing)**

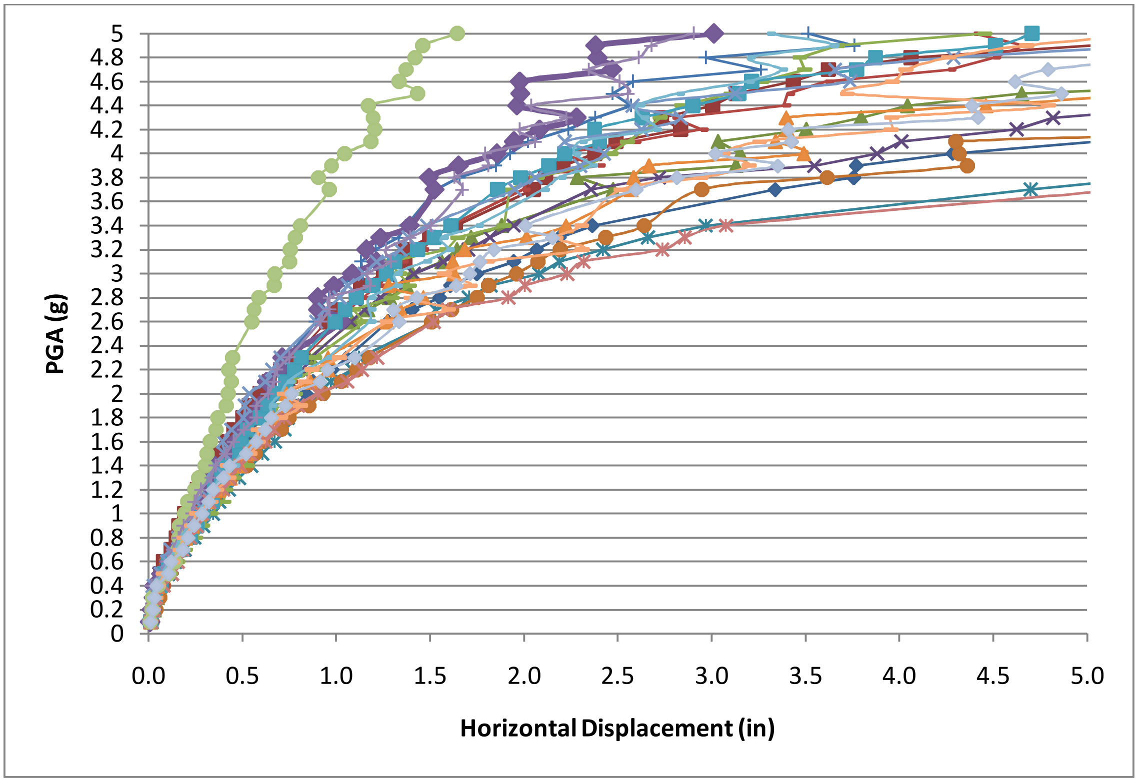


Figure D 10 - PGA vs. Horizontal Displacement Graph for Model PLY 6 (3”/12” Fastener Spacing

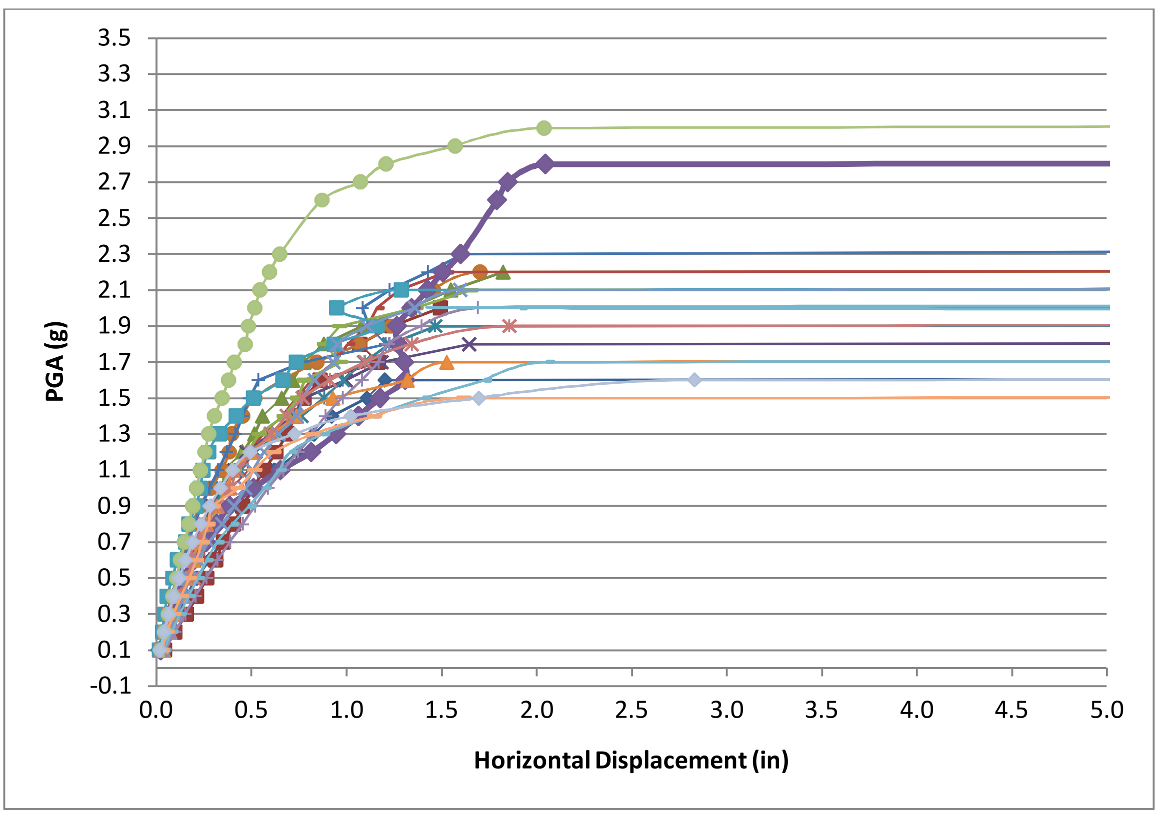


Figure D 11 – PGA vs. Horizontal Displacement Graph for Model C1 (X-Brace)

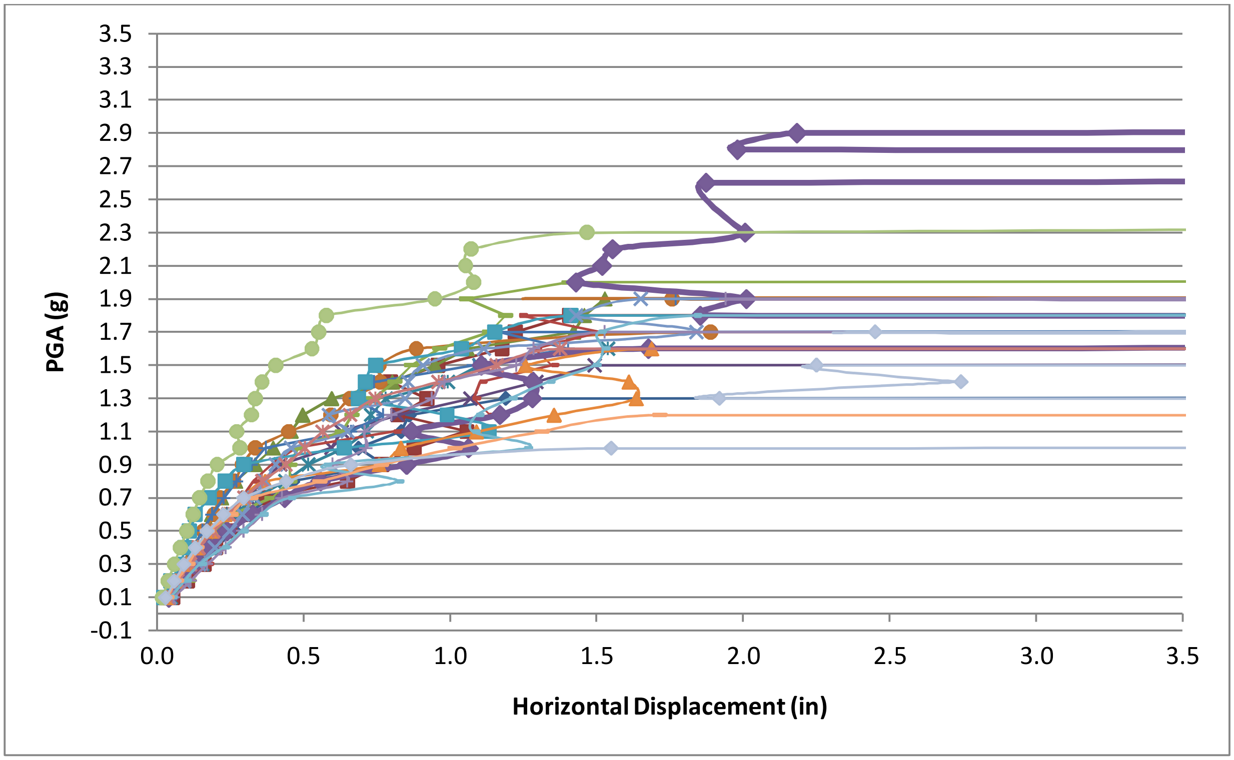


**Figure D 12– PGA vs. Horizontal Displacement Graph for Model C2 (X-Brace)**

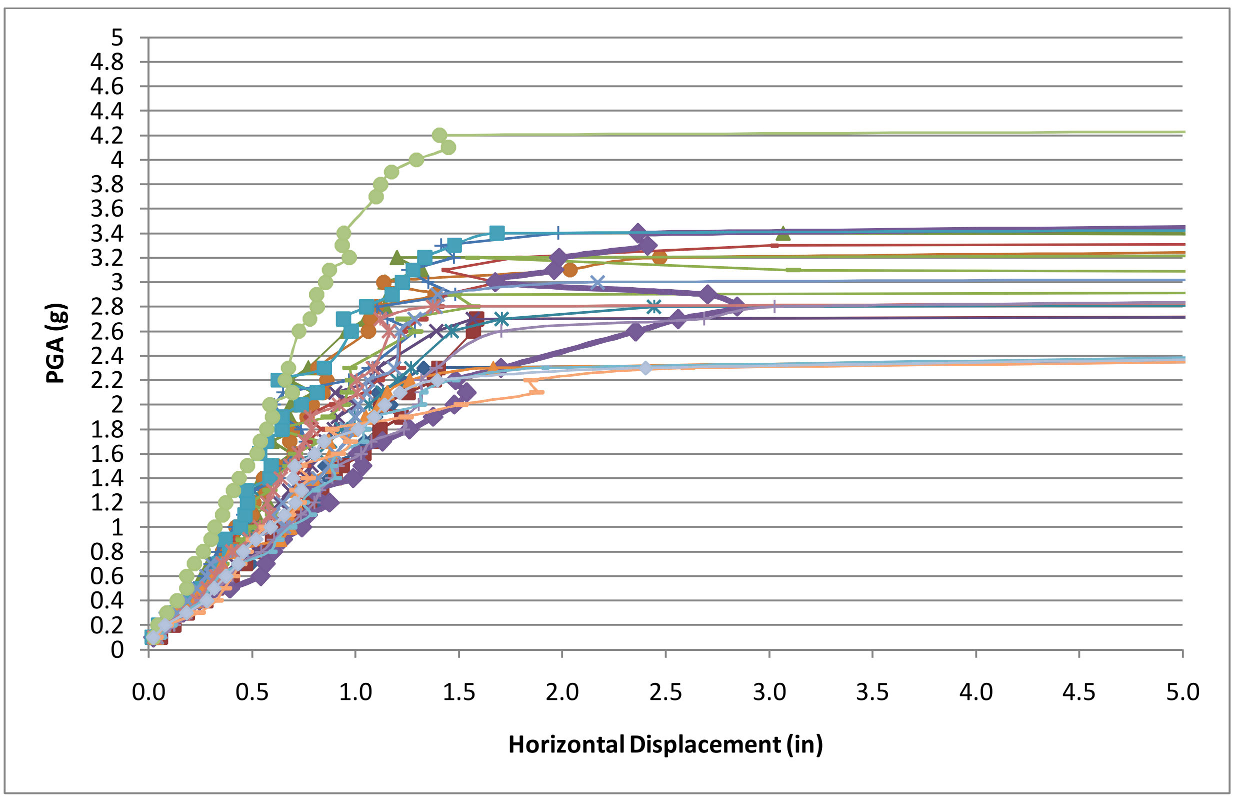


**Figure D 13– PGA vs. Horizontal Displacement Graph for Model C3 (X-Brace)**

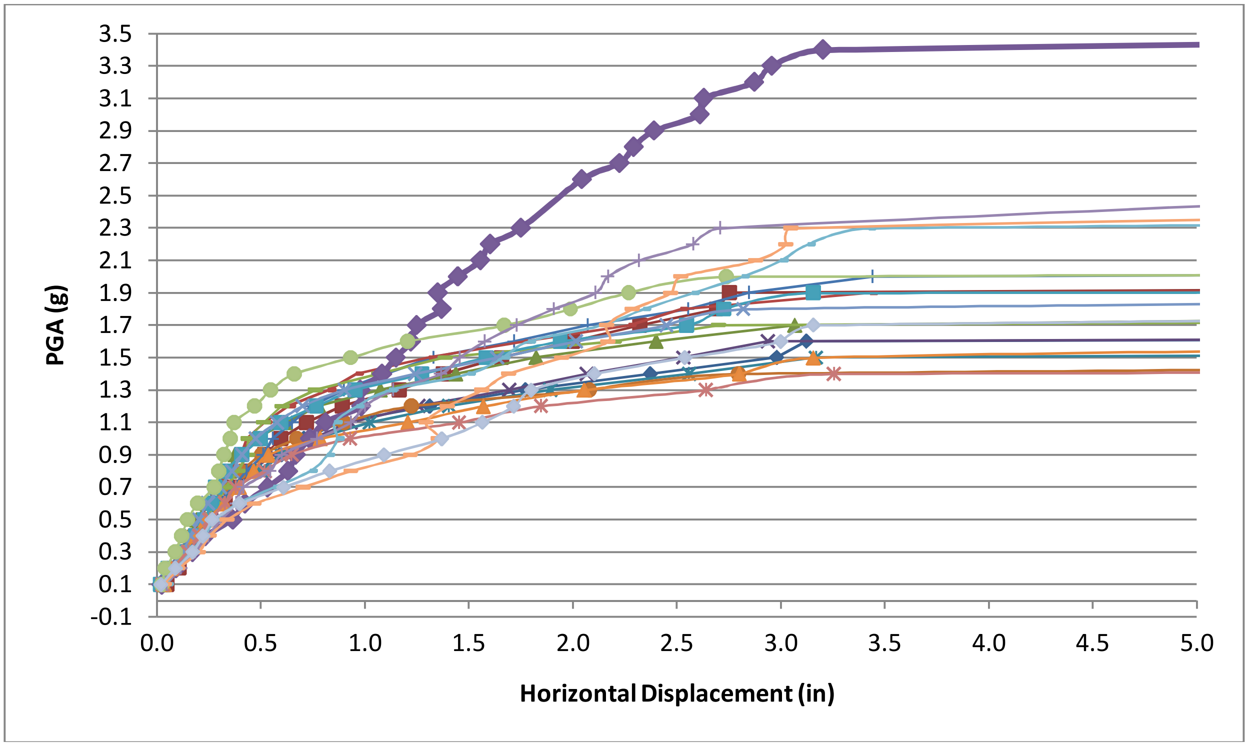


**Figure D 14 – PGA vs. Horizontal Displacement Graph for Model D1 (Steel Sheathing)**

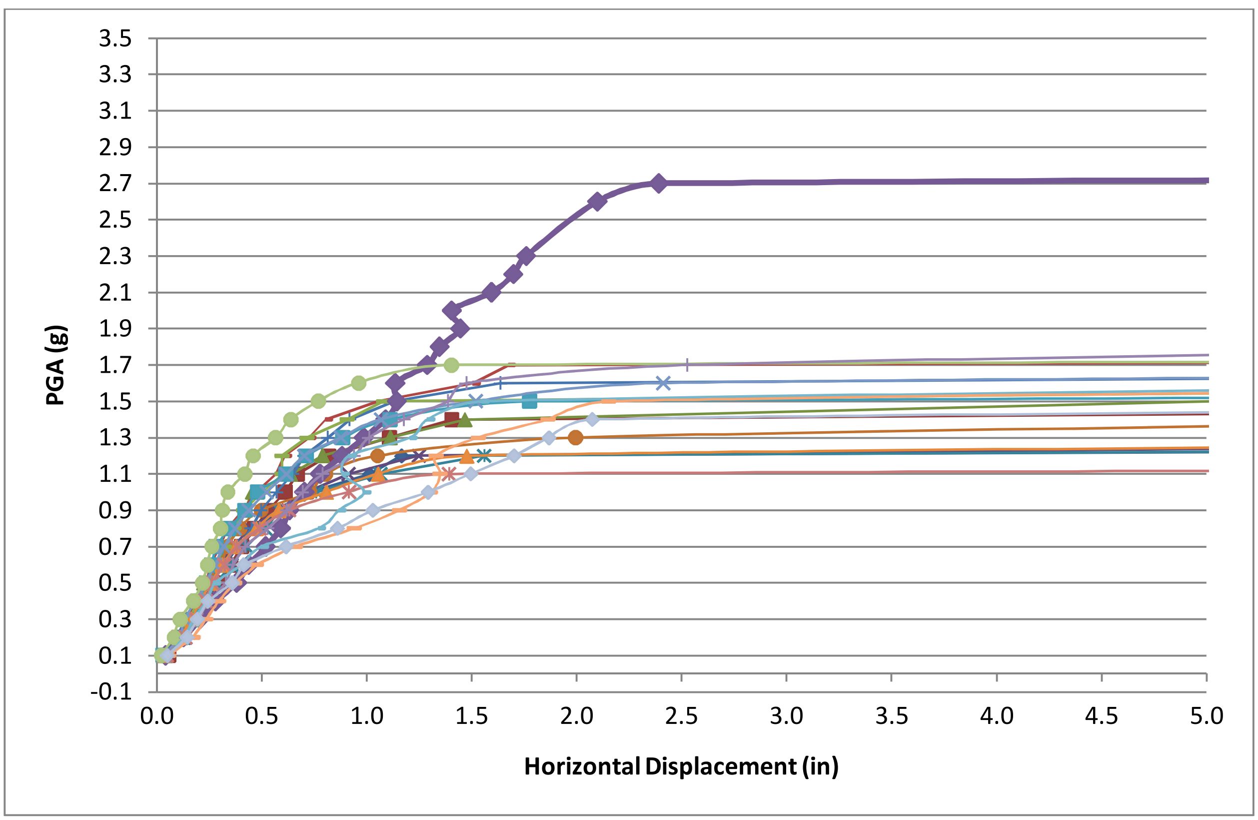


**Figure D 15– PGA vs. Horizontal Displacement Graph for Model D2 (Steel Sheathing)**

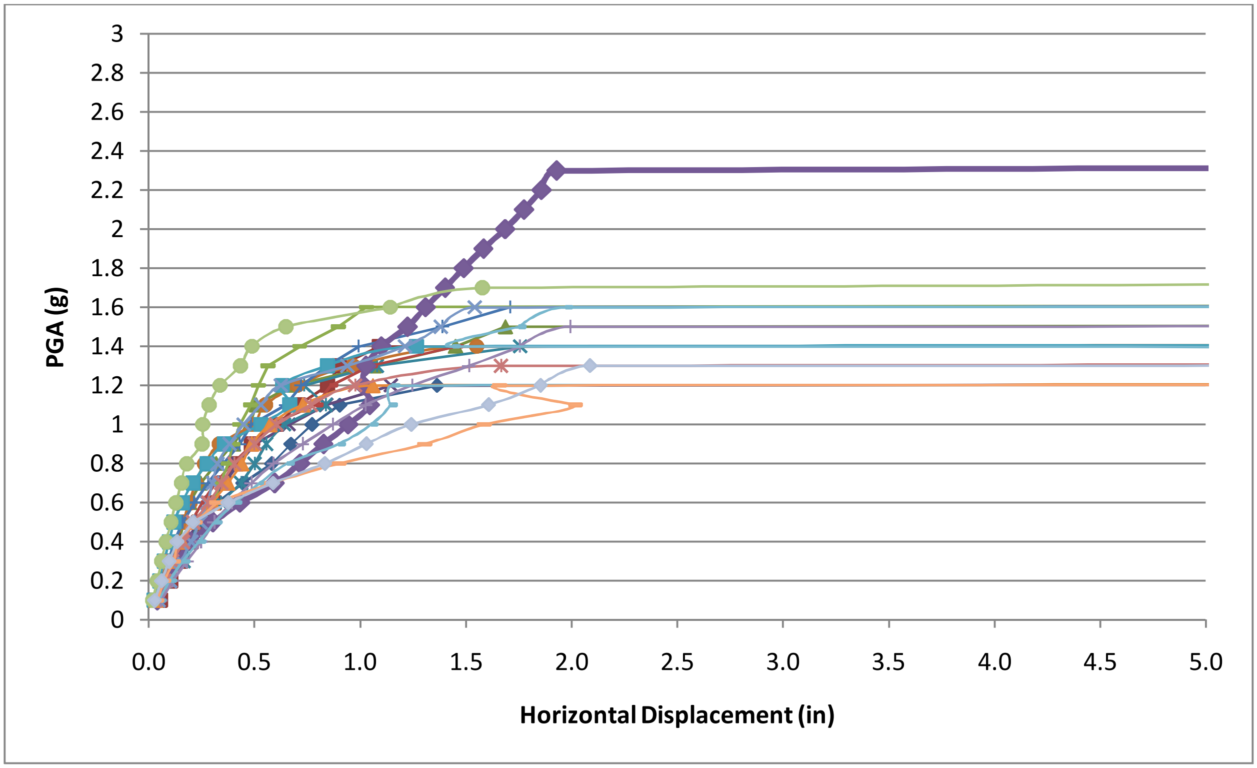


**Figure D 16 - PGA vs. Horizontal Displacement Graph for Model F1 (Steel Sheathing)**

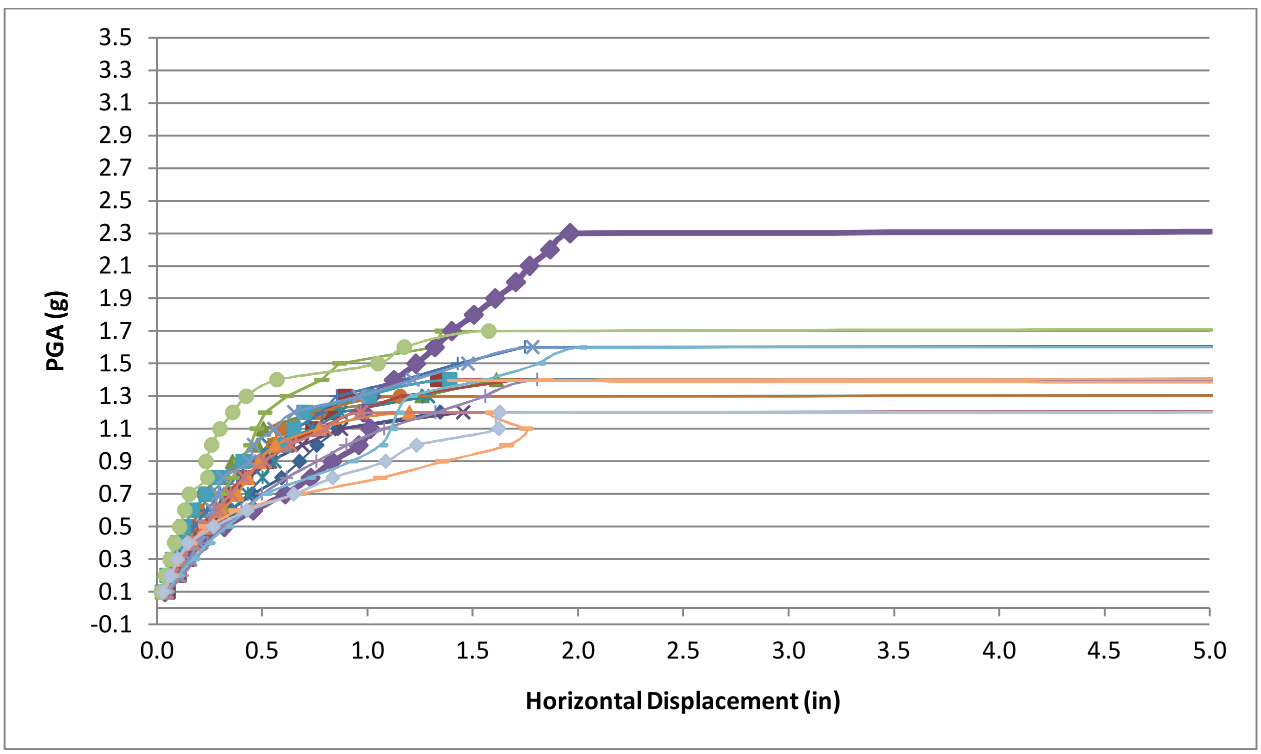


**Figure D 17 – PGA vs. Horizontal Displacement Graph for Model F2 (Steel Sheathing)**